Title
Role of Orai1 in Oral Cancer

Author
Lee, Sung Hee

Publication Date
2016

Peer reviewed|Thesis/dissertation

UNIVERSITY OF CALIFORNIA
Los Angeles

Role of Orai1 in Oral Cancer

A dissertation submitted in partial satisfaction of the

requirements for the degree Doctor of Philosophy

in Oral Biology

by

Sung Hee Lee

2016

ABSTRACT OF THE DISSERTATION

Role of Orai1 in Oral Cancer

by

Sung Hee Lee

Doctor of Philosophy in Oral Biology

University of California, Los Angeles, 2016

Professor Ki-Hyuk Shin, Co-Chair

Professor No-Hee Park, Co-Chair

Oral cancer is the 6th most common cancer worldwide, and more than 30,000 Americans are diagnosed with oral cancer each year. The 5-year survival rate for this group of cancers has been about 50%, despite advances in surgery, radiation, and chemotherapy. In addition to premature death associated with oral cancer, the severe morbidity from cancer treatment makes oral cancer a major public health concern. Thus, although there has been in depth studies for understanding the molecular pathogenesis of oral cancer, further studies of the understanding of the cancer etiology, development, progress and recurrences are warranted. Recent studies have shown that cancer cells, including oral cancer, contain a small population of cancer stem cells (CSCs or alternatively cancer initiating cells) associated with drug resistance, metastasis and recurrence of

the cancer. Therefore, CSCs might be strategically plausible targets for cancer therapies. More recently, many studies indicated that the suppression of Orai1 can diminish malignant phenotypes of cancer cells. Although Orai1 is known as a key calcium channel for store-operated Ca^{2+} entry, the underlying mechanism by which Orai1 regulates cancer progression remains unknown. Here we demonstrate that Orai1 is increased in a stepwise manner during oral/oropharyngeal carcinogenesis and highly expressed in cancer stem-like cell (CSC)-enriched populations of human oral/oropharyngeal squamous cell carcinoma (OSCC). Ectopic Orai1 expression further induced malignant transformation and self-renewal capacity, $ALDH1^{HIGH}$ cell population, increased. Conversely, inhibition of Orai1 suppressed tumorigenic and CSC phenotype in OSCC, indicating that Orai1could be an important element for tumorigenicity and stemness of OSCC. Mechanistically, Orai1 activates its major downstream effector molecule, NFATc3. Knockdown of NFATc3 in the Orai1-overexpressing oral epithelial cells abrogates the effect of Orai1 on CSC phenotype. Antagonist of NFAT signaling also decreases CSC phenotype, implying the functional importance of Orai1/NFAT axis in OSCC CSC regulation. Moreover, Orai1-induced cytokines in HOK-16B/Orai1 cells were commonly upregulated in CSCs and enhanced important CSC phenotypes, *i.e.*, self-renewal in OSCC. Subset of these CSC-specific cytokines were regulated by NFAT signaling, and partially rescued CSC phenotype in Orai1 inactivated OSCC, which suggests a possible role of cytokines in regulating CSC through Orai1-NFAT signaling. This study identifies Orai1 as a novel molecular determinant for OSCC progression by enhancing cancer stemness, suggesting that inhibition of Orai1-NFAT signaling may offer an effective therapeutic modality against OSCC.

The dissertation of Sung Hee Lee is approved.

Yousang Gwack

Mo Kang

Ki-Hyuk Shin, Committee Co-Chair

No-Hee Park, Committee Co-Chair

University of California, Los Angeles

2016

TABLE OF CONTENTS

LIST OF FIGURES AND TABLES

ACKNOWLEDGEMENTS

I would like to express my gratitude to my doctorate dissertation committee members for giving me a full support and guidance throughout my doctorate program.

Because of great mentorship of my committee chairs, Dr. No-Hee Park and Dr. Ki-Hyuk Shin, I was able to complete my doctorate degree. Dr. Shin and Dr. Park has proved their true mentorship by giving me a clear direction in each step of my research projects. Their mentorships are highly recognized when I received the 1st and 2nd research awards at the UCLA School of Dentistry Research Competition in the year of 2012 and 2016, respectively, and the 1st Hatton Award at the 2016 American Association for Dental Research (AADR) Annual Meeting. Also, I deeply appreciate their faith-based mentorship that helped me to grow to be a mature person.

I thank Dr. Mo Kang and Dr. Reuben Kim for their important feedbacks on my research project and their encouragements throughout my doctorate program. I consider Dr. Kang and Dr. Kim as my mentors, because they gave me thoughtful guidance in difficult times throughout my doctorate program and encouraged me to keep my dream and move forward. It has been a great honor to have both mentors for five years, and I would like to take this opportunity to thank them with my sincere heart.

I also thank Dr. Gwack and Dr. Srikanth for their insight and guidance in my research project. Especially, their advice based on his expertise in Immunology and Calcium signaling really helped me to have a clear understanding of the background of my research. I am grateful for their willingness to share their research equipment, many reagents and lab supplies. Also, I would like to acknowledge Dr. Gwack and Dr. KD Kim for all providing me with the chemical 5D and the molecular structure of 5D, which was published in the Journal of Immunology in the

year of 2014: Kim KD, Srikanth S, Tan YV, Yee MK, Jew M, Damoiseaux R, Jung ME, Shimizu S, An DS, Ribalet B, Wascheck JA, Gwack Y. Calcium signaling via Orai1 is essential for induction of the nuclear orphan receptor pathway to drive Th17 differentiation. J Immunol 2014. 192 (1):110-122.

Without many helps and support I received from my colleagues, I could not have completed my program. First, I would like to acknowledge Nicole Rigas for giving me a research insight with her Master's thesis work and a modified figure from her work published in ProQuest: Nicole Rigas. The role of cytokines on oral cancer stem cells. Proquest 2014. UMI 157246.

Also, I would like to thank Justin Lee, Dr. Sol Kim, Dr. Suhjin Sohn, Dr. Kyung Lhi Kang, Dr. Minju Song, Dr. Wei Chen, Paul Yang, Terresa Kim, Cindy Lee, Shebli Mehrazarin, Richard Lee, Zi Xiao, Peter Huh, Sonia Kim, Charlotte Martin, Neha Mohindroo, Abdullah Alshaikh and Calvin Keu for their support, teaching and advice.

Most importantly, I would like to thank my parents for their full support with sacrificial love. I am indebted to you two. Thank you for your companionship throughout the important chapter of my life's journey. Because of your love and support, I am where I am. Thank you and I love you sincerely.

BIOGRAPHICAL SKETCH

NAME Sung Hee Lee	POSITION TITLE Ph.D Candidate in Oral Biology
eRA COMMONS USER NAME (credential, e.g., agency login): N/A	

EDUCATION/TRAINING *(Begin with baccalaureate or other initial professional education, such as nursing, include postdoctoral training and residency training if applicable. Add/delete rows as necessary.)*

INSTITUTION AND LOCATION	DEGREE	Completion Date MM/YYYY	FIELD OF STUDY
University of California, Los Angeles	B.S	12/2008	Biochemistry
University of California, Los Angeles	M.S.	08/2012	Oral Biology
University of California, Los Angeles	Ph.D	*in progress*	Oral Biology

A. Positions and Honors

Position and Employment

2011 – Present Graduate student researcher, Division of Oral Biology & Medicine, UCLA, School of Dentistry

Other Experience and Professional Memberships

2012 – 2015 Associate Member, American Association for Cancer Research (AACR)
2015 – Present Student Member, American Association for Dental Research (AADR)
2015 – Present Student Member, International Association for Dental Research (IADR)

Academic and Professional Honors

2012 Research Award (**1st place** in Master student category), UCLA School of Dentistry Research Day Competition
2016 Research Award (**2nd place** in Ph.D & Post-doctoral category), UCLA School of Dentistry Annual Poster Competition
2016 Hatton Award (**1st place** in Senior category), American Association for Dental Research (AADR)
2016 Selected as the finalist in Unilever Hatton Competition, International Association for Dental Research (IADR)

B. Publication

Original Research Articles:

1. **Lee SH**, Hong SH, Liu ZX, Kim RH, Kang MK, Park NH, Shin KH. TNFα enhances cancer stem cell-like phenotype via Notch-Hes1 activation in oral squamous cell carcinoma cells. *Biochem Biophys Res Commun* 424:58-64, 2012.

2. **Lee SH**, Lee CR, Rigas NR, Kim RH, Kang MK, Park NH, Shin KH. Human papillomavirus 16 (HPV16) enhances tumor growth and cancer stemness of HPV-negative oral/oropharyngeal squamous cell carcinoma cells via miR-181 regulation. *Papillomavirus* 1: 116-125, 2015.
3. Lee CR, **Lee SH**, Rigas NK, Kim RH, Kang MK, Park NH, Shin KH. Elevated expression of JMJD6 is associated with oral carcinogenesis and maintains cancer stemness properties. *Carcinogenesis* 37: 119-128, 2016.
4. **Lee SH**, Park Y, Song M, Srikanth S, Kim S, Kang MK, Gwack Y, Park NH, Kim RH, Shin KH. Orai1 mediates osteogenic differentiation via BMP signaling pathway in bone marrow mesenchymal stem cells. *Biochem and Biophys Res Commun* 473: 1309-1314, 2016.
5. **Lee SH**, Rigas NK, Lee CR, Bang A, Srikanth S, Gwack Y, Kang MK, Kim RH, Park NH, Shin KH. Orai1 promotes tumor progression by enhancing cancer stemness *via* NFAT signaling in oral/oropharyngeal squamous cell carcinoma. *Oncotarget* 7: 43239-43255, 2016.
6. **Lee SH**, Inaba A, Mohindroo N, Ganesh D, Martin CE, Chugal N, Kim RH, Kang MK, Park NH, Shin KH. Three-dimensional sphere-forming cells are unique multipotent cell population in dental pulp cells. *Manuscript submitted.*

Abstracts Presented in Scientific Meetings:

1. **Lee SH**, Kim RH, Kang M, Park NH, Shin KH. Chronic TNFα treatment enhances cancer stem cell-like phenotype via Notch1 activation in oral squamous cell carcinoma cells. Proceedings of 103th Annual Meeting of American Association for Cancer Research, Abstract # 3341, 2012.
2. **Lee SH**, Kim R, Kang M, Park NH, Shin KH. Zoledronic acid inhibits cancer growth and cancer stem cell phenotype in head and neck squamous cell carcinoma. Proceedings of 104th Annual Meeting of American Association for Cancer Research, Abstract # 3715, 2013.
3. **Lee SH**, Rigas N, Lee CR, Han J, Kim RH, Kang MK, Park NH, and Shin KH. Human papillomavirus enhances oral cancer stem cell phenotype by regulating microRNA-181. Proceedings of 105th Annual Meeting of American Association for Cancer Research, Abstract #1948, 2014.
4. Chiang S, Li F, **Lee SH**, Shin KH, Park NH, and Wong D. Salivary piRNA Enhances Re-epithelialization in Oral Wound Healing. American Association for Dental Research, 2016.
5. **Lee SH**, Rigas N, Lee CY, Gwack Y, Kim RH, Kang MK, Park NH, and Shin KH. Orai1 promotes oral cancer progression by enhancing cancer stemness via NFAT signaling. American Association for Dental Research, 2016.
6. **Lee SH**, Kim RH, Kang MK, Park NH, and Shin KH. Three-dimensional spheres derived from dental pulp cells exhibit enhanced stemness. International Association for Dental Research, 2016.
7. **Lee SH**, Rigas N, Lee CY, Gwack Y, Kim RH, Kang MK, Park NH, and **Shin KH**. Orai1 promotes oral cancer progression by enhancing cancer stemness via NFAT signaling. International Association for Dental Research, 2016.

1. INTRODUCTION

1.1 Oral cancer

1.1.1 Prevalence of oral cancer

Oral cancer is the sixth most common cause of death from cancer worldwide with only about 50% chance of 5-year survival (Al-Swiahb et al., 2010). About 90 percent of oral cancer is squamous cell carcinoma, and common site includes tongue, floor of oral cavity and lip (Rivera and Venegas, 2014). The recent annual estimated incidence of oral cancer worldwide is around 275,000 with two thirds of cases occurring in developing countries, including South and Southeast Asia, parts of Eastern and Western Europe, parts of Latin America and Caribbean and in Pacific regions (Warnakulasuriya, 2009). According to the NIH Cancer Statistics Review in 2016, approximately 48,330 cases of oral cancer and pharynx cancer are reported with estimated death of 9,570 cases in the United States (National Cancer Institute, 2016). Estimated new diagnosed and death case associated with oral cancer is commonly in aged population between 55 to 64, and is more prevalent in men than women. Also, rising incidence of oral cancer in young adults is reported in the United States and Europe (Shiboski et al., 2005; Warnakulasuriya, 2009).

1.1.2 Oral cancer risk factors

Well-known Risk factor of oral cancer are tobacco, alcohol and high-risk HPV infection, and their effects can be additive (Hansson et al., 2005; Lee et al., 2005a; Perez-Sayans et al., 2009). All forms of tobacco contain more than 60 different carcinogens (Hecht, 2003). Among these carcinogens, Benzo[a]pyrene (BaP) is the first detected carcinogen implicated as forming DNA adduct, which cause mutation in tumor suppressor gene TP53 gene in the lung cancer

(Denissenko et al., 1996; Pfeifer et al., 2002). Significance of smoking as risk factor for oral cancer is also well-documented. Long-term exposure to BaP converted the immortalized non-tumorigenic oral epithelial cells to tumorigenic cells, indicating the role of BaP in cellular transformation leading to cancer formation (Park et al., 1995). Alcohol is another important factor playing important role in development of several cancers types, including oral cancer (Cao and Giovannucci, 2016). Acetaldehyde, the first and most toxic ethanol metabolites, promotes cancer development through different mechanism, including interference with DNA replication, formation of DNA adducts, and induction of DNA damage (Seitz and Becker, 2007). Combination of alcohol consumption and tobacco consumption significantly increased the permeability of oral mucosa to nitrosonornicotine (NNN), which is one of tobacco carcinogen (Du et al., 2000). HPV is a DNA virus that is typically transmitted through sexual contacts. Many studies revealed that high-risk HPV (*e. g.,* HPV16, HPV18) is an additional independent risk factor for oral cancer(Smith et al., 2004). HPV infection is closely associated with benign and malignant oral lesions and up to 30–40% of oral cancer biopsies contain the viral DNA (Kellokoski et al., 1992; Syrjanen, 1992). Also, the enhancement of oral cancer growth and cancer stemness by HPV16 further augments that of HPV infection is an important risk factor for oral cancer development (Lee et al., 2015).

1.1.3 Current oral cancer treatments

Currently available treatments for oral cancer are chemotherapy and radiotherapy. Surgical resection and/or radiotherapy has been widely used to treat the early stage cancer, and systemic chemotherapy has been employed in advanced cancer. Since the introduction of cisplatin in the 1970s, combining cisplatin with a variety of other drugs have been used for improved clinical

response rate in a number of trials with advanced cancer (Rooney et al., 1985). However, combination therapy is effective in treating 33% of advanced cancer, as compared to its effectiveness in treating 97 percent of early stage cancer (Marcial et al., 1990). Furthermore, the recurrence rates ranges from 30 percent to 47 percent for oral squamous cell carcinoma, affecting the quality of life for the oral cancer patients (Kligerman et al., 1994; Wang et al., 2013). Therefore, implementation of prevention strategies, *e.g.*, early diagnosis, HPV vaccination and education on safe sex, and continuous oral cancer research are crucial to control the incidence and mortality related to oral cancer.

1.2 Cancer stem cells (CSCs) and cancer

1.2.1 Definition of CSCs

CSCs are a subpopulation of cancer cells with self-renewal capacity and a potential to differentiate that establishes heterogeneity of cancer. CSCs are also known as cancer initiating cells and are responsible for the long sustenance of cancer (Beck and Blanpain, 2013a). It has been postulated that CSC might be originated from specific stem cells, progenitor cells or differentiated cells (Beck and Blanpain, 2013a). CSCs have been isolated from various tumor and established cancer cell lines, such as breast, prostate, lung and oral cancer (Chiou et al., 2008; Clevers, 2011; Ginestier et al., 2007; Lang et al., 2009; Singh and Chellappan, 2014).

1.2.2 Identification and isolation of CSCs

CSCs are genetically and epigenetically regulated such that phenotypes of CSCs have been reported to be regulated by several cellular pathways, such as Notch, Hedgehog, and Wnt, all of which are frequently activated in human cancer (Giles et al., 2003; Lee et al., 2012a; Lee et al.,

2015; Liu et al., 2006). In addition to various molecular pathways which provide the means to identify cancer stem cell, other useful methods have been used to isolate CSCs including oral CSCs. Drug resistant property of CSCs has been used to isolate population of cancer cells called side population, which can pump out intracellular toxins. Also, common surface markers used for oral CSCs isolation include $CD44^{high}$ $CD24^{low}$, $CD133^{+}$ and $ALDH1^{high}$, and cells expressing high level of these surface markers have been shown to propagate tumor in mouse xenograft assay, indicating tumorigenic potential of CSCs (Clay et al., 2010; Ginestier et al., 2007; Hermann et al., 2007). ALDH1 is well-known oral cancer stem cell marker, as cells with high expression of ALDH1 have been shown to produce tumor *in vivo* with much higher efficiency than the cells sorted with traditionally used oral cancer surface marker (Clay et al., 2010). Although these surface markers are widely used in research, there is no single biomarker that selectively isolate oral CSCs. Along with these useful markers to isolate oral CSCs, further understanding the unique biology of oral CSCs may enable more selective isolation and generation effective targeted therapy for oral cancer.

1.2.3 Role of CSCs in cancer progression

CSCs are also responsible for drug resistance, metastasis, and recurrence of cancer. Indeed, CSCs plays important role as the driving force of cancer formation and cancer progression, making them strategically plausible target for cancer therapy. As cancer progresses to advanced stages, cancer become more difficult to eradicate mainly due to the property of cancer cells to metastasize. CSCs have been defined as cells that are able to re-form secondary tumor when transplanted in immune-deficient mice, suggesting the role of CSCs in cancer metastasis (Hermann et al., 2007). Their migratory and invasive behavior and cell's morphological change

is the result of changes in molecular events within cancer cells, enabling cancer cells to evade into the circulatory system and metastasize. As most adult tissues possess capacity to generate epithelial to mesenchymal transition (EMT) for the purpose of wound healing and tissue regeneration, CSCs may undergo EMT to initiate metastasis. EMT is cellular process in which cell-cell junction and cell-extracellular matrix breaks apart and undergo morphological change that switches cell to the condition favorable for migration (Chu et al., 2013). Co-expression of ZEB1/ZEB2, key transcriptional factor regulating EMT, was found increased in oral CSCs with capacity of distant metastasis. Silencing ZEB1/ZEB2 in oral CSCs resulted in reduction in distant lung metastasis, Conversely, overexpression of these factors in non-CSCs cells enhanced key mesenchymal markers expression along with CSC phenotypes (Chu et al., 2013). Other important makers of metastasis found in CSCs include vascular endothelial growth factor (VEGF), Zinc finger protein SNAI1 (SNAIL), Vimentin, N-Cadherin, all of which aids CSCs to either migrate or form the secondary tumor (Bhat-Nakshatri et al., 2010; Morel et al., 2008). ALDH1 positive oral CSCs revealed high expression of SNAIL protein, which was shown responsible for invasiveness and also chemo-radioresistance of oral cancer cells (Chen et al, 2009). CSCs express anti-apoptotic genes and high DNA damage response factors to promote DNA repair and become resistant to chemotherapy and radiation therapy (Abdullah and Chow, 2013). CSCs express ATP-binding cassette (ABC) pumps that allows exclusion of cancer therapeutic drugs, therefore is known to have multidrug resistance (MDR), making cancer more difficult to eradicate (Grimm et al., 2012). Role of checkpoint kinase 1 (CHK1) in chemoresistance in $CD133^{+}$ colon and glioma, and CD24+ CD44+ ESA+ pancreatic CSCs is also well-documented (Abdullah and Chow, 2013). In particular, oral cancer stem cells with increased B-Cell Lymphoma-2 (Bcl-2) family proteins was shown to improve oral cancer

prognosis, and ABCB5 overexpression in oral cancer showed strong association of cancer formation and progression (Grimm et al., 2012; Sinevici and O'Sullivan, 2016). Furthermore, Oral CSCs expressing high ALDH1 showed high resistance to chemo-radiotherapy and were capable of forming tumor in vivo at much higher efficiency than non-CSC oral cancer cells (Clay et al., 2010).

1.3 Cellular calcium signaling

1.3.1 Overview of calcium signaling

Ca^{2+} regulates various cellular processes including proliferation, apoptosis, and migration (Monteith et al., 2007). There are many different Ca^{2+} channels on the plasma membrane or on the surface of cellular organelles, *i.e.*, endoplasmic reticulum (ER) and mitochondria Ca^{2+} is derived either from internal store or extracellularly. Intracellular Ca^{2+} is tightly controlled to achieve the regulation of cell signaling pathways in response to stimuli. In a resting state, intracellular Ca^{2+} level is kept low (~100nM) compared to the extracellular level (1.2mM) (Carafoli, 1987). External stimuli that control the Ca^{2+} entry through those channels include membrane depolarization, extracellular agonist, intracellular messengers and depletion of intracellular store, and subsequent Ca^{2+} signaling can be initiated within cells to control various biological processes (Berridge et al., 2000). Largely, there are three different types of Ca^{2+} channels: Voltage-operated, receptor-operated, and second-messenger-operated channels (Berridge et al., 2000). Voltage-operated channels are dominant Ca^{2+} channel on excitable cells, such as neurons and in heart, and is activated by membrane depolarization. For example, Ca^{2+} entered through these channels in heart functions to induce muscle contraction by activating sarcomere. Second messengers-operated channel is controlled by intracellular messengers, such

as arachidonic-acid-sensitive channel, Inositol-1,4,5-triphosphate receptor (Ins(1,4,5)P_3R and sarcoendoplasmic reticulum Ca^{2+}-ATPase (SERCA) expressed on the ER membrane (Cancela et al., 2002; Lukyanenko et al., 2001; Mignen and Shuttleworth, 2000). Some Ca^{2+} channel opens in response to external signal, such as receptor-operated channels. N-methyl-D-aspartate receptor (NMDAR) receptor that opens in responds to the binding of glutamate on the channel. Store-operated channels are the plasma membrane-bound channel, which can open upon depletion of ER Ca^{2+} store. Ca^{2+} which made entry through these channels relay various cellular signaling pathway by activation of Ca^{2+}-dependent effectors. Ca^{2+} signaling can be either spatial and temporal (Berridge et al., 2000). Ca^{2+} channels and cellular proteins form complexes that function together to modulate Ca^{2+} entry, and it can function as independent unit. For example, the cardiac Ca^{2+} channel unit, which comprise of Ryanodine receptor 2 (RynR2) and other interacting proteins, can work independently from its neighbor to control Ca^{2+} entry to produce regional graded contraction (Berridge et al., 2000). Temporally, single Ca^{2+} channel unit can activate other channels to spread the local Ca^{2+}signal to create the Ca^{2+} oscillation (Berridge et al., 2000).

1.3.2 Calcium signaling and stem cell maintenance

Hallmarks of stem cell are self-renewal capacity and multi-lineage differentiation, and studies have shown the role of intracellular Ca^{2+} in maintaining stem cells of different origin. Numerous reports highlight the role of Ca^{2+} as a key regulator of the cell cycle, and lowering extracellular Ca^{2+} decrease cell proliferation (Berridge et al., 2000; Hazelton et al., 1979; Hickie et al., 1983; Kahl and Means, 2003; Whitfield et al., 1979). Indeed, flow cytometry analysis revealed that changes in intracellular Ca^{2+} has been detected in different stages of cell cycle,

especially as cells passed through G1 phase (Pande et al., 1996). In the same manner, spontaneous Ca^{2+} oscillations were found during cell cycle embryonic stem cells (ESC). Mechanistically, recent study on mouse ESC revealed that induction of Ca^{2+} signaling by lysophosphatidic acid (LPA) receptor coupled to G-Protein coupled receptor (GPCR) resulted in the induction of *c-myc* and increased cell proliferation (Todorova et al., 2009). Another similar study has shown that the activation Ca^{2+}/Calmodulin-dependent kinase (CaMKII) and Jun-N-terminal Kinase (JNK) by Wnt11 can regulate the differentiation function of cardiac stem cell(Biteau et al., 2008). Number of reports also emphasized the significance of Ca^{2+} in cellular differentiation process. A study on human mesenchymal stem cell revealed the importance of intracellular Ca^{2+} content and stimulation of intracellular Ca^{2+} oscillation in in osteogenic differentiation (Sun et al., 2007). Moreover, store-operated Ca^{2+} entry was detected in human mesenchymal stem cells, and specific transient receptor potential (Trp) Ca^{2+} channel isoforms were expressed in cells of the megakaryocytes or platelets lineage of monocytes (den Dekker et al., 2001).

1.4 Calcium and cancer

1.4.1 Calcium signaling in cancer survival and growth

Increasing number of studies have demonstrated the importance of Ca^{2+} in regulating cancer cell proliferation. As the matter of fact, Ca^{2+} channels with altered expression in cancer are directly involved in cancer growth. Importance of Ca^{2+} channels for cell proliferation is reported in breast, colorectal, prostate and gastric cancer cells (Lehen'kyi et al., 2007; Panner and Wurster, 2006). For example, inhibition of Ca^{2+} entry using Ca^{2+} channel blocker suppressed human lung and colon cancer, and U87 MG glioma cells growth (Benzaquen et al., 1995; Panner and

Wurster, 2006). Furthermore, expression of plasmalemmal Ca^{2+}-APTase (PMCAs), which efflux Ca^{2+} outside the cell, was reduced in oral cancer and transformed skin and lung fibroblast, giving an advantage to cancer to utilize Ca^{2+} signaling for cancer growth (Endo et al., 2004; Saito et al., 2006). Importance of Ca^{2+} signaling is also highlighted by in the studies on the Ca^{2+}-dependent proteins. Nuclear factor of activated T cells (NFATs) have been shown to regulate cell cycle-related genes responsible for cell cycle progression to S phase in mouse 3T3-L1 fibroblast (Neal and Clipstone, 2003). Also, constitutively active NFATc1 mutant promoted cell proliferation of 3T3-L1 fibroblast and induced cell transformation. NFATc1 overexpression directly upregulates *c-myc* transcription, which resulted in cell proliferation and anchorage-independent growth in pancreatic cancer (Buchholz et al., 2006b).

Due to complex biology of ever transforming cancer, Ca^{2+}-induced apoptosis and death signaling is tightly controlled. In the proliferative cancer cells, the disruption of the balance between cell survival and cell death signals are detected. It is reported that increased intracellular Ca^{2+} level due to Endoplasmic reticulum (ER) depletion of Ca^{2+} or increased Ca^{2+} influx leads to Ca^{2+} overload in the mitochondria, sensitizing cells to apoptotic stimuli (Rizzuto et al., 2003). In order to promote proliferation, cancer cell's Ca^{2+} signaling is regulated by anti-apoptotic proteins, such as B-cell lymphoma 2 (BCL2) and B-cell lymphoma-extra large (BCL-$X_{L)}$, and Protein kinase B (PKB) proteins (Roderick and Cook, 2008). Suppression of Ca^{2+} depletion from ER by BCL2-related proteins has been shown to increase apoptosis resistance in cancers, which seem paradoxical to the reports suggesting the importance of Ca^{2+} signaling in cancer growth (Pinton et al., 2000; Vanden Abeele et al., 2002). However, recent report indicated that BLC2 inhibited apoptosis without inhibiting Ca^{2+} oscillation and NFAT activation in T cells, showing that it is possible to modify Ca^{2+}-induced apoptotic signal while not altering Ca^{2+} signaling (Zhong et al.,

2006). Also, concurrent overexpression of Ca^{2+} influx channel and efflux channel were found in breast cancer cells lines, owing to the possibility that cancer can modulate Ca^{2+} content favorable for its growth (Lee et al., 2002; Tsavaler et al., 2001). These data suggest the importance of Ca^{2+} signaling in cancer growth with tight control of Ca^{2+}-induced apoptosis.

1.4.2 Calcium signaling in cancer progression

Clinically, intracellular Ca^{2+} level is strongly linked to poor overall and recurrence-free survival in different cancer types, such as human esophageal SCC (Lee et al., 2012b; Zhang et al., 2013) and non-small cell lung cancer (Zhan et al., 2015) due to their malignant phenotype. Ca^{2+} promoted cancer cell migration/invasion (Yang et al., 2009a), drug resistance (Schmidt et al., 2014), both phenotypes of which are well known for CSC characteristics (Beck and Blanpain, 2013a; Beck and Blanpain, 2013b; Ribatti, 2012).

Metastatic cancer cells display highly migratory and invasive phenotype, and Ca^{2+} plays important role in acquiring these phenotypes in cancer cells. Migrating cells exhibit transient intracellular Ca^{2+} gradient from the front of the cell to rear, which is responsible for cell retraction (Brundage et al., 1991). Also, there are aberrant expression of Ca^{2+}-handling proteins as well as Ca^{2+}-dependent effector, leading to increased focal adhesion turnover and extracellular matrix remodeling, the key features of cell migration (Prevarskaya et al., 2011). As a secondary messenger in cellular signaling pathways, Ca^{2+} is required for the activation of focal adhesion-localized proline-rich tyrosine kinase (PYK), which in turn phosphorylates focal adhesion kinase (FAK) and Paxillin in order to form a focal adhesion complex (Du et al., 2001). Several reports showed the significant role of Ca^{2+} channels in cancer motility and invasive property of cancer (Yang et al., 2009a; Yang et al., 2009b; Zhu et al., 2014a). In particular, genetic and chemical

inhibition of store-operated Ca^{2+} channel resulted in significant inhibition of breast cancer cell migration in vitro and lung metastasis in vivo (Yang et al., 2009a). Also, Transient receptor potential channel subfamily V member 2 (TRPV2) promotes migration of prostate cancer by inducing matrix metalloproteinase 2 (MMP2) and MMP9, both of which are important protein for remodeling of ECM (Monet et al., 2010).

Metastatic cancer also is highly resistant to cancer drugs. Ca^{2+} signaling has been shown to be involved in the resistance of cancer to chemotherapy. As disruption of ER Ca^{2+} content leads the activation apoptosis signaling in cells, acquisition of chemoresistance may require compensating change in a molecular level. Study on chemoresistant lung cancer lines revealed reduced Ca^{2+} content of the ER and SERCA expression (Schrodl et al., 2009). Furthermore, paclitaxel-resistant adenocarcinoma cells showed lower ER Ca^{2+} content and high anti-apoptosis protein called BCL2 compared to non-resistant cells. (Padar et al., 2004). While maintenance of Ca^{2+} content is crucial for the cellular homeostasis, the role of Ca^{2+} in various mechanism regulating drug resistance is recognized. Recent report showed the drug resistance in hepatocellular carcinoma cells is regulated by Ca^{2+} via transient receptor potential canonical 6 (TRPC6)/signal tranducer and activator of transcription-3 (STAT3) signaling pathway (Wen et al., 2016). Also, store operated Ca^{2+} entry through Orai1 Ca^{2+} channel revealed importance of Ca^{2+} in cisplatin-resistant ovarian cancer and the role of phosphatidylinositol 3-kinases (PI3K)-protein kinase B (Akt), a known target of Ca^{2+}-dependent Calmodulin, in the regulation of Ca^{2+} entry. As Ca^{2+}-activated Calmodulin phosphorylase targets, such as Akt, STAT3, have been reported to promote drug resistance in cancer (Lee et al., 2014; West et al., 2002), modulation of Ca^{2+} is very plausible in the malignant progression of cancer. Thus, Ca^{2+}, Ca^{2+} channels and

Ca^{2+}-regulated effector molecules play important role in cancer cell migration, invasion and drug resistance to further progress cancer to metastatic phenotypes.

1.5 Pathological role of cytokines and chemokines in cancer

1.5.1 Chronic inflammation and cancer

Inflammation is the process by which body's immune system respond to infection or injury and eradicate the foreign invader followed by repair of damaged tissue. In particular, within a process of inflammation, immune cells and cells exposed to foreign antigens produce cytokines and chemokines acting in autocrine or paracrine fashion to recruit immune cells to eradicate evading antigen within an organism (Balkwill and Coussens, 2004). Chronic inflammation is marked by sustained inflammatory condition in the site of infection or injury causing accumulation of genomic mutation in cells, which may lead to carcinogenesis. The inflammatory microenvironment in cancer is characterized by the presence of host immune cells promoting cancer growth (Balkwill and Mantovani, 2001). Cancer microenvironment contains immune cells, such as tumor associated macrophages (TAM), neutrophils, T and B lymphocyte, along with cancer cells and their surrounding stroma cells, and these diverse cells produce cytokines and chemokines acting in autocrine or paracrine fashion to control and promote cancer progression. Indeed, in cancer microenvironment, pro-tumorigenic inflammatory signal prevails over anti-tumorigenic inflammatory signal and allow caner to use the inflammatory signal to proliferate and progress.

1.5.2 Function of cytokine and chemokine

Within a process of inflammation, immune cells and cells exposed to foreign antigens produce cytokines and chemokines acting in autocrine or paracrine fashion to recruit immune cells to eradicate evading antigen within an organism. Cytokines are secretory proteins that are released by different cell types, including immune cells, stromal cells and cancer cells, and they function to recruit immune cells to the site of damage, serve as growth factor for B cell maturation and T cell activation, and induce apoptosis of infected cells (Feghali and Wright, 1997). Chemokines are secretory proteins (8-11 kDa) that are produced by immune cells and cells of inflammatory microenvironment in responds to stimuli, including inflammatory cytokines and growth factors (Mueller et al., 2007). They mostly signal through G-proteins mediated pathways. Main function of chemokine is to localize cells toward the source of chemoattractant, and G-protein-dependent chemokine receptor signaling induce activation of signaling involved in cell polarization and cell migration, such as F-actin polymerization and transcription of matrix metalloproteinases (MMPs) (O'Hayre et al., 2008). Also, some chemokines can activate other signaling, such as cell survival or anti-apoptotic signal, and proliferative signals (O'Hayre et al., 2008).

1.5.3 Significance of cytokines and chemokines in tumorigenesis

Different cytokine and chemokine promote tumor development through activation of transcriptional factor, such nuclear factor kappa-light-chain enhancer of activated B cell (NF-kB), activator protein 1 (AP-1) and signal transducer and activator of transcription (STAT), to transcribe pro-inflammatory cytokine and promote the initiation, growth and progression of cancer (Grivennikov et al., 2010). Previous findings suggested that inflammatory

microenvironment can increase mutation in cells, as inflammatory cells play role in producing cytokines that stimulate of reactive oxygen species and inactivation of DNA damage, which may act as another driving force of cancer initiation (Grivennikov et al., 2010). Also, cytokines can regulate transformed stem-like cancer cells to proliferate. It is reported that macrophages-derived tumor necrosis factor-α (TNF-α) promote cancer initiation by activating Wnt signaling in gastric mucosa (Oguma et al., 2008). Also, activation NF-kB signaling by chronic inflammation enhanced Wnt/ß-catenin signaling, which resulted in hyper-proliferation of and anti-apoptosis of colonic crypt (Umar et al., 2009). Also, blocking IL-4 signaling using the neutralizing antibody resulted in higher sensitization of colon cancer stem cells to the chemotherapy, suggesting that IL-4 plays role in survival and maintenance cancer stem cell population, the driving force of cancer initiation and progression (Francipane et al., 2008). Thus, activation of inflammatory signaling and prolong exposure of cells to cytokine play important role in promoting tumorigenesis.

1.5.4 Role of cytokines and chemokines in cancer progression

Clinically, cancer mortality is closely related to cancer metastasis. Also, it is important to note that collaboration among the cancer cells, immune and inflammatory cells, and stromal cells is required for cancer metastasis (Grivennikov et al., 2010). Cytokines plays important role in the progression of various cancer types. Cancer-promoting signaling through NF-kB, STAT and caspases have shown to be activated by various cytokines, such as IL-1, IL-4, IL-6, IL-10, IL-12, IL-23, TGF-β, TNF-α and TRAIL (Lin and Karin, 2007). In inflammatory human tumor environment, cytokines function to enhance proliferation and survival. IL4, pro-inflammatory cytokine, has been shown to promote cancer cell survival and expansion by inducing the

expression of anti-apototic genes (Todara et al., 2007). Also, cancer cells themselves produce IL4 in autocrine fashion and confer drug resistance, which then allow cancer cells to escape from cancer drug-induced death (Conticello et al., 2004). In addition, the role of cytokines in cancer metastasis is highlighted in different scientific reports. Cytokines play important role in every step of metastasis: extravasation, circulation, colony expansion. As EMT is the hallmark of migratory phenotype of cells, cytokines may affect cells morphological change by regulating known EMT transcriptional factors. TNF-α induction by NF-kB activation induced zinc finger protein SNAI1 transcriptional factor. Furthermore, STAT-mediated twist-related protein (Twist) transcriptional factor was known to promote EMT phenotype in cancer (Yu et al., 2009). In order for the cancer cells to invade, proteolysis of extracellular matrix by MMP is required during metastasis. Secretion of IL-1, TNF- α by cancer induce expression of MMP by activation of NF-kB and STAT signaling in immune cells and promote invasive property of cancer (Yu et al., 2007). Particularly, IL-1β knockout mice showed significant decrease in local metastasis of melanoma, prostate, and mammary cells, and this suggested that IL-1β may control tumor invasiveness as well as metastasis (Voronov et al., 2003).

2 MATERIALS AND METHODS

2.1 Cell culture and reagents

Primary normal human oral keratinocytes (NHOK) were prepared from oral mucosa and cultured in Keratinocyte Growth Medium (KGM, Lonza) as described previously (Park et al., 1991). Three non-tumorigenic immortalized oral epithelial cell lines, NOK-SI (Castilho et al., 2010), OKF6/tert (Dickson et al., 2000), and HOK-16B (Park et al., 1991), were also cultured in KGM. Ten human OSCC cell lines, HOK-16B BapT, SCC4 (Min et al., 1994), SCC15, SCC1, SNU1041, SNU1076, SCC9/TNF (Lee et al., 2012a), YD9 (Lee et al., 2005b), YD15M, and UM17b (Lin et al., 2007), were cultured in DMEM/Ham's F12 (Invitrogen) supplemented with 10% FBS (Gemini Bioproducts) and 0.4 μg/ml hydrocortisone (Sigma-Aldrich). Orai1 chemical blocker, Compound 5D (Kim et al., 2014b), was obtained from Dr. Yousang Gwack (UCLA David Geffen School of Medicine). Antagonist of NFAT signaling, cyclosporine A (CsA), was purchased from Sigma-Aldrich.

2.2 Western blotting

Western blotting was performed as described previously (Lee et al., 2012a). Briefly, Whole cell extracts were isolated using the lysis buffer (1% Triton X-100, 20 mM Tris –HCl pH 7.5, 150 mM NaCl, 1mM EDTA, 1mM EDTA, 2.5 mM sodium pyrophosphate, 1 μ M β -glycerophosphate, 1 mM sodium orthovanadate, 1 mg/ml PMSF). Cytoplasmic and nuclear proteins were isolated using the NE-PER® Nuclear and Cytoplasmic Extraction Reagents kit (Pierce, Rockford) following the manufacturer's instructions. Briefly, harvested cell pellet was resuspended in iced-cold cytoplasmic extraction reagent (CER) I, vortexed vigorously for 15 seconds and incubated on ice for 10 minutes. Ice-cold CER II were added followed by additional

5 second vortex. After centrifugation at maximum speed (~16,000 x g), supernatant (cytoplasmic extract) was transferred to a separate tube. Then, the pellet was resuspended in ice-cold nuclear extraction reagent (NER) followed by 15 second vortexing for four times every 10 minutes. After centrifugation, the supernatant (nuclear extract) fraction was transferred to a separate tube. The extracts were then fractionated by SDS-PAGE and transferred to Immobilon protein membrane (Millipore). The membranes were incubated successively with the primary and the secondary antibodies,and exposed to the chemiluminescence reagent (Amersham) for signal detection. We used the following primary antibodies for our study: Orai1 (AB9868; EMD Millipore), NFATc3 (sc-8405; Santa Cruz Biotech), NFATc1 (8032S; Cell Signaling Tech), Lamin B1 (sc-20682; Santa Cruz Biotech), α-tubulin (T9026; Sigma) and GAPDH (FL-335; Santa Cruz Biotech).

2.3 Immunohistochemistry

Tissue specimens that were previously collected for diagnostic purposes were obtained from the Oral Pathology Diagnostic Laboratory at the UCLA School of Dentistry. All tissue specimens were collected and processed according to the guidelines of the University of California at Los Angeles Institutional Review Board. Immunohistochemical staining was performed as described previously (Shin et al., 2011). Briefly, four to five-micrometer tissue sections were cut from the block and deparaffinized in an oven at 60°C for 30 minutes followed by rehydration in xylenes twice and a graded series of ethanol three times. Antigen was retrieved using citrated buffer in a pressure cooker for 20 minutes. The endogenous peroxidase activity was quenched with 3% solution of H_2O_2 for 15 minutes and washed in the running water to wash off the peroxide residues. After incubation with 1X PBST for 5 minutes, tissues samples were

blocked with 10% serum for 30 minutes and incubated with antibodies at 1:100 overnight in humid chamber. The optimal concentration (1:100) of Orai1 antibody (AB9868; EMD Millipore) was first established using serially diluted primary antibody along with IgG as a negative control. In the following day, the tissue samples were washed with 1X PBST 5 minutes for three times, and the secondary antibody was incubated for 1 hour followed by 30 minutes incubation with HRP. After another three times of washing using 1X PBST, tissues were then developed with the 3,3'-diaminobenzidine (DAB) chromogen substrate for 3–4 minutes. Two independent examiners scored the immunohistochemical expression of Orai1 protein. The level of Orai1 staining pattern was scored into four subgroups: (1) weak; (2) moderate; and (3) strong (+++); (4) very strong. Representative images were taken at 50X and 150X.

2.4 Confocal laser scanning microscopy

Five thousand cells were seeded on the 4 chamber slides (Thermo Fisher Scientific) one day prior to the immunofluorescence staining. After cell permeabilization using TNT buffer containing 20mM Tris-HCl pH.7.4, 150mM NaCl, and 0.5% Triton-X 100, cells were blocked with TNT buffer with 3% Bovine Serum Albumin (BSA) for 30 minutes at room temperature. Then, cells were probed with NFATc3 primary antibody in 1X PBS supplemented with 3% goat serum overnight, then with Alexa Fluor 594 dye-conjugated secondary antibody and DAPI (blue-green) for confocal laser scanning. Confocal laser scanning microscopy was performed using Fluoview FV10i Confocal Microscope (Olympus), and images were captured with 60x oil objective under different gain settings. The laser diode 559 nm was used to capture NFATc3 staining, and the diode 405 nm laser was used to capture DAPI nuclear stain. Image acquisition and further adjustment of brightness was performed using Olympus Fluoview Ver.

4.2a. Fluorescent images of cells were taken as single channel images then converted to overlay images and all images were saved in TIFF format.

2.5 Ectopic expression of dominant negative Orai1 E106Q mutant and wild-type Orai1

The retroviral pMSCV-CITE-eGFP-Puro vectors encoding ORAI1^{WT} and ORAI1^{E106Q} (Gwack et al., 2007) were used to prepare viruses as described previously (Kim et al., 2010). Briefly, for retroviral expression plasmids encoding human Orai proteins, Orai1 cDNAs with FLAG epitope tags introduced at the C terminus were cloned between the XhoI and EcoRI sites of pMSCV-CITE-eGFP-PGK-Puro. The endogenous termination codon was substituted with the coding sequence of the FLAG tag (AADYKDDDDK) followed by a TAG termination codon. For mutagenesis of Orai1, the QuikChange site-directed mutagenesis kit (Life Technologies) was used according to the manufacturer's instructions. These vectors were transfected into GP2-293 universal packaging cells (Clonetech, Mountain View, CA, USA). First vector master mix was prepared by mixing the vectors with pVSV-G envelope plasmid and pCMV-dR8.9 packaging plasmid with Opti-MEM medium (Life Technologies) in a tube, and Opti-MEM with lipofectamine 2000 (Life Technologies) were mixed together in another tube. After 5 minutes of incubation, two tubes are mixed together and incubated for 20 minutes in room temperature. Complete mixtures were added to the cells gently in dropwise. Additional 4 ml of pre-warmed Opti-MEM is added to the culture plate after 3 hours of incubation. Next day, viral soup was collected and centrifuged under 20,000rm for 90 minutes to collect the viral pellet. Then, the vial pellets were incubated in 1 ml of the serum and antibiotics free cell culture medium overnight. Cells were then infected with 300ul of viral soup in 1.2ml of pre-warmed culture medium for 3 hours. Infected cells were selected with 0.5μg/ml puromycin for two weeks and used for

experiments. The GFP fluorescence was used to check the efficiency of viral infection and selection.

2.6 SOCE assay (Single-cell Ca^{2+} imaging)

Cells were plated on UV-sterilized coverslips using poly-L-lysine one day prior to imaging. Next day, cells were loaded with 1 mM Fura 2-AM for 45 min at 25^{o}C. Intracellular $[Ca^{2+}]_i$ measurements were performed using essentially the same methods as previously described (Kim et al., 2011). Briefly, cells were mounted in an RC-20 closed bath flow chamber (Warner Instrument Corp., Hamden, CT, USA) and analyzed on an Olympus IX51 epifluorescence microscope (Olympus, Center Valley, PA, USA) with SlideBook (Intelligent Imaging Innovations Inc., Denver, CO, USA) imaging software. Cells were perfused with Ca^{2+}-free Ringer solution, and Ca^{2+} stores were passively depleted with 1 μM thapsigargin. Fura-2 emission was detected at 510 nm with excitation at 340 and 380 nm, and the Fura-2 emission ratio (340/380) was acquired at every 5-s interval after subtraction of the background. For each experiment, 50 to 100 individual cells were analyzed using OriginPro (OriginLab Corp., Northampton, MA, USA) analysis software. Acquisition and image analysis including measurement of the Pearson correlation coefficient was performed using SlideBook (Intelligent Imaging Innovations Inc.) software, and graphs were plotted using OriginPro 8.5 (OriginLab Corp.).

2.7 Anchorage-independent growth

To determine colony-forming efficiency in semi-solid medium, 1 x 10^4 cells were plated in culture medium, DMEM/F12, containing 0.3% agarose over a base layer of serum-free medium

containing 0.5% agarose. Briefly, bottom agarose gel is prepared by mixing 0.15g of Agar Noble (DIFCO) with the 45ml DMEM/F12 followed by melting by microwave. As soon as the gel solution cools to 50˚C, 5ml of FBS were added, and 4ml of the bottom gel solution is poured into 60mm dish. Top agarose gel is prepared in the same manner but with 0.5% agarose, and the agarose gel solution was kept in tubes in a 37 ˚C until cells were ready. Once cells are ready, cells and top agarose gel solution is mixed together and transferred on top of the bottom agarose gel. The cultures were incubated with 95% air, 5% CO_2 and 100% humidity at 37°C. Next day, 1ml of the culture medium was added to each well in order to prevent the dry and keep the humidity. After three weeks of incubation in the incubator, colonies were counted using the light microscope. The experiment was performed in triplicate with 60mm dishes. The assay was performed as described previously (Lee et al., 2012a).

2.8 *In vivo* xenograft tumor assay

Each cell lines were grown to confluency in 100mm dishes to subcutaneously inject ten million cells into the flank of five immunocompromised mice (strain nu/nu, Charles River Laboratories). After counting cells, cell pellets were resuspended in 1.2ml of serum free culture medium, the volume enough for injecting six mice. Cell suspension, 0.5cc syringes and other equipment for the procedure were taken down to the vivarium in a sterile secondary container. Five mice were anesthetized with inhalant isoflurane inside the fume hood, and each cell lines were injected into the flank regions in sterile condition. Upon completion of the injection, mice were laid on the heat pad until they become conscious. The kinetics of tumor growth was determined by measuring the volume in three perpendicular axes of the nodules using micro-scaled calipers. After six weeks of incubation, tumors were excised for histological validation by

hematoxylin and eosin (H&E) staining. The animal study was performed according to the protocol approved by UCLA Animal Research Committee.

2.9 Tumor sphere formation assay

Three thousand cells were prepared from the monolayer culture grown in 100mm dish. Then, cells were directly added to tubes which contains 3 ml of conditioned medium to grow self-renewing cells. Conditioned medium consisted of serum-free DMEM/F12 media supplemented with 1:50 B27 (Life Technologies), 20 ng/mL EGF, 20 ng/mL, 10μg/mL insulin, penicillin, streptomycin, and amphotericin B. Cells were transferred to the Ultra-Low Attachment 6-well Plates (Corning) to grow cells in suspension for 6-10 days (Lee et al., 2012a). Additional 1ml of medium was added every 5 days in order to prevent the medium evaporation. After incubation in 95% air, 5% CO_2 and 100% humidity at 37°C, the number of cells grown in spheres are counted, and photographs were taken under the light microscope. The experiment was done in triplicates.

2.10 Quantitative real-time PCR (qPCR)

RNA isolation was done using TriZol (Life Technologies). Briefly, 1ml of TriZol was added to the cells grown on 100mm dish. Then, 0.2 ml of chloroform was added to the solution, vortexed for 60 seconds, and incubated at room temperature for 10 minutes. After centrifugation at 12,000 rpm for 15 minutes, supernatant was mixed with 0.5ml of isopropyl alcohol and incubated for additional 10 minutes. Following the second round of centrifugation, the RNA pellets were washed twice with 70% ethanol, air dried and resuspended in RNase-free water. To synthesize cDNA, 5ug of total RNA was mixed with Random Primer (Life Technologies) and dNTP (Promega) in the PCR microtubes and incubated at 65˚C for 5 minutes. Then, RNA

samples were chilled on ice to add reverse transcriptase mixture containing SuperScript first-strand synthesis system (Life Technologies), 0.1M DTT and 5X buffer. Complete mixture was incubated at 25°C for 12 minutes, 42°C for 50 minutes and 70°C for 15 minutes to complete the synthesis. We used 1 µl cDNA for quantitative PCR amplification using SYBR Green I Master mix (Roche) and LightCycler 480 II (Roche). The primer sequences were obtained from the Universal Probe Library (Roche). The quantitative PCR cycle conditions were 1 cycle of 10 minute pre-incubation at 95°C and 55 cycles of 10s at 95°C, 45s at 55°C and 10s at 72°C. Second derivative Cq value determination method was used to compare fold-differences according to the manufacturer's instructions.

2.11 ALDH1 assay

Using Aldehyde Dehydrogenase-Based Cell Detction Kit (STEMCELL), ALDH enzymatic activity was determined. Total of 1 x10^6 cells were re-suspended in the ALDEFLUOR Assay Buffer in the volume of 1ml. Fluorescent nontoxic ALDEFLUOR Reagent BODIPY^{TM} (1.25µl) was added as a substrate to measure ALDH enzymatic activity in intact cells. Immediately after adding the substrate reagent, 0.5ml of the cell suspension was transferred into the control tube which contains specific inhibitor for ALDH, diethylaminobenzaldehyde (DEAB) for calculating background fluorescence. Then, cells were incubated at 35˚C for 30 minutes and fluorescence data acquisition was made by using a BD FACScan flow cytometer (BD Biosciences).

2.12 Migration and invasion assays

Cell migration was measured using transwell chambers with polycarbonate membranes (Corning) as described in our previous publication (Chen et al., 2016; Lee et al., 2012a). Briefly,

1 x10^4 cells were resuspended in serum-free culture medium were seeded in the upper chamber of 24-well transwell inserts with 8 μm pores (Corning, NY). The bottom chambers were filled with the culture medium (DMEM/F12 with 1% FBS). After 96 hours, non-migrated cells on the upper surface of the chamber were mechanically removed with a cotton, and the migrated cells on the lower surface of chamber were fixed with formalin and stained with 1% crystal violet, and photographs were taken using the light microscope at 20X and 50X. For quantification of migrated cells, three different random areas were chosen from the photographed images of the whole transwell to count cells, and average cell number from three areas were calculated. All experiments were done in triplicate.

2.13 siRNA-mediated gene knockdown

Orai1and NFATc3 were knocked down by duplex corresponding siRNAs or the control, scrambled siRNA (Santa Cruz Biotech), which was introduced using Lipofectamine RNAiMAX (Invitrogen). Cells (2 x 10^5) were plated in 60-mm dishes one day prior to the transfection with siRNA. On the day of transfection, 500 μl of transfection solution was made by adding 20 μl of 10 μM siRNA, 10ul of Lipofectamin RNAiMAX, and 470 μl of antibiotics-free and serum-free DMEM/F12 and was incubated in the room temperature for 5 minutes. Meanwhile, old cell medium was aspirated from the dish and changed to fresh complete culture medium. Then, 500 μl of the transfection solution was added to the dish and incubated overnight. Next day, medium was changed to fresh culture medium next day. The cultures were harvested after two-day post-transfection for expression and functional analyses.

2.14 Laser-captured microdissection

Epithelial layers from the paraffin-embedded dysplastic and oral cancer tissue samples were excised by laser-captured microdissection (LCM) using Leica (LMD) 7000 system (Leica Microsystems Inc, Richmond, IL) at the California NanoSystems Institute at UCLA (Los Angeles, CA). RNAs from LCM-derived tissue were extracted using a high pure RNA paraffin kit (Roche). RT was performed with RNA isolated from the tissue sections using a SuperScript first-strand synthesis system (Life Technologies) with random primers (Life Technologies) according to the manufacturer's instructions. Transcript expression was analyzed by quantitative PCR with the LightCycler® 480 system (Roche). All experiments were repeated in triplicate.

2.15 Determination of cytokine rescue effect in Orai1-inhibited OSCC

Rescue effect of cytokine on self-renewal in Orai1-inhibited OSCC was determined by growing SCC4/EV control and SCC4/E106Q cells in tumor sphere medium with IL4 (204-IL-010; R&D) and CCL3 (270-LD-010/CF; R&D). 5000 cells were seeded in the Ultra-Low Attachment 6-well Plates (Corning) in triplicate with 10ng/ml of IL4 and CCL3 recombinant protein and were cultured for 6 days. Non-treated cells were used as the controls. After incubation in 95% air, 5% CO_2 and 100% humidity at 37°C, the number of cells grown in spheres are counted, and photographs were taken under the light microscope. The effect of cytokines on cell migration in Orai1-inhibited OSCC was also determined by examining the effect of either IL4 and CCL3 treatment on cell migration in SCC4/EV control and SCC4/E106Q cells. 10ng/ml of IL4 and CCL3 recombinant proteins were added to the bottom chamber containing DMEM/F12 supplemented with 1% FBS. Then, 1 x10^4 cells were seeded on the top

chamber in DMEM/F12 without FBS. After 96 hours, non-migrated cells on the upper surface of the chamber were mechanically removed with a cotton, and the migrated cells on the lower surface of chamber were fixed with formalin and stained with 1% crystal violet, and photographs were taken using the light microscope at 50X. For quantification of migrated cells, three different random areas were chosen from the photographed images of the whole transwell to count cells, and average cell number from three areas were calculated. All experiments were done in triplicate.

3. The role of Orai1 in OSCC progression

3.1 Status of Orai1 expression during oral carcinogenesis

To investigate the role of Orai1 in oral/oropharyngeal carcinogenesis, we first determined the expression level of Orai1 protein in normal human oral keratinocytes (NHOK), non-tumorigenic immortalized oral epithelial cell lines (NOK-SI, OKF6/tert, and HOK-16B), and OSCC cell lines (HOK-16B-BapT, SCC4, SCC15, SCC1, SNU1041, YD9, YD15M, UM17B, SNU1076 and SCC9/TNF) by western blot analysis. All of the OSCC cell lines expressed higher level of Orai1 protein compared to the tested immoralized cell lines (**Figure 1A**). All immoralized cell lines showed higher expression of Orai1 protein compared to NHOK (**Figure 1A**). Our findings suggested a stepwise increase of Orai1 expression during oral/oropharyngeal carcinogenesis. To extend our findings, immunohistochemical (IHC) staining for Orai1 was performed using normal human oral epithelia (NHOE), oral dysplasia, and OSCC tissues. The results of *in vivo* Orai1 staining are summarized in **Figure 1B**, and a typical Orai1 staining observation in NHOE, dysplasia and OSCC tissue is shown in **Figure 1C**. In 13 NHOE, weak Orai1 staining was detected in 11 cases (84.6%), and moderate staining detected in 2 cases (15.4%). Of 15 dysplastic tissues, weak staining was detected in 2 cases (13.3%), moderate staining detected in 8 cases (53.3%), and strong staining detected in 5 cases (33.3%). In 19 OSCC samples, 16 cases (84.2%) demonstrated strong staining and 3 cases (15.8%) with very strong staining. Mean IHC scores for Orai1 in NHOE, dysplasia, and OSCC were 1.15, 2.2, and 3.16, respectively, showing statistical significant difference ($P<0.0001$ between NHOE and dysplasia; $P<0.0001$ between dysplasia and OSCC). Using laser capture microdissection (LCM), we determined the level of Orai1 mRNA in dysplasia and OSCC tissues and found that Orai1 mRNA is also increased in OSCC compared to dysplastic tissues (**Figure 1D**). Taken together,

our findings clearly indicate a stepwise elevation of Orai1 protein during oral/oropharyngeal carcinogenesis, suggesting an important role of Orai1 in the progression of OSCC.

3.2 Effect of Orai1 inhibition on tumorigenic potential of OSCC

Many studies reported the efficacy of targeting Orai1to suppress cancer growth (Flourakis et al., 2010; Kim et al., 2014a; Liu et al., 2011; Yang et al., 2009a; Zhu et al., 2014b). A point mutation in the negatively charged residues of Orai1 is known to function as a dominant negative mutant (Gwack et al., 2007). To investigate the role of Orai1 in OSCC growth, we inhibited Orai1 using a dominant negative Orai1 mutant (E106Q). SCC4, a human tongue squamous carcinoma cell line, was infected with retroviral vector expressing E106Q or empty vector (EV) as a control. As shown in Figure 2A, treatment of SCC4/EV with 1 μM thapsigargin (TG), an ER Ca^{2+}-ATPase inhibitor, resulted in a rapid rise in intracellular Ca^{2+} level, consistent with depletion of ER Ca^{2+} stores. Subsequent addition of Ca^{2+} to the extracellular bath solution triggered another increase in the Ca^{2+} level, consistent with Ca^{2+} influx from the extracellular solution. However, SCC4/E106Q failed to show the increase in Ca^{2+} influx. Our finding indicated that E106Q successfully impaired Orai1-mediated SOCE in OSCC cells, confirming the inactivation of Orai1 (**Figure 2A**). E106Q slightly lowered proliferation capacity of SCC4 (**Figure 2B**).

Effect of Orai1 inactivation on tumorigenic potential of OSCC was then evaluated using *in vitro* anchorage independent growth and *in vivo* tumor xenograft assay. E106Q significantly reduced formation of colonies in soft agar suggesting decreased anchorage independent growth ability by Orai1 inactivation (**Figure 2C**). As demonstrated by xenograft tumor assay in nude mice, 3 out of 5 animals inoculated with SCC4/EV formed tumors, whereas the animals

inoculated with SCC4/E106Q failed to form tumor *in vivo* (**Figure 2D**). These findings indicate that Orai1 is required for tumorigenicity of OSCC.

3.3 Effect of Orai1 inhibition on oral CSCs

A key feature of CSCs is self-renewal capacity, which appears to be a driving force for the initiation and maintenance of tumorigenicity (Beck and Blanpain, 2013b). Our data revealed the crucial role of Orai1 function in tumorigenicity of OSCC. To determine the role of Orai1 on CSC phenotype of OSCC, we first employed tumor sphere formation assay in which CSCs can be enriched in non-adherent tumor spheres (Wang et al., 2011). Thus, abundance and the growth kinetics of tumor spheres are indicative of CSC content and self-renewal capacity in a given culture of heterogeneous cancer cells. We determined the effect of E106Q on self-renewal capacity of two OSCC cell lines, SCC4 and HOK-16B BapT. Tumor sphere formation assay revealed that E106Q significantly inhibits the tumor sphere forming ability of both cell lines (**Figure 3A and 3B**), indicating that Orai1 is indeed essential for sustaining self-renewal capacity of CSCs. ALDH1 activity is one of CSC markers and known to enrich CSCs in solid malignancies, including head and neck cancer (Monroe et al., 2011). Thus, we investigated whether Orai1 inhibition could affect CSC property by performing ALDH1 assay. The assay revealed a significant decrease in ALDH1 activity in SCC4/E106Q compared to their control SCC4/EV (**Figure 3C**). Because another well-known property of CSCs is their metastatic potential (Beck and Blanpain, 2013b), we examined the effect of Orai1inhibiton on metastatic potential of OSCC *in vitro*. As demonstrated by a transwell migration assay (**Figure 3D**), E106Q markedly suppressed migration of SCC4 cells. We also found a significant inhibitory effect of E106Q on invasion ability using Matrigel invasion assay (**Figure 3E**). This is consistent

observation reported by other (Yang et al., 2013; Yang et al., 2009a). To extend these observations, we determined whether a chemical inhibitor of Orai1 also suppresses CSC phenotype. We treated OSCC cells with non-cytotoxic dose of the Orai1-specific small molecular blocker, *compound 5D* (Kim et al., 2014b) (**Figure 4A**), and found that the Orai1 inhibitor dramatically inhibited tumor sphere forming ability (**Figure 4B**), secondary sphere forming ability (**Figure 4C**). Also, *compound 5D* significantly suppressed AlDH1 activity (**Figure 4D**) and migration (**Figure 4E**) at the dose of 15 μM. We observed no significant effect of compound 5D on cell proliferation at the same dose, indicating that the inhibitory effect of compound 5D on CSC phenotype was unlikely an artifact of slower cell proliferation and a cytotoxic effect of the chemical. Similar to the effects of E106Q and compound 5D on CSC phenotype, successful Orai1 knockdown (**Figure 4F**) reduced self-renewal and migration ability of SCC4 (**Figure 4G and 4H**).

3.4 Orai1 overexpression in CSC-enriched oral cancer population

To further examine the importance of Orai1 in CSC, we compared Orai1 expression of CSC-enriched populations with that of non-CSC populations. Orai1 expression is highly enriched in tumor spheres compared with their corresponding adherent monolayer cells (**Figure 5A and 5B**). Similarly, stemness transcription factors, Nanog, Oct4, KLF4, Lin28, and Sox2 were enriched in tumor spheres (**Figure 5A**). We also observed robust induction of CSC marker, ALDH1, in tumor spheres (**Figure 5A**), confirming that tumor spheres are CSC-enriched cell population. Furthermore, we sorted the $ALDH1^{HIGH}$ and $ALDH1^{LOW}$ cell populations from SCC4 according to ALDH1 activity (**Figure 5C**) and examined Orai1 expression in these two cell populations. The $ALDH1^{HIGH}$ population expressed higher Orai1 protein than the $ALDH1^{LOW}$ population

(**Figure 5D**). Overall, our data clearly indicate that Orai1 is enriched in CSC and essential for maintenance of CSC phenotype in OSCC.

3.5 Effect of Orai1 on tumorigenic potential in non-tumorigenic oral epithelial cells

Having established that increased Orai1 is associated with OSCC progression and is necessary for CSC phenotype, we next examined whether ectopic Orai1 expression confers tumorigenic capacity and CSC phenotype on non-tumorigenic immortalized oral epithelial cells. As shown in **Figure 6A**, we overexpressed Orai1 in non-tumorigenic immortalized oral epithelial cells, HOK-16B, using the lentiviral vector expressing Orai1 or empty vector (EV) as a control. Orai1 overexpression was also confirmed by immunohistochemistry for Orai1. We first examined the effect of Orai1 on cell proliferation and found that Orai1 overexpression led to robust increase in proliferation capacity of HOK-16B *in vitro* (**Figure 6B**). To further examine the effect of Orai1 on tumor growth *in vivo*, we injected the cells into nude mice and observed tumor formation. Three out of 5 mice injected with HOK-16B/Orai1 developed tumor, whereas, as expected, the mice injected with HOK-16B/EV failed to form tumor (**Figure 6C**). Histological examination of tumors grown in mice injected with HOK-16B/Orai1 revealed the presence of malignant cells, with hyperchromatic nuclei, prominent nucleoli, and active mitosis (**Figure 6D**), indicating that Orai1 conferred tumorigenicity to the non-tumorigenic cells.

3.6 Effect of Orai1 overexpression on non-tumorigenic oral epithelial cells

Next, we investigated the effect of Orai1 on CSC phenotype in HOK-16B. Ectopic Orai1 expression resulted in robust induction in tumor sphere formation, indicating the acquisition of

self-renewal capacity by Orai1 (**Figure 7A**). The flow analysis revealed a significant increase in ALDH1+ cell population in HOK-16B/Orai1 compared to HOK-16B/EV (13.1% vs. 1.4%; **Figure 7B**). As demonstrated by a transwell migration assay (**Figure 7C**), HOK-16B/Orai1 migrated significantly faster than HOK-16B/EV. The effect of Orai1 on CSC phenotype was further validated by qPCR analysis of stemness transcription factors and CSC-related genes (**Figure 7D**). Orai1 increased stemness transcription factors (*i.e., Nanog*, *Oct4, Sox2, KLF4, and Myc) and CSC-related genes (i.e.*, *Ezh2, Gli1, Hes1, Zeb2, FGF4, and IL4)*. Our findings indicate that Orai1 indeed conferred CSC phenotype on the non-tumorigenic oral epithelial cells. We then determined the effect of *compound 5D* on self-renewal and cell migration on HOK-16B cells. Treatment of non-cytotoxic *compound 5D* (**Figure 8A**) significantly suppressed Orai1-induced self-renewal (**Figure 8B**) and cell migration (**Figure 8C**), which further confirms the importance of Orai1 in CSC phenotype acquisition in HOK-16B cell.

3.7 Status of NFAT signaling for Orai1-induced CSC phenotype

It is well documented that Orai1-mediated SOCE activates downstream responses including NFAT signaling pathway (Parekh, 2007; Parekh and Putney, 2005). Emerging evidence has suggested that NFAT signaling plays an important role in tumorigenesis (Mancini and Toker, 2009a). Thus, we investigated whether Orai1 promotes CSC phenotype through NFAT signaling pathway. We treated HOK-16B/Orai1 with the NFAT antagonist, cyclosporine A (CsA) (Martinez-Martinez and Redondo, 2004), and subsequently performed the assays for CSC properties. NFAT inhibitor significantly inhibited self-renewal (**Figure 9A**) and migration (**Figure 9B**) of HOK-16B/Orai1. With minimal effect of CsA on cell viability (**Figure 9C**), it

also suppressed self-renewal and migration in OSCC cells (**Figure 9D and 9E**). Our data indicate that NFAF signaling is required for Orai1-induced CSC phenotype.

3.8 Effect of Orai1 on NFATc3

Four isoforms of NFAT, NFATc1, NFATc2, NFATc3, and NFATc4, were identified (Daniel et al., 2014). To determine which of the NFAT isoforms are involved in Orai1-induced CSC phenotype, we first examined the expressions of the isoforms in HOK-16B/EV and HOK-16B/Orai1. Among these four members, we found that NFATc3 was the dominant isoform and increased by Orai1 in HOK-16B (**Figure 10A**). We also found that NFATc3 is the dominant isoform in various OSCC cell lines (data not shown). Notably, NFATc3 was primary found in the cytoplasm of HOK-16B/EV but accumulated in the nucleus of HOK-16B/Orai1 (**Figure 10B and 10C**), indicative of NFATc3 activation by Orai1(Mancini and Toker, 2009a).

3.9 Function of NFATc3 in Orai1-induced CSC phenotypes

To further assess the functional role of NFATc3 in Orai1-induced CSC phenotype, we knocked down NFATc3 using siRNA in HOK-16B/Orai1 (**Figure 11A**). Knockdown of NFATc3 showed significant suppressive effect on tumor sphere formation (**Figure 11B**) and migration (**Figure 11C**) in HOK-16B/Orai1 cells. Furthermore, treatment CsA reduced self-renewal (**Figure 11E**) and cell migration in HOK-16B (**Figure 11F**) without severely affecting cell viability (**Figure 11D**). We also demonstrated that silencing of NFATc3 (**Figure 12A**) resulted in significant suppression of tumor sphere formation and migration ability in OSCC cells (**Figure 12B and Figure 12C)**. Orai1 knockdown and treatment of compound 5D

suppressed NFATc3 expression, indicating that revealed that NFATc3 is regulated by Orai1 (**Figure 12D**). Our findings indicate that Orai1 promotes CSC phenotype through NFATc3, suggesting the role of Orai1/NFAT axis in CSC regulation

3.10 Global human transcription profile upregulated by Orai1

To further study the mechanism by which Orai1 regulates CSC phenotypes, we decided to conduct a microarray of human genome to investigate the genes regulated as the result of Orai1 overexpression using HOK-16B/EV and HOK-16B/Orai1 cells. Analysis of raw microarray data using strict fold change limit of 2-folds or higher, we have found significant upregulation of immunity-related genes expression. Analysis of genes revealed that out of 279 canonical pathways regulated by Orai1 overexpression in HOK-16B, 79 immunity-related signaling pathways were significantly upregulated. (**Figure 13**) These signaling pathways include cytokine and chemokine signaling, T cell and B cell activation and differentiation, and immune cell communication (**Figure 14**).

3.11 Identification of cytokines regulated by Orai1/NFATc3 axis

Cytokines are demonstrated to regulate CSCs, *i.e.*, self-renewal, drug resistance and tumorigenicity, in different cancer types, including oral cancer (Lee et al., 2012; Lee et al. 2016). To validate the significant change in cytokine and chemokines genes expression from the microarray data, cytokines and chemokine genes expression were determined using qPCR. Among the 25 cytokine genes tested, 14 cytokine genes, *i.e.*, *IL1α, IL1β, IL4, IL5, IL6, IL8, IL15, IL17, IL36RN, CCL3, RANTES, TNFα, and VEGF*, were upregulated by Orai1 in HOK-16B

compared to the EV control, suggesting that they are Orai1-induced cytokines (**Figure 15A**). To further investigate cytokines regulated in Orai1-NFATc3 axis, we then performed qPCR to determine the effect of NFATc3 knockdown on the 14 Orai1-induced cytokines in HOK-16B/Orai1. Out of 14 Orai1-induced cytokines, 9 were downregulated by NFATc3 knockdown (**Figure 15B and Figure 16A**) .We also examined whether these 9 cytokine were regulated by NFAT activation, OSCC cells were treated with NFAT activator, PMA/Ionomycin, and/or NFAT inhibitor, CsA. When the cells were stimulated by NFAT activator, expression level of 5 cytokines, *i.e*., *IL4, IL5, CCL3, RANTES and VEGF*, increased significantly, and CsA treatment reverted the induction significantly (**Figure 16B**), indicating downstream cytokines of Orai1-NFATc3 axis,

3.12 Role of the Orai1/NFATc3 cytokines in CSC phenotypes

To investigate the role of the Orai1/NFATc3 cytokines in oral CSCs, we first determine the expression of 5 Orai1/NFTc3 cytokines in CSC-enriched OSCC. As demonstrated earlier (**Figure 5**), we used tumor sphere assay and ALDH1 assay to isolate CSC-enriched OSCC. Among the 5 cytokines, *IL4* and *CCL3* were commonly upregulated significantly both in SCC4/Sphere compared to SCC4 adherent monolayer (**Figure 17A**) and $ALDH1^{high}$ cells compared to $ALDH1^{low}$ cells (**Figure 17B**).

Next, to determine the role of IL4 and CCL3 in regulating Orai1-dependent CSC phenotypes, we tested the effect of each cytokine on self-renewal in Orai1 inhibited OSCC, SCC4/E106Q. As expected, SCC4/E106Q showed suppression of self-renewal compared to the EV control, but subsequent addition of IL4 and CCL3 resulted in rescue of self-renewal comparable to the EV control (**Figure 18A**). To further investigate if these cytokines are

required for the CSC phenotype regulated by Orai1, we tested the rescue effect of cytokines on cell migration in Orai1-inhibited OSCC. Again, SCC4/E106Q showed dramatic suppression of cell migration compared to the EV control. Addition of CCL3 partially rescued suppressed cell migration in SCC4/E106Q, but addition of IL4 did not have any effect (**Figure 18B**). These data indicate the role of IL4 and CCL3 in regulating different CSC phenotypes and possible involvement of other Orai1 target genes in CSC regulation.

3.13 Role of Orai1-induced stem cell and cancer/metastasis markers

Along with upregulation of cytokine genes, stem cell and cancer/metastasis genes were also upregulated. Gene ontology analysis of genes upregulated 2 folds or higher also revealed that 22 stem cell pathways and 24 cancer/metastasis pathways out of 275 pathways were upregulated by Orai1 in HOK-16B cells (**Figure 19A**). Validation of 15 out of 22 genes in these pathways showed significant induction, *i.e.*, *ALSH1A3, CPT1A, ID1, ID2, AKAP12, COL12A1, DLX2, DLX6, DPP4, FABP4, MAF, LOX2, LOXL2, SERPINB1*, and *SEMA3A*. To identify Orai1-induced stem cell and cancer/metastasis-related genes regulated by NFAT, we determined the effect of NFATc3 knockdown on these genes expression. Out of 15 genes, 4 genes were significantly downregulated by NFATc3 knockdown (**Figure 19B**), indicating that these genes are regulated by Orai1-NFATc3 axis.

DISCUSSION

In this study, we demonstrate for the first time that Orai1 is a novel molecular regulator of tumorigenicity and stemness of OSCC. Orai1 expression is elevated in a stepwise manner during oral/oropharyngeal carcinogenesis and enriched in CSC populations. Ectopic Orai1 expression confers *in vivo* tumorigenic capacity and CSC phenotype on non-tumorigenic immortalized oral epithelial cells. Moreover, inhibition of Orai1 suppresses tumorigenicity and CSC phenotype in OSCC. We also provide the evidence that Orai1 enhances CSC phenotype through NFAT signaling, indicating the importance of Orai1/NFAT axis in oral CSC. Therefore, our study highlights the functional significance of Orai1 signaling in malignant progression of OSCC by enriching cancer stemness.

Emerging role of Orai1 in human cancer has been reported. Upregulation of Orai1 expression was observed in various human cancers, including esophageal cancer (Zhu et al., 2014b). A high expression of Orai1 protein is also strongly linked to poor prognosis and aggressive behavior of human cancers. However, no information is available regarding Orai1 expression during oral/oropharyngeal carcinogenesis. Our results showed that Orai1 is highly expressed in OSCC compared to precancerous and normal tissues *in vivo*. Moreover, precancerous oral epithelial cells express higher Orai1 protein than normal oral epithelial cells, suggesting that Orai1 plays an important role in cancer progression. To our knowledge, our finding is the first report showing a stepwise elevation of Orai1 in multistep carcinogenesis *in vivo* and further oncogenic transformation of immortalized cells by Orai1 overexpression. Consistent with previous observation (Zhu et al., 2014b), our immunohistochemistry study confirmed localization of Orai1 in the plasma membrane. We also observed diffused staining of Orai1 in both the cytoplasm and nucleus. Since the tissue sections were obtained from 3 dimensional tissue structures, there

could be some overlap with another cell layer positioned in different orientation compared to monolayer-cultured cells. Indeed, we were able to detect predominant Orai1 staining to the plasma membrane in the monolayer-cultured cells of HOK-16B/Orai1. Our study clearly demonstrated that Orai1 is required for tumorigenicity of OSCC *in vivo*. Inactivation of Orai1 by the dominant negative Orai1 mutant not only suppressed SOCE, but also abolished *in vivo* tumorigenic potential of OSCC. Conversely, ectopic Orai1 expression further transformed non-tumorigenic oral epithelial cells to tumorigenic cells. This finding is consistent with the results of a previous study reporting that Orai1 inhibition led to significant decreases in cancer growth *in vivo* and *in vitro* (Kim et al., 2014a; Liu et al., 2011; Zhu et al., 2014b). Our findings support the hypothesis that Orai1 is a novel molecular determinant of oral/oropharyngeal cancer progression.

Self-renewal is the critical characteristic by which CSCs regenerate themselves, suggesting the driving force of tumorigenesis. CSCs are viewed as the seed of cancer and hence as effective target of anti-cancer therapies. Therefore, findings from our studies are of paramount important for the development of more effective cancer therapies. By phenotypic and functional analysis, we demonstrate that Orai1 is an important regulator of CSC phenotype in OSCC. Orai1 is highly expressed in CSC-enriched cell populations, such as tumor spheres and $ALDH1^{HIGH}$ population of OSCC. Furthermore, Orai1 endowed non-tumorigenic immortalized oral epithelial cells with self-renewal and concomitantly increased stemness transcription factors, *i.e.*, Nanog, Oct4, Sox2, KLF4, and Myc.

These stemness factors, especially Nanog, Oct4 and Sox2, serve as the key pluripotency transcriptional factor, which dictates formation of embryo. Octamer 3/4 (Oct4), a member of the POU family, is known as an essential transcription factor during human embryogenesis thus is considered important stem cell marker (Lee et al., 2006). Recently, there have also been reports

about the presence of Oct 4 in benign and malignant human cancer cells which serves to enhance cancer stemness and cancer progression (Tai et al., 2005). Sox2 is a member of the Sox (SRY-Related HMG box) gene family that serves as the transcriptional factors with a single HMG DNA-binding domain. Sox2 is another well-known embryonic stem cell marker and is considered to function important role in the formation of early pluripotent embryonic cells. Also, Sox2 sustains stemness of the neural progenitor cells by prohibiting the differentiation (Bani-Yaghoub et al., 2006). Nanog is known to function in conjunction with Oct4 and Sox2 to form embryonic stem cells and maintain their self-renewal during embryogenesis (Chambers et al., 2003; Pan and Thomson, 2007). Oct4, Sox2, and Nanog is also aberrantly expressed in several cancers such as breast, colon, lung and oral cancer cells, and they serves important function tumorigenesis and metastasis (Schoenhals et al., 2009)((Ezeh et al., 2005). These evidences support the role of Orai1 in conferring tumorigenic potential in non-tumorigenic oral epithelial cells in our study.

Orai1 also promoted other CSC properties, ALDH1 activity and migration. Ectopic Orai1 expression markedly increases ALDH1+ cell population in the non-tumorigenic oral epithelial cells. ALDH1 has been found to be a marker for stem cells in different types of cancer, including OSCC (Clay et al., 2010; Ota et al., 2014a). $ALDH1^+$ cancer cells displayed higher self-renewal, migration, and tumorigenic potential than $ALDH1^-$ cells (Clay et al., 2010; Ota et al., 2014b; Richard et al., 2013). Orai1 also markedly increases motility of the non-tumorigenic cells. Our finding is consistent with previous reports showing the importance of Orai1 in cell migration. Knockdown of Orai1 in invasive breast cancer cell lines decreased cell migration, whereas its overexpression promoted cellular motility (Lee et al., 2012b). However, underlying mechanism by which Orai1 enhances oral epithelial cell migration has not been understood. Therefore,

effects of Orai1 on epithelial-to-mesenchymal transition (EMT) and metastasis-related gene expression should be warranted to investigate (Davis et al., 2012). In multiple OSCC cell lines, inhibition of Orai1 led to suppression of such CSC phenotype. We conclude that Orai1 increases not only the number of CSCs, but also CSC properties. Thus, we hypothesize that Orai1 promotes malignant progression of OSCC by enriching CSC phenotype. Therefore, Orai1 could be an effective therapeutic target for OSCC.

We also found that Orai1 regulates the expression of several important CSC-related genes, *i.e., Ezh2, Gli1, Hes1, Zeb2, FGF4,* and *IL4*. Studies have shown the important role of these genes in acquisition and maintenance of CSC phenotype. For instance, our previous study demonstrated that Hes1 is upregulated in OSCC, and the suppression of Hes1 in oral cancer cells inhibits self-renewal capacity of OSCC, suggesting the important role of Hes1 in OSCC CSC (Lee et al., 2012a). In addition, other reports also revealed the crucial roles of Hes1 in the maintenance of CSC properties, such as metastasis, chemotherapy resistance, and EMT (Liu et al., 2015). Zeb1 and Zeb2 are significantly increased in head and neck CSCs compared to non-CSCs (Chu et al., 2013). Knockdown of Zeb1 and Zeb2 in head and neck cancer cells decreased their CSC properties such as self-renewal capacity, the expression of stemness markers, and drug resistance. Moreover, their suppression inhibited *in vivo* tumor growth and the rate of metastasis to distant site (Chu et al., 2013). Conversely, co-overexpression of Zeb1 and Zeb2 enhanced sphere-forming ability of head and neck cancer cells (Chu et al., 2013). FGF4 is shown to play a key role in maintaining self-renewal capacity of normal and cancer stem cells (Jordan et al., 2011; Yasuda et al., 2014). FGF4 promoted self-renewal of CSC-enriched population (Yasuda et al., 2014).

Orai1-mediated SOCE activates NFAT, a family of transcription factors composed of four members, NFATc1, NFATc2, NFATc3, and NFATc4 (Daniel et al., 2014; Parekh, 2007; Parekh and Putney, 2005). NFATs are first elucidated in immune cells, NFATs are activated as a result of calcium flux from endoplasmic reticulum stores and from the extracellular environment through the activation of store-operated channels on the plasma membrane. In the basal state NFATs are hyperphosphorylated in the cytoplasm. Following the stimulation and increase in intracellular Ca^2 level, NFATs are activated by the phosphatase calcineurin-dependent dephosphorylated, and active NFAT form then can translocate to the nucleus, where they cooperate with other factors and co-activators to promote gene transcription (Mancini and Toker, 2009b). The calcium-regulated isoforms NFATc1–4 share two conserved domains: the Rel-homology region (RHR) and conserved NFAT homology region (NHR). NHR domain contains the transactivation region of NFATs, which binds to gene promoter to initiate gene transcription, and numerous serine residues that can be phosphorylated by protein kinase again to transfer NFAT back to the cytoplasm (Chen et al., 1998).

NFATs also have an important role in maintaining the balance between quiescence and proliferation in stem cells (Horsley et al., 2008). When hair follicle stem cells enter quiescent state, NFATc1 activation by bone morphogenic protein 4 (BMP4) serves to repress cycline-dependent kinase 4 (CDK4) and repress cell cycle progression. Conversely, activation of NFATc1 drives stem cells to enter the proliferative stage and allow differentiation (Mancini and Toker, 2009b; Mani et al., 2008). This suggests the role of NFATc1 in maintaining stemness in stem cells and is involved in biological cue which directs transition of stem cells from the undifferentiated state to the differentiation state. Emerging evidence has suggested that NFAT signaling plays an important role in tumorigenesis by regulating various target genes involved in

cancer development (Mancini and Toker, 2009a). For instance, NFATc1 induced malignant cell growth phenotype in pancreatic cancer cells by upregulating Myc (Buchholz et al., 2006a) and promoted metastasis of mammalian cancer cells *via* MMP-2 upregulation (Chen et al., 2011; Liu et al., 2013; Velupillai et al., 2010). NFATc2 was overexpressed in multiple cancer types (Chen et al., 2011; Liu et al., 2013), and its depletion suppressed migration/invasion of cancer cells (Liu et al., 2013).

Despite these reports, the role of NFAT proteins in OSCC has not been documented. In our study, we showed that treatment of OSCC cells with NFAT inhibitor suppressed self-renewal and migration. Similar effect of the NFAT inhibitor was also observed in HOK-16B/Orai1, suggesting that NFAT is required for Orai1-induced CSC phenotype. Furthermore, our studies revealed that NFATc3 is dominant isoform in oral epithelial cells and activated by Orai1 overexpression. Silencing NFATc3 in HOK-16B/Orai1 led to suppression of CSC phenotype, suggesting the funtional role of Orai1/NFAT axis in the regualtion of CSC.

The role of cytokines during inflammation include sending signals to immune cells via ligand-receptor interaction to help resolve infection, and studies suggests oncogenic role of these cytokines signaling (Sriuranpong et al., 2003). Generally, secreted cytokines can send signals in an autocrine or paracrine fashion. Chronic inflammation is a sustained inflammatory condition in the site of injury which may lead to environments that promote genomic mutation and initiation of cancer. About 20% of cancer formation and progression are reported to be linked to chronic inflammation (Aggarwal et al, 2009). Inflammatory tumor microenvironment is populated with a many different cell types, which includes groups of the innate immune cells (neutrophils, macrophages, mast cells, dendritic cells, myeloid derived suppressor cells and natural killer cells), adaptive immune cells (B and T lymphocytes), stromal cells (fibroblasts, endothelial cells,

pericytes and mesenchymal cells) and cancer cells. (de Visser et al, 2006). Recent scientific evidences inferring the significant role of immune system in cancer growth and progression in inflammation (Blair and Cook, 2008). The role of pro-inflammaotry cytokines in tumorigenesis of various cancer types is generally well-documented in research. NF-Kβ, STAT and caspases are activated by various cytokines, including IL-1, IL-4, IL-6, IL-10, IL-12, IL-23, TGF-β, TNF-α and TRAIL, and can also sustain the inflammatory microenvironment (Lin and Karin, 2007).

To investigate the role of cytokines in Orai1-induced CSC phenotypes, we first examined the global expression of human genome using high-throughput microarray using HOK-16B/EV and HOK-16B/Orai1 cells. Interestingly enough, HOK-16B/Orai1 revealed significant number of genes increased by Orai1. Among those genes, there were significant number of genes involved in immunity-related canonical signaling pathway. These pathways include cytokine and chemokine receptor-mediated inflammatory signaling, immune cell activation and differentiation signaling, and inflammatory signaling in involved in different human diseases. Along with our previous study demonstrating enhanced oral CSC phenotypes by chronic inflammatory cytokine exposure (Lee et al., 2012a), this microarray data provides another valuable information that these genes involved immunity-related canonical pathways may also participate in regulating CSC phenotype in HOK-16B cells.

Evidences revealed overexpression of IL4 in many cancers including lung, colon, breast and thyroid cancer (Todaro et al., 2007b). IL4 is well-known pro-inflammatory cytokine with multifunction which can promote cancer formation by enhancing proliferation and inhibiting apoptosis (Li et al., 2008; Prokopchuk et al., 2005). It has previously been demonstrated that IL4 confer apoptosis resistance in chronic lymphocytic leukemia B-cells and enhance the anti-apoptotic proteins expression in cancers cell lines, such as breast, prostate and bladder. IL4 is

reported to promote cancer cell survival and expansion by inducing the expression of anti-apototic genes (Todara, 2007). Also, cancer cells producing IL4 in autocrine fashion showed drug resistance thereby escaping from chemotherapy-induced cell death (Conticello et al., 2004). Many studies demonstrated that cytokines increased CSC population and phenotype (Asiedu et al., 2011; Lee et al., 2012a; Sansone et al., 2007; Storci et al., 2010; Todaro et al., 2007a). We also previously reported that inflammatory cytokine enhanced CSC phenotype of OSCC (Lee et al., 2012a). Its role in CSC is also highlighted. IL4 secretion by colon CSCs conferred chemoresistance (Di Stefano et al., 2010; Todaro et al., 2007b). Indeed, many evidences indicate the role of IL-4 cytokine in cancer progression and is found to be associated with cancer initiation and CSC regulation. In our study, we found an increase in IL-4 expression in OSCC cell lines and increased CSC phenotypes, *e.g.*, self-renewal capacity and cell migration and invasion.

CCL3, also known as macrophage inflammatory protein 1α (MIP-1α), is a pro-inflammatory cytokine belonging to the CC chemokine subfamily and is a ligand for CCL3 receptors, CCR1, CCR3, CCR4 and CCR5. On the site of inflammation, CCL3 is known to have function to elicit chemotactic activities of immune cells including lymphocytes, macrophages, and monocytes (Schall et al., 1993). Also, it has been reported that various cancers secrete or stimulate different complex chemokine networks in immune cells and stromal cells that directs immune cell recruitment to tumor microenvironment as well as growth, drug resistance, angiogenesis and metastasis of cancer (Gales et al., 2013; Mueller et al., 2007). CCL3 promote cancer cell growth, angiogenesis and metastasis of different tumors such as melanoma, colorectal cancer, and renal cell carcinoma (Arabzadeh et al., 2013; Hsu et al., 2013; Wu et al., 2008). Recent report highlighted the important metastatic role of CCL3 by inducing expression and secretion of

MMPs, which digest extracellular matrix and help cell migration in cancer (Wu et al., 2008). In human chondrosarcoma cells, activation of MMP and secretion dependent on CCL3. In one study, CCL3 induced MMP-2 expression and secretion while introduction of MMP-2 inhibitor suppressed cell migration induced by CCL3 (Hsu et al., 2013). Also, upregulation of cytokines and chemokines, such as CCL3 and IL8, by exposure to carcinogen called benzo[a]pyrene increased migration and invasion of lung cancer (Zhang et al., 2016). Along with these phenotypes of cancer, CCL3 has been shown to promote expansion leukemic initiating cells, indicating its role in regulating stemness in leukemia (Baba et al., 2013). CCL3 can initiates cellular signaling pathway upon binding to its receptor. Activation of CCR5 signaling by CCL3 in cancer-associated fibroblast allowed fibroblast to accumulate near the colon cancer during the late phase of colitis-associated colon carcinogenesis, and chemical inhibition of CCR5 suppressed tumor formation in vivo (Tanabe et al., 2016), which also emphasizes the significance role CCL3 in perpetuating the inflammatory environment favorable for carcinogenesis. These evidence are in line with our finding that CCL3 functions to regulate CSC phenotypes in oral cancer.

Due to significant involvement of chemokines in cancer progression, further investigation should be warranted to determine whether chemokines are plausible oral cancer therapeutic target. In this study we demonstrated the possible regulation mechanism of these chemokines. We showed that IL4 and CCL3 are overexpressed in SCC4 spheres and ALDH1^{high} cells compared to the monolayer cells ALDH1^{low} cells, respectively (**Figure 17A** and **17B**). Ectopic Orai1 expression resulted in the significant induction of these cytokine/chemokine expression (**Figure 15A**), indicating that these cytokines expression are dependent on Ca^{2+} entry via Orai1. As NFAT is the well-known effector of Orai1 and is the transcriptional factor that regulates

transcription of various cytokines, we speculated that NFAT signaling may be involved in Orai1-induced cytokine/chemokine expression. As expected, these cytokines were consistently upregulated by NFAT activator, PMA and Ionomycin, and down-regulated by subsequent inhibition of NFAT signaling using CsA in SCC4. Moreover, specific knockdown of NFATc3 also consistently downregulated these genes expression. Gene ontology and canonical pathway analysis of our microarray data revealed regulation of significant number of immunity-related genes expression, which also support the idea that cytokines may play a major role in regulating Orai1-induced tumorigenic potential by conferring CSC phenotypes in HOK-16B, non-tumorigenic immortalized oral epithelial cell.

In addition to delineating the molecular signaling that regulates these cytokine expression, we showed their function in CSC regulation. Effect of CCL3 and IL4 on self-renewal of different oral cancer cell lines indicate that these secretory molecules may direct the autocrine and paracrine signals specifically to stem cells to promote their growth. In order to determine the role of these cytokines in regulating important CSC phenotypes, we investigated whether cytokines can rescue CSC phenotypes suppressed by NFAT inhibition. IL4 and CCL3 treatment rescued self-renewal and CCL3 but not IL4 partially rescued migration capacity of SCC4/E106Q. These data suggest involvement of various network of cytokines and possibly different effectors of Orai1orchestrating the oral cancer progression in NFAT-independent manner.

Gene ontology analysis also identified Orai1-induced cancer stem cell and cancer/metastasis-related genes in HOK-16B. Gene ontology analysis of genes upregulated 2 folds or higher revealed upregulation of 22 stem cell and 24 cancer/metastasis-related pathways. Validation of Orai1-induced genes in the HOK-16B by qRT-PCR revealed 15 genes upregulated by Orai1. Among those genes regulated by Orai1, many genes including ID1, ID2, LOX and LOXL2, were

previously reported as cancer stem cell marker or genes involved in malignant cancer progression in different cancer types. Among the four isoforms of Inhibitor of DNA binding (ID) proteins, we identified ID1 and ID2 which were overexpressed by Orai1 in HOK-16B. Both ID1 and ID2 has implication in tumorigenesis and cancer progression. ID1 overexpression and knockdown study has revealed its function in maintenance of self-renewal, chemoresistance and tumorigenic potential in colon cancer, and maintenance of glioma stem cells population (Niola, et al., 2013; O'Brien et al., 2012). Also, ID2 has been reported to play important function in tumor initiation, proliferation and angiogenesis in retinoblastoma mutant mice (Lasorella et al., 2005). ID2 loss of function study showed that ID2 knockdown resulted in more differentiated cell phenotype in human salivary gland cancer cells, with less aggressive phenotype, such as reduction of EMT marker and suppression of cell proliferation (Sumida et al., 2016). Moreover, upregulation of lysyl oxidase (LOX), which functions to catalyze the cross-linking of collagen and elastin in the extracellular matrix, was found crucial in cancer metastasis. According to the report from Erler et al., LOX expression showed positive correlation with overall survival in estrogen receptor-negative breast cancers and head and neck cancer patients. In the same report, they demonstrated that chemical inhibition of LOX inhibited cell invasion in breast cancer and head and neck squamous cell carcinoma, indicating important function of LOX in cancer metastasis (Erler et al., 2006). Moreover, expression of Lysl oxidase-like 2 (LOXL2) was increased in different tumor types such as colon and esophageal cancer (Fong et al., 2007), and was shown to promote invasion of breast cancer and gastric cancer (Akiri et al., 2003) and metastasis of gastric carcinoma cells *in vitro* and *in vivo* (Peng et al., 2009). From our study, we showed that Orai1 indeed confers CSC phenotype in HOK-16B, non-tumorigenic oral epithelial cells, and we provide another line of evidence that Orai1 induced a network of stem cell and

cancer metastasis-related genes expression may promote oral cancer progression by regulating CSC phenotype. Also, as we identified Orai1 target genes which were regulated by either NFAT-dependent or NFAT-independent pathways (**Figure 20**), Orai1 may regulate CSC phenotypes in oral cancer *via* many signaling pathways. Therefore, studying the role of Orai1-induced stem cell and cancer/metastasis genes in CSC regulation is warranted.

Nonetheless, we have shown the important oral CSC regulating axis: Orai1-NFATc3-Cytokine. Orai1-NFATc3 target cytokines, IL4 and CCL3, has been shown to regulate CSC phenotype regulated by Orai1 in OSCC. Based on our finding, we speculate that cytokines secreted by oral CSCs in the tumor environment may regulate CSC phenotypes in autocrine manner as well as exerts molecular signals in neighbor cells in paracrine manner to promote oral cancer growth and further progression (**Figure 21**). Due to various mechanisms by which CSCs regulate themselves and manipulating cell-cell signaling networks to their own advantage within the tumor environment, and its drug resistance and metastatic phenotypes, targeting CSCs would prevent recurrence of cancer. Our study demonstrates that Orai1is the key regulator of tumor formation as well as CSC phenotypes. With the potent Orai1-specific chemical blocker *compound 5D* identified to suppress Orai1 function (Kim et al., 2014), our study proposes for the first time that targeting Orai1 by using Orai1 chemical inhibitor 5D may offer a therapeutic modality against oral cancer (**Figure 22**).

In conclusion, we demonstrate that Orai1 is a novel molecular regulator of tumorigenicity and stemness of OSCC. Orai1 enhances CSC phenotype through NFAT signaling. Cytokine and chemokine genes expression induced by Orai1-NFATc3 axis also participate in regulating important CSC phenotypes, *e.g*., self-renewal and cell migration in OSCC. Thus, the Orai1/NFAT axis could be an important therapeutic target in OSCC.

4. SUMMARY AND CONCLUSION

Oral cancer is the 6th most common cancer worldwide with poor survival rate. Recent studies evidence the presence of cancer stem cells (CSCs or alternatively cancer initiating cells) that are subpopulations of tumor cells considered as the driving force of tumorigenesis. CSCs are also potentially responsible for drug resistance, metastasis, and recurrence of cancers. Thus, this dissertation aims to investigate the novel pathway specifically involved in the maintenance of CSCs and explore the potential use of this unique pathway as a novel therapeutic target for CSCs. Orai1, a major pore subunit of Ca^{2+} channel of non-excitatory cells, has been involved in carcinogenesis and cancer progression. To investigate the significance of Orai1 in oral cancer, the study was designed to specify the role of Orai1 and its underlying mechanism by which Orai1 regulates oral cancer stemness. Here, we report very notable findings from our study that:

- ✓ Orai1 is gradually increased from normal to OSCC cancer cells and tissues.
- ✓ Orai1 is overexpressed the CSC-enriched population in OSCC.
- ✓ Orai1 gain-of-function and loss-of-function experiments demonstrate that Orai1 is required for the tumorigenicity and CSC maintenance of OSCC.
- ✓ Orai1 overexpression in non-tumorigenic epithelial cells activated NFATc3.
- ✓ NFATc3 knockdown reverted Orai1-induced CSC phenotypes.
- ✓ Orai1-NFATc3 target cytokines, *i.e*., *IL4* and *CCL3*, are highly expressed in CSC-enriched cells and regulate CSC phenotypes in OSCC**.**
- ✓ Orai1also induced inflammation, stemness and cancer/metastasis-related genes in a NFATc3-independent manner.

Based on these findings, we show that Orai1 maintains oral cancer stemness via activation of NFATc3 signaling. Also we provide evidence that CSC-specific cytokines regulated by Orai1-NFATc3 axis play a role in regulating oral CSC phenotype. Indeed, we claim that Orai1-NFATc3 axis is the novel CSC regulating pathway in oral cancer and this finding may offer a targeted therapeutic modality against cancer.

5. FIGURES AND FIGURE LEGENDS

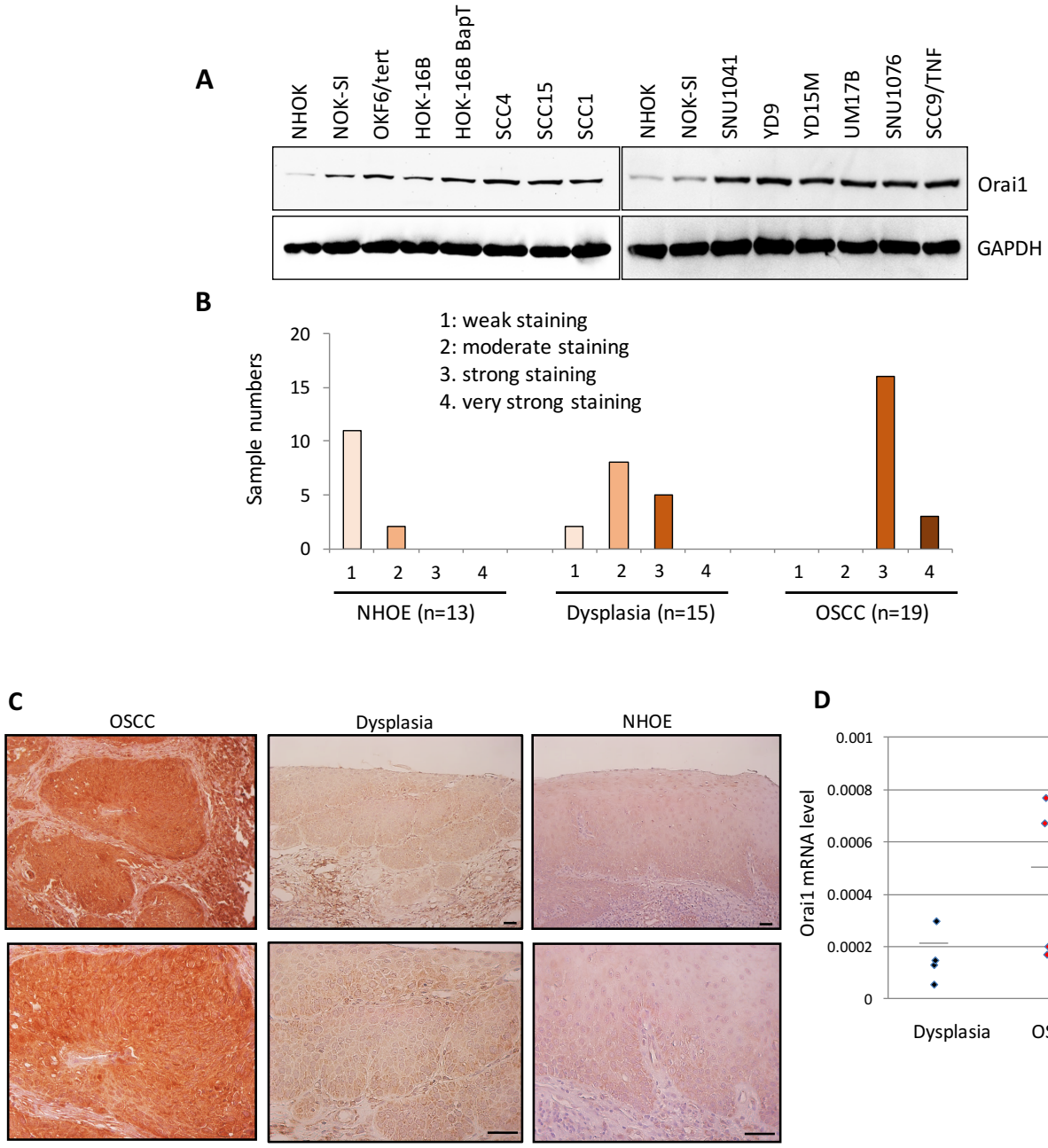
A
NHOK
NOK-SI
OKF6/tert
HOK-16B
HOK-16B BapT
SCC4
SCC15
SCC1
NHOK
NOK-SI
SNU1041
YD9
YD15M
UM17B
SNU1076
SCC9/TNF
Orai1
GAPDH
B
1: weak staining
2: moderate staining
3. strong staining
4. very strong staining
Sample numbers
20
15
10
5
0
1 2 3 4
1 2 3 4
1 2 3 4
NHOE (n=13)
Dysplasia (n=15)
OSCC (n=19)
C
OSCC
Dysplasia
NHOE
D
Orai1 mRNA level
0.001
0.0008
0.0006
0.0004
0.0002
0
Dysplasia
OSCC

Figure 1. A stepwise increase of Orai1 in oral/oropharyngeal carcinogenesis.

(A) Level of Orai1 protein was determined in normal human oral keratinocyte (NHOK), 3 precancerous, non-tumorigenic immortalized oral epithelial cell lines (NOK-SI, OKF6/tert, and HOK-16B) and 10 OSCC cell lines (HOK-16B-BapT, SCC4, SCC9/TNF, UM17b, and YD38) by performing Western blot. GAPDH was used as a loading control. (B) *In vivo* Orai1 expression was determined in normal human oral epithelia (NHOE), oral dysplasia and OSCC tissues by immunohistochemical staining. (C) Representative examples of Orai1 immunohistochemical staining in NHOE, oral dysplasia and OSCC tissues *in vivo*. Bar indicates 100 μm. (D) OSCC and dysplastic cells were microdissected from oral cancer tissue and oral dysplastic tissue, respectively. The levels of Orai1 mRNA were measured by qRT-PCR and normalized with the expression of GAPDH.

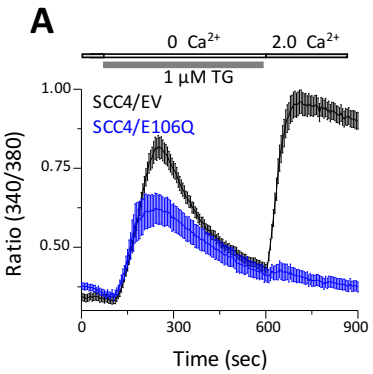

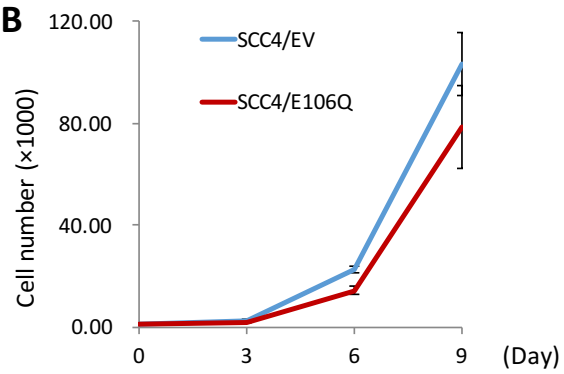

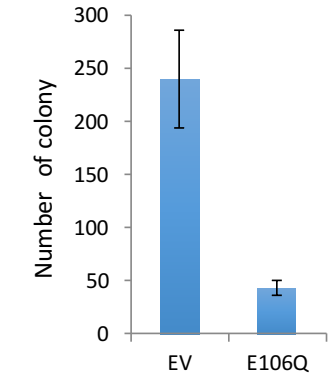

D

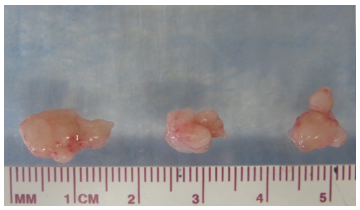

Group	*In vivo* tumorigenicity
SCC4/EV	3/5
SCC4/E106Q	0/5

Figure 2. The dominant negative Orai1 mutant (E106Q) suppresses tumorigenicity of OSCC *in vivo*.

(A) SCC4 cells were infected with retroviruses containing E106Q or empty vector (EV) as a control. Intracellular Ca^{2+} imaging assay was performed to confirm the inactivation of Orai1 function. Intracellular Ca^{2+} stores were depleted with 1 μM TG in the absence of extracellular Ca^{2+}, followed by re-addition of 2 mM Ca^{2+}. Ca^{2+} influx was analyzed by single-cell video imaging of Fura2-labeled, GFP+ cells. More than 30 GFP+ cells were analyzed in each experiment. (B) Effect of E106Q on cell proliferation of SCC4 was determined by cell counting. Data are means ± SD of triplicate experiments. (C) Effect of E106Q on anchorage independent growth of SCC4 was determined by soft agar assay. Data are means ± SD of triplicate experiments. $*P < 0.001$ by two-tailed Student's *t* test. (D) Effect of E106Q on *in vivo* tumorigenicity of SCC4 was determined by xenograft tumor assay. SCC4/EV and SCC4/E106Q were injected subcutaneously into five nude mice. Mice were killed at week 6, and tumors were surgically removed from all animals and photographed.

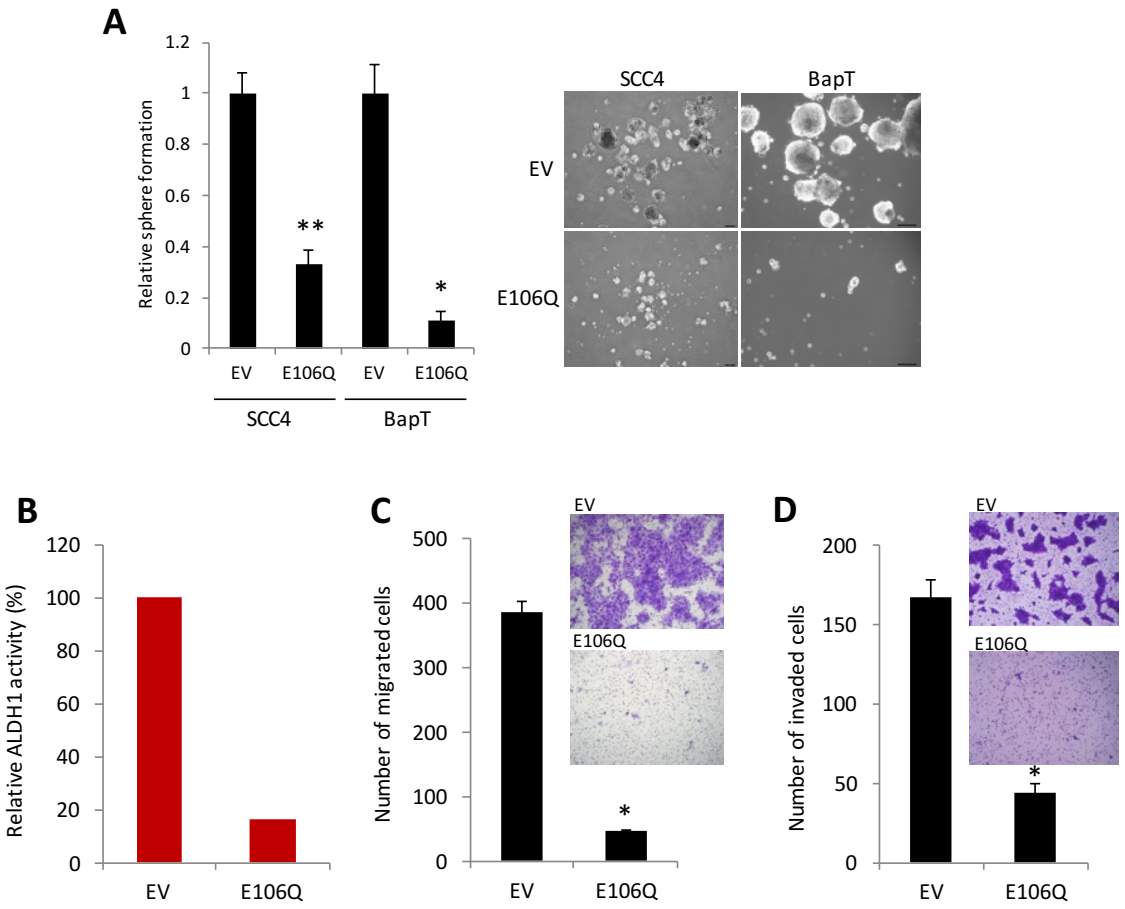
A
Relative sphere formation
1.2
1
0.8
0.6
0.4
0.2
0
**
*
EV
E106Q
EV
E106Q
SCC4
BapT
SCC4
BapT
EV
E106Q
B
Relative ALDH1 activity (%)
120
100
80
60
40
20
0
EV
E106Q
C
Number of migrated cells
500
400
300
200
100
0
*
EV
E106Q
EV
E106Q
D
Number of invaded cells
200
150
100
50
0
*
EV
E106Q
EV
E106Q

Figure 3. The dominant negative Orai1 mutant (E106Q) inhibits CSC phenotype.

(A) Effect of *E106Q* on self-renewal capacity of two OSCC cell lines, SCC4 and HOK-16B BapT, was determined by tumor sphere formation assay. Data are means ± SD of triplicate experiments. $*P < 0.01$ and $**P < 0.05$ by two-tailed Student's *t* test. Representative images of tumor spheres formed by E106Q-transduced OSCC cell lines (SCC4/E106Q and BapT/E106Q) and their corresponding controls (SCC4/EV and BapT/EV). The photographs were taken at a magnification of 50X. (B) Effect of *E106Q* on ALDH1 activity in SCC4 was determined by Aldefluor assay. (C) Effect of *E106Q* on migration ability in SCC4 was determined by transwell migration assay. Migration ability was described as number of migrated cells per field with data as mean ± SD for *3 randomly selected fields*. $*P < 0.01$ by two-tailed Student's *t* test. Representative images of transwell migration assay are shown on the right. (D) Effect of *E106Q* on invasion ability of SCC4 was determined by Matrigel invasion assay. Invasion ability was described as the number of invaded cells per field with the data as mean ± SD for *3 randomly selected fields*. $*P < 0.01$ by two-tailed Student's *t* test. Representative images of Matrigel invasion assay are shown on the right.

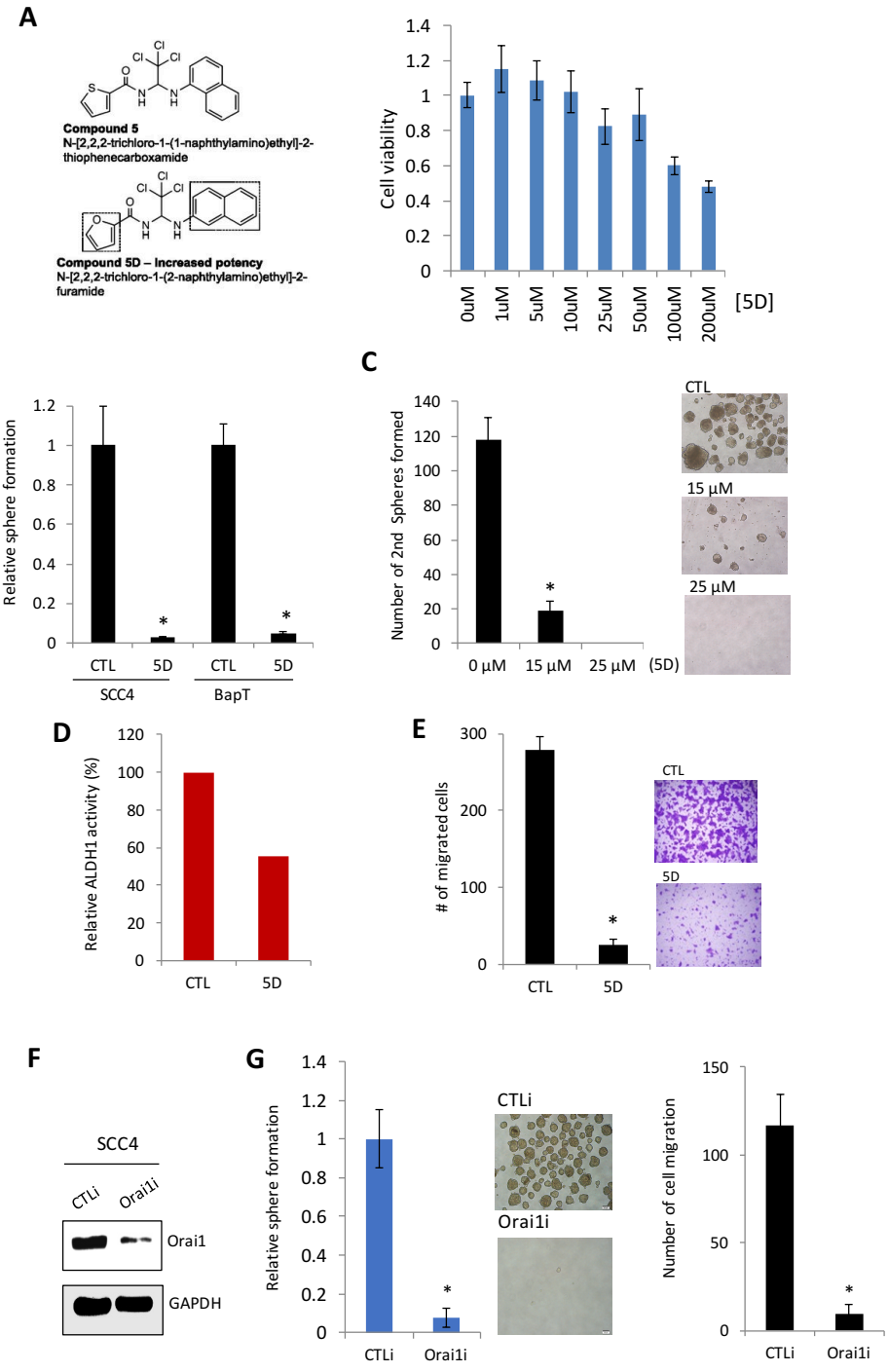
A
Compound 5
N-[2,2,2-trichloro-1-(1-naphthylamino)ethyl]-2-thiophenecarboxamide
Compound 5D – increased potency
N-[2,2,2-trichloro-1-(2-naphthylamino)ethyl]-2-furamide
Cell viability
0uM
1uM
5uM
10uM
25uM
50uM
100uM
200uM
[5D]
B
Relative sphere formation
CTL
5D
SCC4
BapT
C
Number of 2nd Spheres formed
0 µM
15 µM
25 µM
(5D)
CTL
15 µM
25 µM
D
Relative ALDH1 activity (%)
E
# of migrated cells
F
SCC4
CTLi
Orai1i
Orai1
GAPDH
G
Relative sphere formation
Number of cell migration

Figure 4. Chemical and Orai1 knockdown suppress CSC phenotype.

(A) Orai1-specific chemical blocker**,** *compound 5D,* was used to observe the effect of Orai1 inhibition on CSC phenotype. Efficiency of 5D in blocking the function of Orai1 is determine previously (Kim, et al, 2014). Effect of *compound 5D* on cell viability was determined by MTT assay. (B) Effect of *compound 5D* on self-renewal capacity of two OSCC cell lines, SCC4 and HOK-16B BapT, was determined by tumor sphere formation assay. $*P < 0.01$ by two-tailed Student's *t* test. (C) In order to confirm the effect of *compound 5D* on self-renewal, secondary sphere assay was performed using 5000 dissociated primary sphere cells. Experiment was done in triplicate and images are taken at 50X. $*P < 0.01$ by two-tailed Student's *t* test. (D) Effect of 5D on ALDH1 activity was measured using ALDH1 Aldefluor kit. (E) Effect of *compound 5D* on migration ability in SCC4 was determined by transwell migration assay. $*P < 0.01$ by two-tailed Student's *t* test. Representative images of transwell migration assay are shown on the right. (F) Endogenous Orai1 was knocked down in SCC4 using siRNA against Orai1 (Orai1i: Santa Cruz) and was confirmed by Western Blot. The cells transfected with control siRNA (CTLi) were included for comparison. (G) Effect of Orai1 knockdown on self-renewal capacity of SCC4 was determined by tumor sphere formation assay. Data are means ± SD of triplicate experiments. (H) Effect of Orai1 knockdown on migration ability of SCC4 was determined by transwell chamber. Migration ability was described as number of migrated cells per field with data as mean ± SD for 3 randomly selected fields.

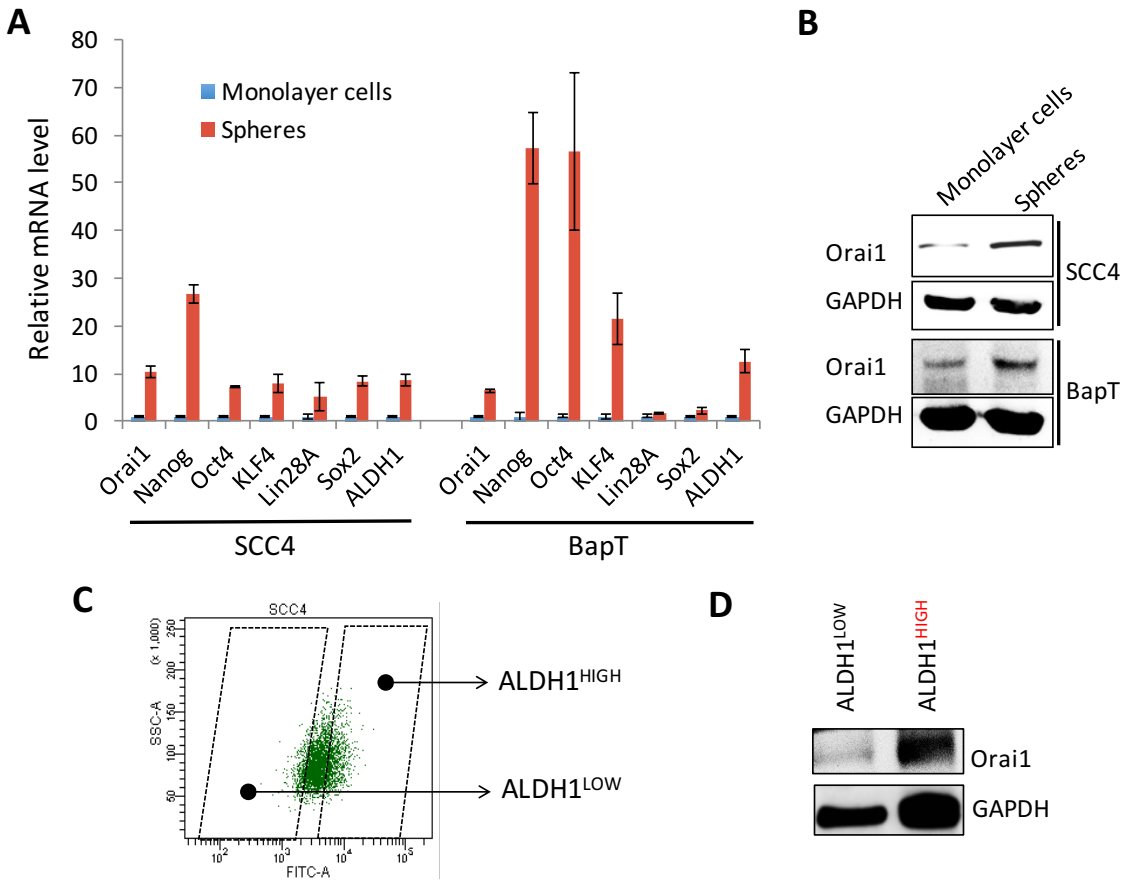
A
Relative mRNA level
80
70
60
50
40
30
20
10
0
Monolayer cells
Spheres
Orai1
Nanog
Oct4
KLF4
Lin28A
Sox2
ALDH1
SCC4
BapT
B
Monolayer cells
Spheres
Orai1
GAPDH
SCC4
Orai1
GAPDH
BapT
C
SCC4
SSC-A
FITC-A
ALDH1HIGH
ALDH1LOW
D
ALDH1LOW
ALDH1HIGH
Orai1
GAPDH

Figure 5. Orai1 expression is enriched in CSC populations of OSCC.

(A) Expressions of Orai1, stemness transcription factors (Nanog, Oct4, KLF4, Lin28A, and Sox2) and ALDH1were assessed in tumor spheres (CSC-enriched population) and corresponding adherent monolayer cells (non-CSC population) derived from SCC4 and HOK-16B BapT by real-time qPCR. Levels of the genes were normalized with the level of GAPDH. Their levels in tumor spheres were plotted as fold induction against those in their corresponding adherent monolayer cells. (B) Level of Orai1 protein was assessed in tumor spheres and corresponding adherent monolayer cells by Western blot analysis. (C) Demonstration of the strategy for sorting $ALDH1^{HIGH}$ (CSC-enriched population) and $ALDH1^{LOW}$ (non-CSC population) cell population. $ALDH1^{HIGH}$ and $ALDH1^{LOW}$ cell populations were sorted from SCC4 cells by flow cytometry. (D) Level of Orai1 protein was determined in $ALDH1^{HIGH}$ and $ALDH1^{LOW}$ cell population by Western blot analysis.

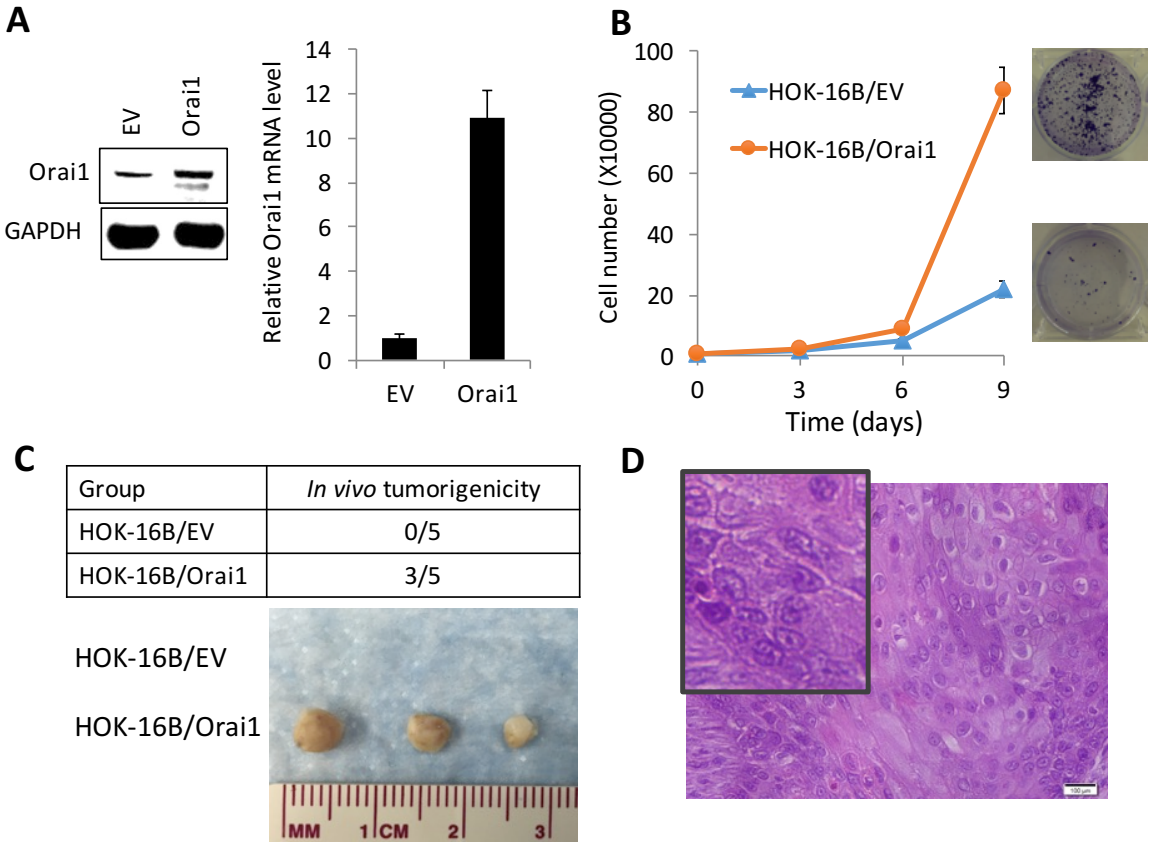
A
EV
Orai1
Orai1
GAPDH
Relative Orai1 mRNA level
14
12
10
8
6
4
2
0
EV
Orai1
B
100
80
60
40
20
0
HOK-16B/EV
HOK-16B/Orai1
Cell number (X10000)
0
3
6
9
Time (days)
C
Group
In vivo tumorigenicity
HOK-16B/EV
0/5
HOK-16B/Orai1
3/5
HOK-16B/EV
HOK-16B/Orai1
MM
1 CM
2
3
D

Figure 6. Ectopic Orai1 expression endows non-tumorigenic immortalized oral epithelial cells with tumorigenic potential *in vivo*.

(A) Orai1 expression was forced in non-tumorigenic immortalized oral epithelial cells, HOK-16B, by infecting with retroviral vector expressing Orai1, and its ectopic expression was confirmed by Western blot analysis and real-time qPCR. Localization of Orai1 is confirmed by Immunohistochemistry using Orai1 antibody. (B) Effect of Orai1 on cell proliferation of HOK-16B was determined by cell counting. Data are means ± SD of triplicate experiments. Representative images of clonogenic assay are also shown on the right. (C) Effect of Orai1 on *in vivo* tumorigenicity of HOK-16B was determined by xenograft tumor assay. HOK-16B/EV and HOK-16B/Orai1 were injected subcutaneously into five nude mice. Mice were killed at week 6, and tumors were surgically removed from all animals and photographed. (D) Morphology characteristics of xenografts formed by HOK-16B/Orai1 were observed *via* hematoxylin and eosin (H&M) staining. Insert showing magnified image.

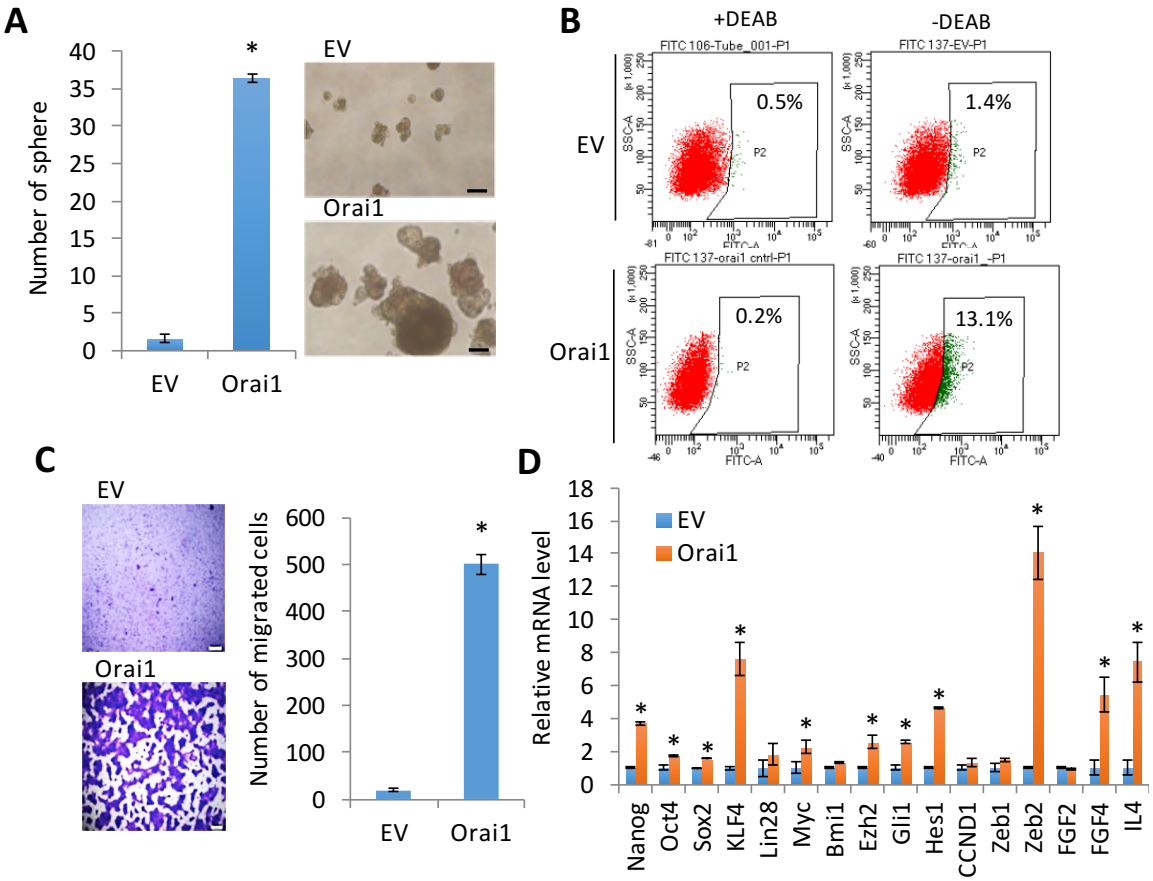
A
Number of sphere
40
35
30
25
20
15
10
5
0
EV
Orai1
*
EV
Orai1
B
+DEAB
-DEAB
EV
Orai1
FITC 106-Tube_001-P1
FITC 137-EV-P1
FITC 137-orai1 cntrl-P1
FITC 137-orai1_-P1
0.5%
1.4%
0.2%
13.1%
P2
SSC-A
FITC-A
C
EV
Orai1
Number of migrated cells
600
500
400
300
200
100
0
*
EV
Orai1
D
Relative mRNA level
18
16
14
12
10
8
6
4
2
0
EV
Orai1
Nanog
Oct4
Sox2
KLF4
Lin28
Myc
Bmi1
Ezh2
Gli1
Hes1
CCND1
Zeb1
Zeb2
FGF2
FGF4
IL4

Figure 7. Ectopic Orai1 expression promotes CSC phenotype in non-tumorigenic immortalized oral epithelial cells.

(A) Effect of *Orai1* on self-renewal capacity of HOK-16B was determined by tumor sphere formation assay. *$P < 0.01$ by two-tailed Student's *t* test. Representative image of tumor spheres formed by HOK-16B/EV and HOK-16B/Orai1 are shown on the right. (B) Effect of *Orai1* on ALDH1 activity in HOK-16B was determined by Aldefluor assay. Cells were labeled with Aldefluor combined with or without the ALDH1 inhibitor DEAB and analyzed by flow cytometry. The gate for ALDH1 + cells is determined in relation to the DEAB control (+DEAB) and shows the brightly fluorescent ALDH1 population versus the side scatter, a population that is absent/decreased in the presence of DEAB. The number shown in each panel reflects the percentage of ALDH1+ cells in each cell type. (C) Effect of *Orai1* on migration ability in HOK-16B was determined by transwell migration assay. *$P < 0.001$ by two-tailed Student's *t* test. Representative images of transwell migration assay are shown on the left. (D) Effects of *Orai1* on stemness transcription factors (Nanog, Oct4, Sox2, KLF4, Lin28, Myc, and Bmi1) and CSC-related genes (Ezh2, Gli1, Hes1, CCND1, Zeb1, Zeb2, FDF2, FGF4, and IL4) in HOK-16B were determined by real-time qPCR. Their levels in HOK-16B/Orai1 were plotted as fold induction against those in HOK-16B/EV. *$P < 0.05$ by two-tailed Student's *t* test.

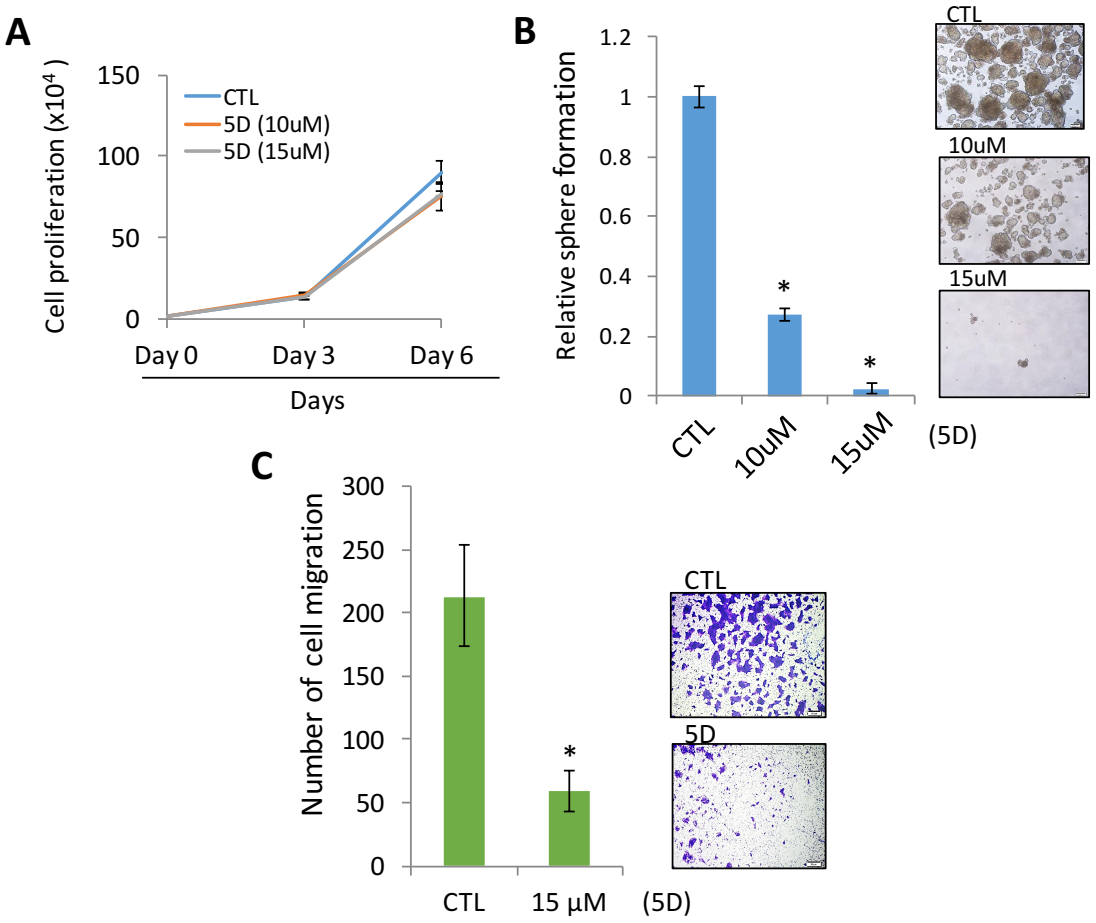
A
Cell proliferation (x10^4)
150
100
50
0
CTL
5D (10uM)
5D (15uM)
Day 0
Day 3
Day 6
Days
B
Relative sphere formation
1.2
1
0.8
0.6
0.4
0.2
0
*
*
CTL
10uM
15uM
(5D)
CTL
10uM
15uM
C
Number of cell migration
300
250
200
150
100
50
0
*
CTL
15 µM
(5D)
CTL
5D

Figure 8. Chemical inhibition of Orai1 suppresses CSC phenotype in HOK-16B/Orai1.

(A) Effect of *compound 5D* on cell proliferation was determined by cell proliferation assay. $1x10^4$ cells were seeded in 6 well plate in triplicate and grown for 3 dasys and 6 days. Cell number was averaged and compared with non-treated control groups. Effect of *compound 5D* on self-renewal capacity of HOK-16B/Orai1 and EV control was determined by tumor sphere formation assay using different dose of *compound 5D*. $*P < 0.005$ by two-tailed Student's *t* test. Representative images were taken at 50X magnification. (C) Effect of *compound 5D* on migration ability in HOK-16B/Orai1 and EV control was determined by transwell migration assay. Three random fields were chosen to count the migrated cells, averaged and compared with the EV control $*P < 0.01$ by two-tailed Student's *t* test. Representative images of transwell migration assay are shown on the right**.**

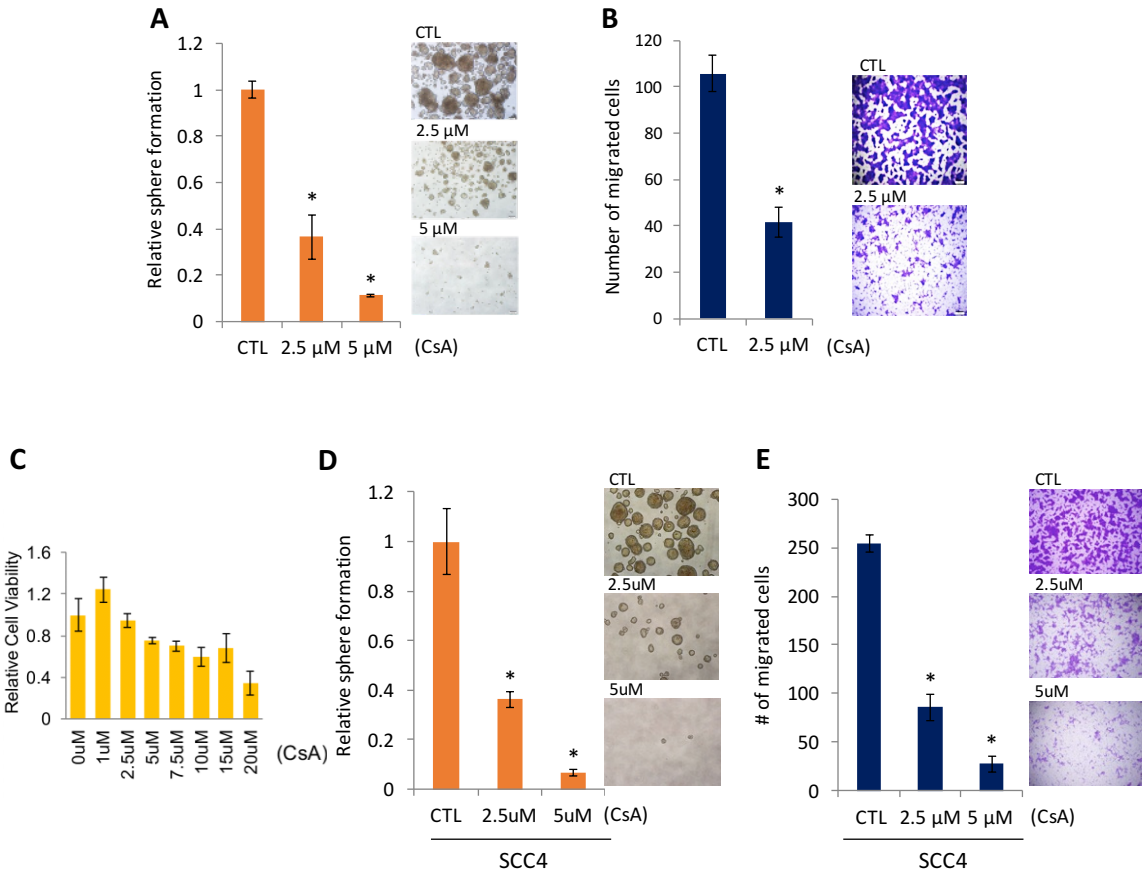
A
Relative sphere formation
1.2
1
0.8
0.6
0.4
0.2
0
CTL
2.5 µM
5 µM
(CsA)
CTL
2.5 µM
5 µM
B
Number of migrated cells
120
100
80
60
40
20
0
CTL
2.5 µM
(CsA)
CTL
2.5 µM
C
Relative Cell Viability
1.6
1.2
0.8
0.4
0
0uM
1uM
2.5uM
5uM
7.5uM
10uM
15uM
20uM
(CsA)
D
Relative sphere formation
1.2
1
0.8
0.6
0.4
0.2
0
CTL
2.5uM
5uM
(CsA)
SCC4
CTL
2.5uM
5uM
E
# of migrated cells
300
250
200
150
100
50
0
CTL
2.5 µM
5 µM
(CsA)
SCC4
CTL
2.5uM
5uM

Figure 9. Inhibition of NFAT signaling suppress CSC phenotype in HOK-16B/Orai1 and OSCC.

(A) Effect of NFAT antagonist, cyclosporine A (CsA), on self-renewal capacity of HOK-16B/Orai1 was determined by tumor sphere formation assay. *$P < 0.05$ by two-tailed Student's *t* test. Representative images of tumor spheres formed by HOK-16B/Orai1 exposed to the NFAT inhibitor are shown on the right. (B) Effect of the NFAT inhibitor on migration ability in HOK-16B/Orai1 was determined by transwell migration assay. *$P < 0.05$ by two-tailed Student's *t* test. Representative images of transwell migration assay are shown on the right. (C) Effect of NFAT inhibitor CsA on cell viability of SCC4 determined by MTT assay. 2000 cells were seeded in 96-well plate with different doses of CsA and grown for 6 days and cell viability was measured using he MTT assay kit. (D) Effect of NFAT inhibitor CsA on self-renewal capacity of SCC4 was determined by tumor sphere formation assay. *$P < 0.01$ by two-tailed Student's *t* test. Representative images of tumor spheres formed by SCC4 exposed to CsA are shown on the right. (E) Effect of NFAT inhibitor CsA on migration ability in SCC4 was determined by transwell migration assay. *$P < 0.01$ by two-tailed Student's *t* test. Representative images are shown on the right.

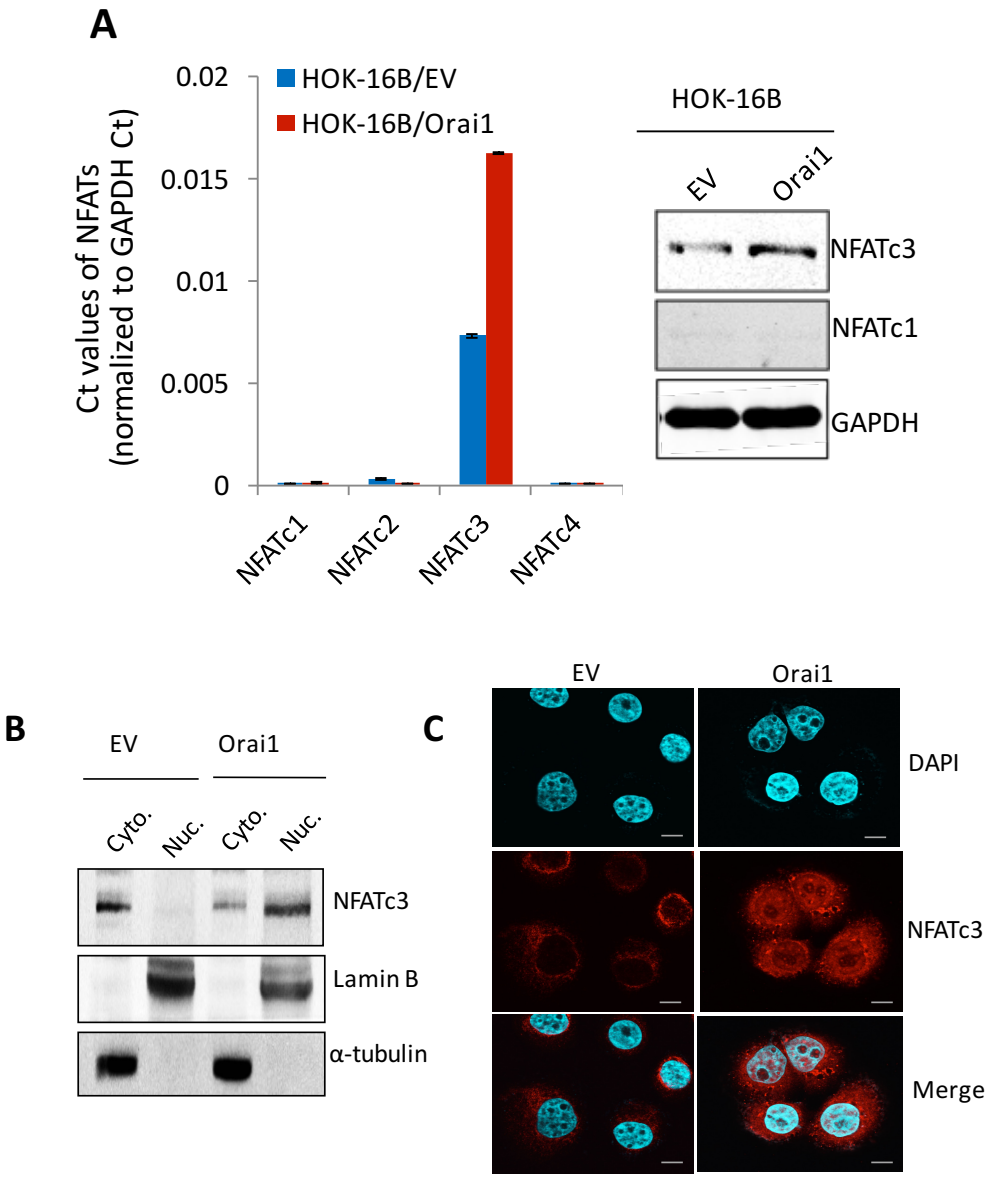
A
0.02
0.015
0.01
0.005
0
HOK-16B/EV
HOK-16B/Orai1
Ct values of NFATs
(normalized to GAPDH Ct)
NFATc1
NFATc2
NFATc3
NFATc4
HOK-16B
EV
Orai1
NFATc3
NFATc1
GAPDH
B
EV
Orai1
Cyto.
Nuc.
Cyto.
Nuc.
NFATc3
Lamin B
α-tubulin
C
EV
Orai1
DAPI
NFATc3
Merge

Figure 10. NFATc3 is increased and activated by Orai1 in HOK-16B.

(A) Effect of Orai1on the expression of NFAT isoforms (NFATc1, NFATc2, NFATc3, and NFATc4) in HOK-16B was determined by real-time qPCR (left) and Western blot analysis (right). The Ct values for 4 NFAT isoforms were normalized by the CT value of GAPDH. (B) Effect of Orai1 on the intracellular localization of NFATc3 was determined by Western blot analysis using the cytoplasmic (Cyto.) and nuclear (Nuc.) extracts. Lamin B is a nuclear protein. α-tubulin is a cytoplasmic protein. (C) Effect of Orai1 on the intracellular localization of NFATc3 was determined by confocal laser scanning microscopy. After cell permeabilization and blocking, cells were probed with NFATc3 primary antibody overnight, then with Alexa Fluor 594 dye-conjugated secondary antibody and DAPI (blue-green) for confocal laser scanning. HOK-16B/EV has NFATc3 immunofluorescence staining (red) mainly in the cytoplasm while HOK-16B/Orai1 has stronger staining both in the cytoplasm and the nucleus, which indicates increased NFATc3 expression as well as dominant nuclear translocation. Representative images were taken at 50X.

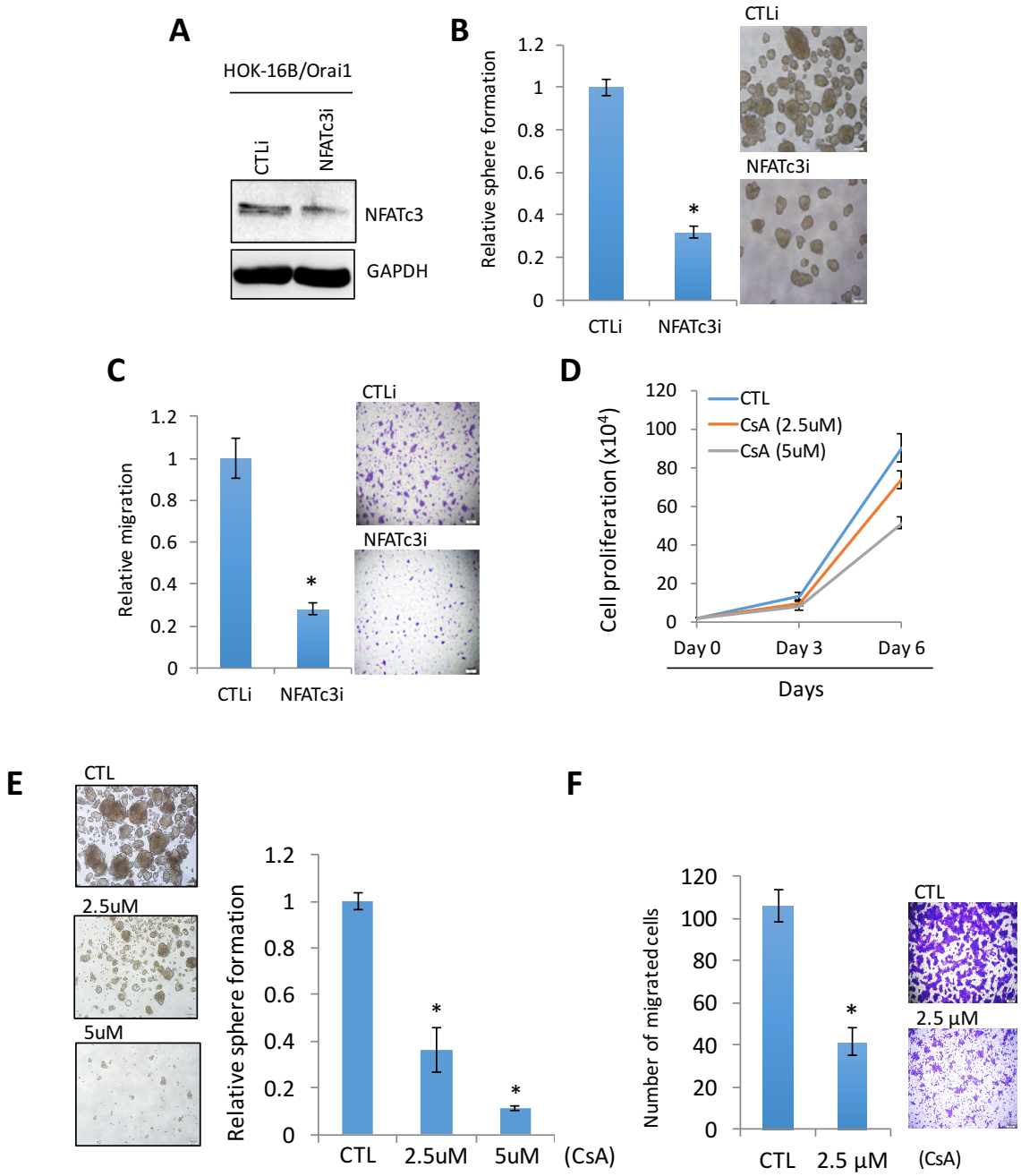
A
HOK-16B/Orai1
CTLi
NFATc3i
NFATc3
GAPDH
B
Relative sphere formation
1.2
1
0.8
0.6
0.4
0.2
0
CTLi
NFATc3i
*
CTLi
NFATc3i
C
Relative migration
1.2
1
0.8
0.6
0.4
0.2
0
CTLi
NFATc3i
*
CTLi
NFATc3i
D
Cell proliferation (x10⁴)
120
100
80
60
40
20
0
CTL
CsA (2.5uM)
CsA (5uM)
Day 0
Day 3
Day 6
Days
E
CTL
2.5uM
5uM
Relative sphere formation
1.2
1
0.8
0.6
0.4
0.2
0
*
*
CTL
2.5uM
5uM
(CsA)
F
Number of migrated cells
120
100
80
60
40
20
0
*
CTL
2.5 µM
(CsA)
CTL
2.5 µM

Figure 11. NFATc3 knockdown suppresses CSC phenotype in HOK-16B/Orai1.

(A) Endogenous NFATc3 was knocked down in HOK-16B/Orai1 using siRNA against NFATc3 (NFATc3i). The cells transfected with control siRNA (CTLi) were included for comparison. Knockdown of NFATc3 was confirmed by Western blot analysis. (B) NFATc3 knockdown effect on self-renewal capacity of HOK-16B/Orai1 was determined by tumor sphere formation assay. Representative images of tumor spheres formed by HOK-16B/Orai1 transfected with control siRNA (HOK-16B/Orai1/CTLi) and NFATc3 siRNA (HOK-16B/Orai1/NFATc3i) are shown on the right. (C) NFATc3 knockdown effect on migration ability in HOK-16B/Orai1 was determined by transwell migration assay. Representative images of transwell migration assay are shown on the right. (D) The effect of CsA on cell viability of HOK/16B was determined by MTT assay. (E) Effect of CsA on self-renewal was determine by tumor sphere formation assay. 3000 cells were seeded in 6-well ultralow gravity plate and grown in conditioned medium for 7 days. (F) Effect of CsA on cell migration was determined by transwell migration assay. Bottom chamber was incubated with CsA for 96 hours.

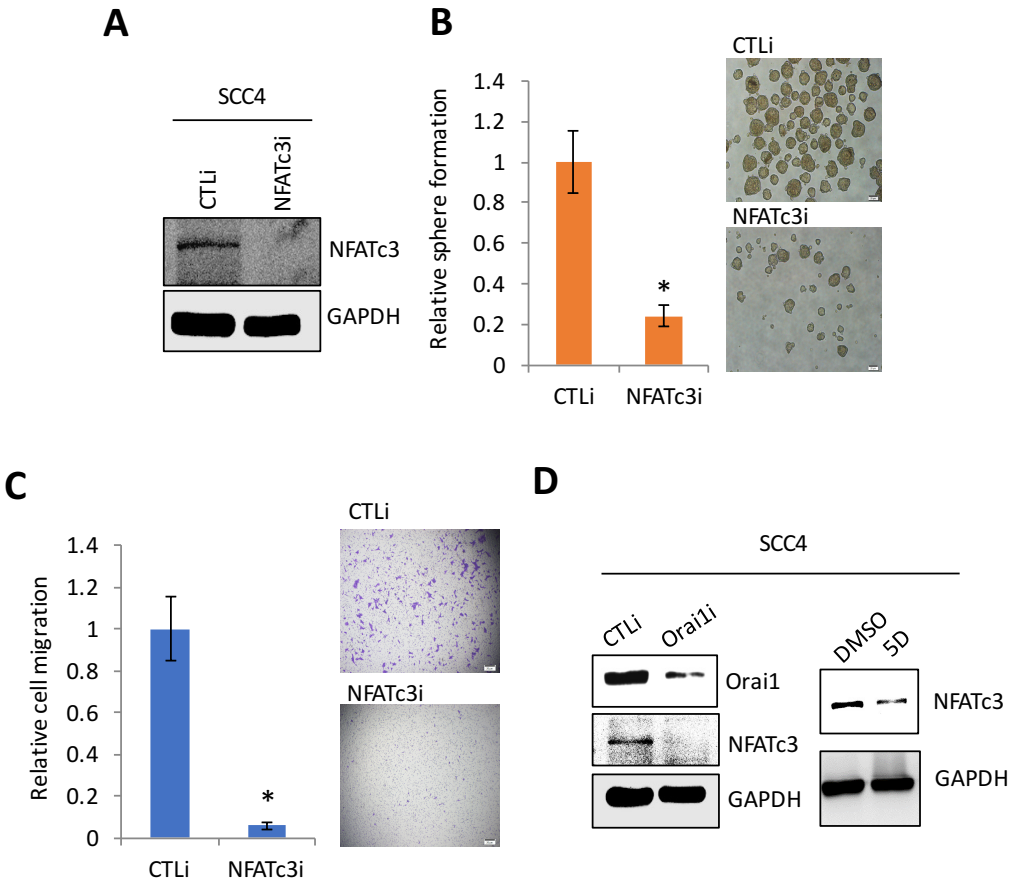
A
SCC4
CTLi
NFATc3i
NFATc3
GAPDH
B
Relative sphere formation
1.4
1.2
1
0.8
0.6
0.4
0.2
0
*
CTLi
NFATc3i
CTLi
NFATc3i
C
Relative cell migration
1.4
1.2
1
0.8
0.6
0.4
0.2
0
*
CTLi
NFATc3i
CTLi
NFATc3i
D
SCC4
CTLi
Orai1i
Orai1
NFATc3
GAPDH
DMSO
5D
NFATc3
GAPDH

Figure 12. Inhibition of NFATc3 suppresses CSC phenotypes in OSCC.

(A) Endogenous NFATc3 was knocked down in SCC4 using siRNA against NFATc3 (NFATc3i). The cells transfected with control siRNA (CTLi) were included for comparison. (B) Effect of NFATc3 knockdown on self-renewal capacity of SCC4 was determined by tumor sphere formation assay. Data are means ± SD of triplicate experiments. Represntative images were taken at 50X magnification. (C) Effect of NFATc3 knockdown on migration ability of SCC4 was determined by transwell chamber. Migration ability was described as number of migrated cells per field with data as mean ± SD for 3 randomly selected fields. *$P < 0.05$ by two-tailed Student's *t* test. (D) Direct effect of Orai1 knock down and *compound 5D* on NFATc3 expression level in SCC4 was determined by Western Blot. Cell lysates were prepared after 2-day post Orai1i and compound 5D treatment.

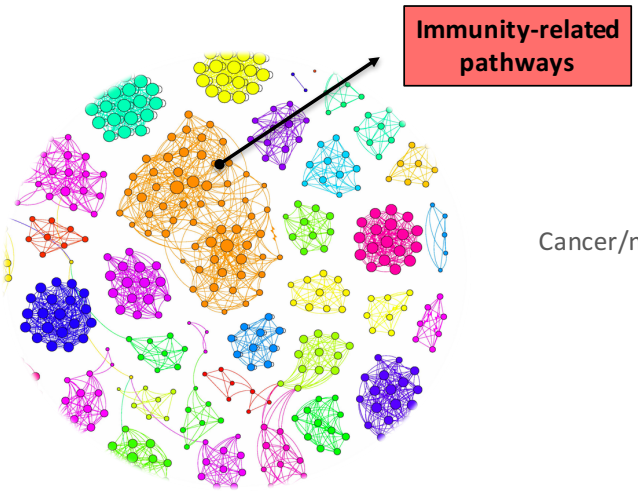

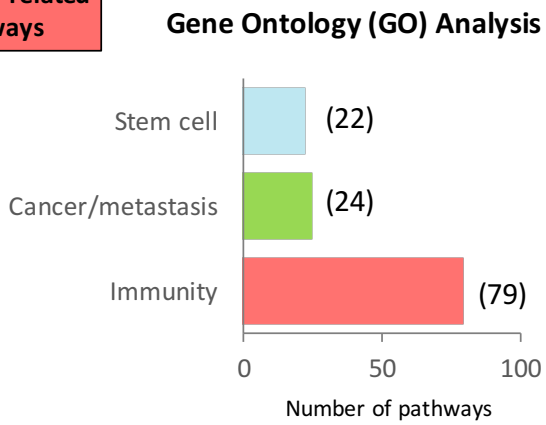

- Genes upregulated 2-folds or higher were used for the gene ontology (GO) analysis.
- Orai1 upregulated 275 pathways

Figure 13. Orai1 globally upregulated human transcription profile in HOK-16B.

Using HOK-16B/EV and HOK-16B/Orai1 cells, expression level of global human genes were determined by performing a high-throughput microarray using Human Genome U133 Plus Array. Analysis of the microarray was performed by UCLA Technology Center for Genomics & Bioinformatics. Gene ontology analysis of genes upregulated 2 folds or higher revealed upregulation of 275 pathways, including stem cell, cancer/metastasis-related and immunity-related pathway.

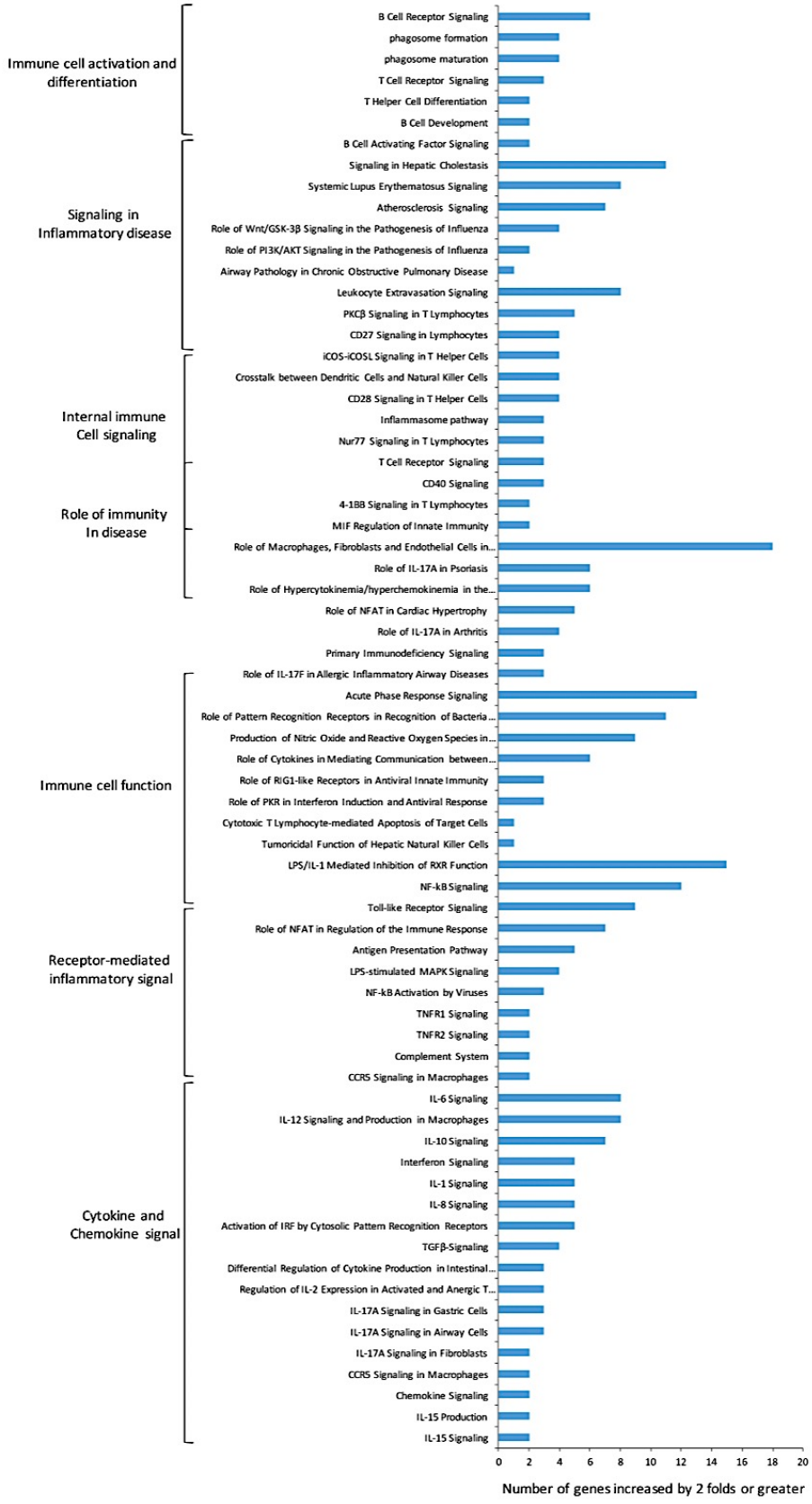
Immune cell activation and differentiation
Signaling in Inflammatory disease
Internal immune Cell signaling
Role of immunity In disease
Immune cell function
Receptor-mediated inflammatory signal
Cytokine and Chemokine signal
B Cell Receptor Signaling
phagosome formation
phagosome maturation
T Cell Receptor Signaling
T Helper Cell Differentiation
B Cell Development
B Cell Activating Factor Signaling
Signaling in Hepatic Cholestasis
Systemic Lupus Erythematosus Signaling
Atherosclerosis Signaling
Role of Wnt/GSK-3β Signaling in the Pathogenesis of Influenza
Role of PI3K/AKT Signaling in the Pathogenesis of Influenza
Airway Pathology in Chronic Obstructive Pulmonary Disease
Leukocyte Extravasation Signaling
PKCβ Signaling in T Lymphocytes
CD27 Signaling in Lymphocytes
iCOS-iCOSL Signaling in T Helper Cells
Crosstalk between Dendritic Cells and Natural Killer Cells
CD28 Signaling in T Helper Cells
Inflammasome pathway
Nur77 Signaling in T Lymphocytes
T Cell Receptor Signaling
CD40 Signaling
4-1BB Signaling in T Lymphocytes
MIF Regulation of Innate Immunity
Role of Macrophages, Fibroblasts and Endothelial Cells in...
Role of IL-17A in Psoriasis
Role of Hypercytokinemia/hyperchemokinemia in the...
Role of NFAT in Cardiac Hypertrophy
Role of IL-17A in Arthritis
Primary Immunodeficiency Signaling
Role of IL-17F in Allergic Inflammatory Airway Diseases
Acute Phase Response Signaling
Role of Pattern Recognition Receptors in Recognition of Bacteria ...
Production of Nitric Oxide and Reactive Oxygen Species in ...
Role of Cytokines in Mediating Communication between...
Role of RIG1-like Receptors in Antiviral Innate Immunity
Role of PKR in Interferon Induction and Antiviral Response
Cytotoxic T Lymphocyte-mediated Apoptosis of Target Cells
Tumoricidal Function of Hepatic Natural Killer Cells
LPS/IL-1 Mediated Inhibition of RXR Function
NF-kB Signaling
Toll-like Receptor Signaling
Role of NFAT in Regulation of the Immune Response
Antigen Presentation Pathway
LPS-stimulated MAPK Signaling
NF-kB Activation by Viruses
TNFR1 Signaling
TNFR2 Signaling
Complement System
CCR5 Signaling in Macrophages
IL-6 Signaling
IL-12 Signaling and Production in Macrophages
IL-10 Signaling
Interferon Signaling
IL-1 Signaling
IL-8 Signaling
Activation of IRF by Cytosolic Pattern Recognition Receptors
TGFβ-Signaling
Differential Regulation of Cytokine Production in Intestinal...
Regulation of IL-2 Expression in Activated and Anergic T...
IL-17A Signaling in Gastric Cells
IL-17A Signaling in Airway Cells
IL-17A Signaling in Fibroblasts
CCR5 Signaling in Macrophages
Chemokine Signaling
IL-15 Production
IL-15 Signaling
0
2
4
6
8
10
12
14
16
18
20
Number of genes increased by 2 folds or greater

Fig 14. Orai1 overexpression induced global upregulation of genes involved in immunity-related signaling in HOK-16B/Orai1 cells.

From gene ontology analysis of the microarray data revealed groups of upregulation of various immunity-related canonical pathways by overexpression of Orai1 in HOK-16B cells. Fold induction greater than or equal to 2 was used for the analysis. Number of genes regulated in each pathway is indicated next to the name of each pathway.

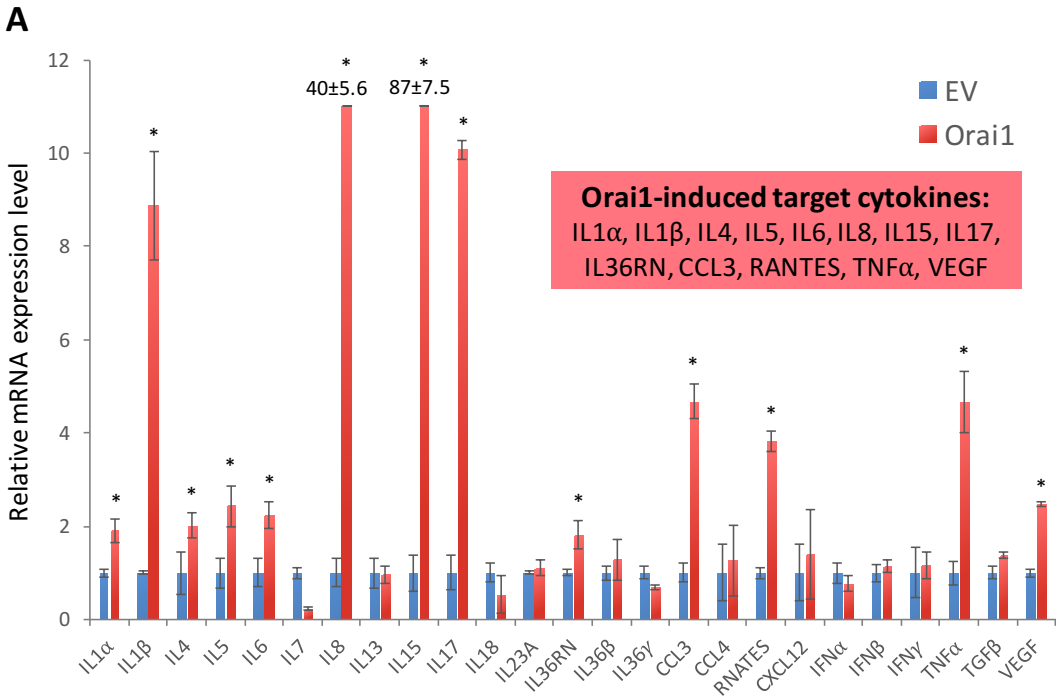
A
Relative mRNA expression level
12
10
8
6
4
2
0
40±5.6
87±7.5
EV
Orai1
Orai1-induced target cytokines:
IL1α, IL1β, IL4, IL5, IL6, IL8, IL15, IL17,
IL36RN, CCL3, RANTES, TNFα, VEGF
IL1α
IL1β
IL4
IL5
IL6
IL7
IL8
IL13
IL15
IL17
IL18
IL23A
IL36RN
IL36β
IL36γ
CCL3
CCL4
RNATES
CXCL12
IFNα
IFNβ
IFNγ
TNFα
TGFβ
VEGF

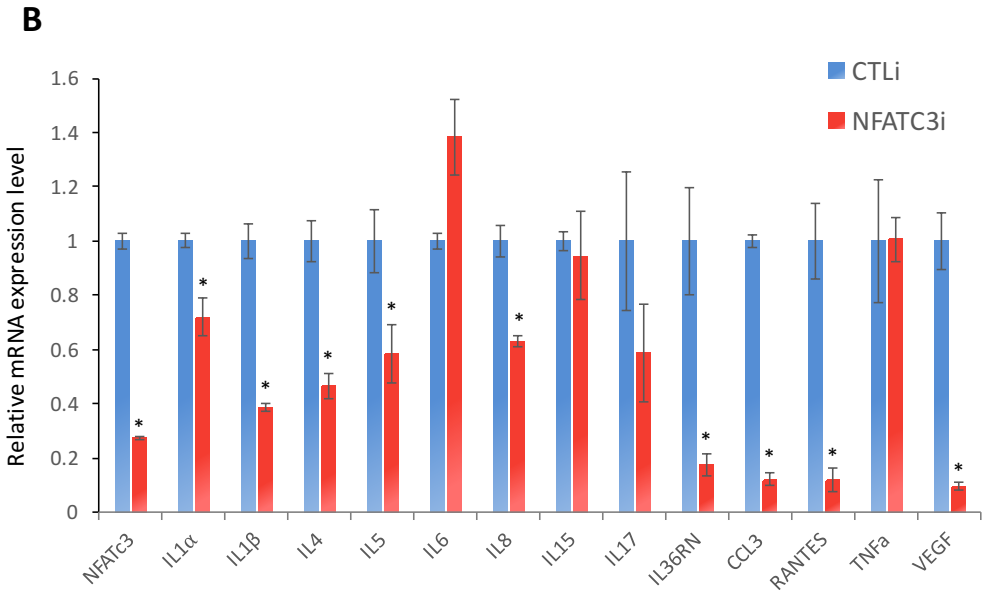
B
Relative mRNA expression level
1.6
1.4
1.2
1
0.8
0.6
0.4
0.2
0
CTLi
NFATC3i
NFATc3
IL1α
IL1β
IL4
IL5
IL6
IL8
IL15
IL17
IL36RN
CCL3
RANTES
TNFa
VEGF

Figure 15. Cytokine genes expression are regulated in Orai1-NFATc3 axis.

(A) Cytokine gene expression was compared between the HOK-16B/EV and HOK-16B/Orai1 cells by qPCR analysis. The Ct values for each gene were normalized by the CT value of GAPDH. *$P < 0.05$ by two-tailed Student's *t* test. (B) Expression of subset of Orai1-induced cytokine genes were compared between the HOK-16B/Orai1 and HOK-16B/Orai1/NFATc3i cells. Fold induction of cytokine genes expression in HOK-16B/Orai1 is relative to HOK-16B/EV control cells (indicated as dashed line), and the same in HOK-16B/Orai1/NFATc3i is relative to HOK-16B/Orai1/CTLi cells. *$P < 0.005$ by two-tailed Student's *t* test.

A **Gene Signatures**

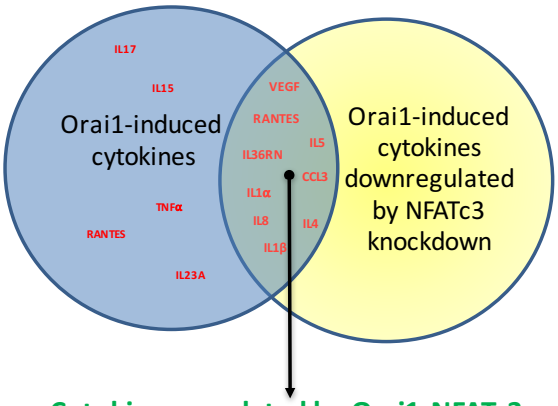

Cytokines regulated by Orai1-NFATc3 axis

(IL1α, IL1β, IL4, IL5, IL8, IL36RN, CCL3, RANTES, VEGF)

B

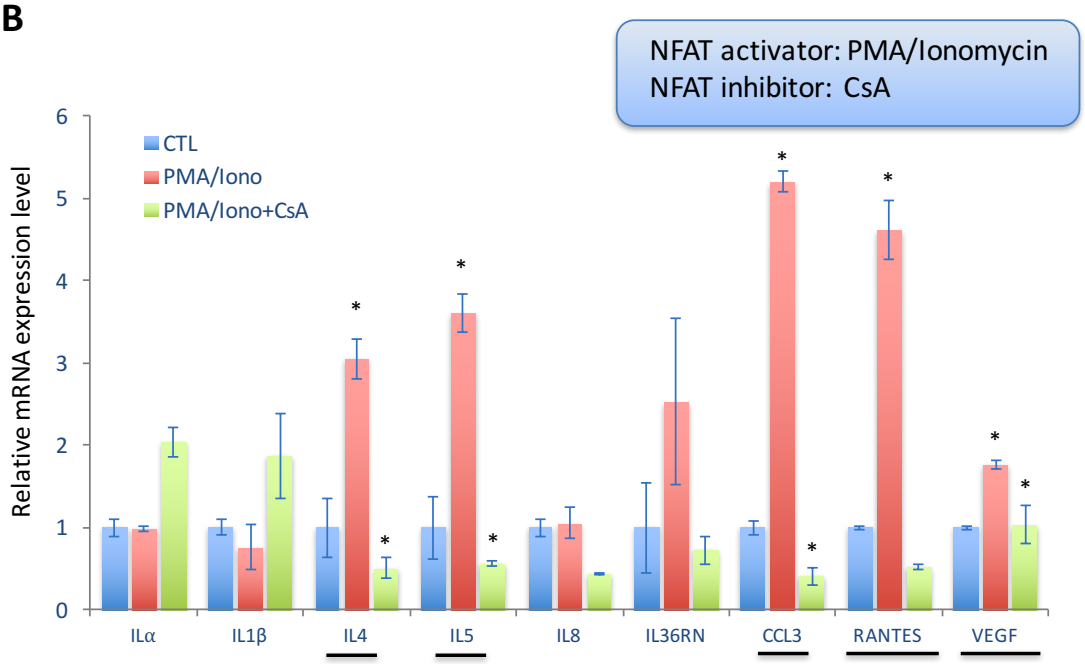

Figure 16. Orai1-induced cytokines are regulated by NFAT signaling.

(A) Gene signature demonstrating the cytokines regulated by Orai1-NFATc3 axis. (B) Regulation of cytokines by NFAT signaling is determined by comparing each gene expression in SCC4 treated with and/or without NFAT activator or inhibitor. 100nM of PMA/Ionomycin and 10uM of CsA was used to treat cells for 2 days prior to collection and the level of cytokine genes expression was determined by qPCR. Cytokines upregulated in HOK-16B/Orai1 cells are underlined. *$P < 0.05$ by two-tailed Student's *t* test. (*Figure obtained from Master's thesis work of Nicole Rigas*)

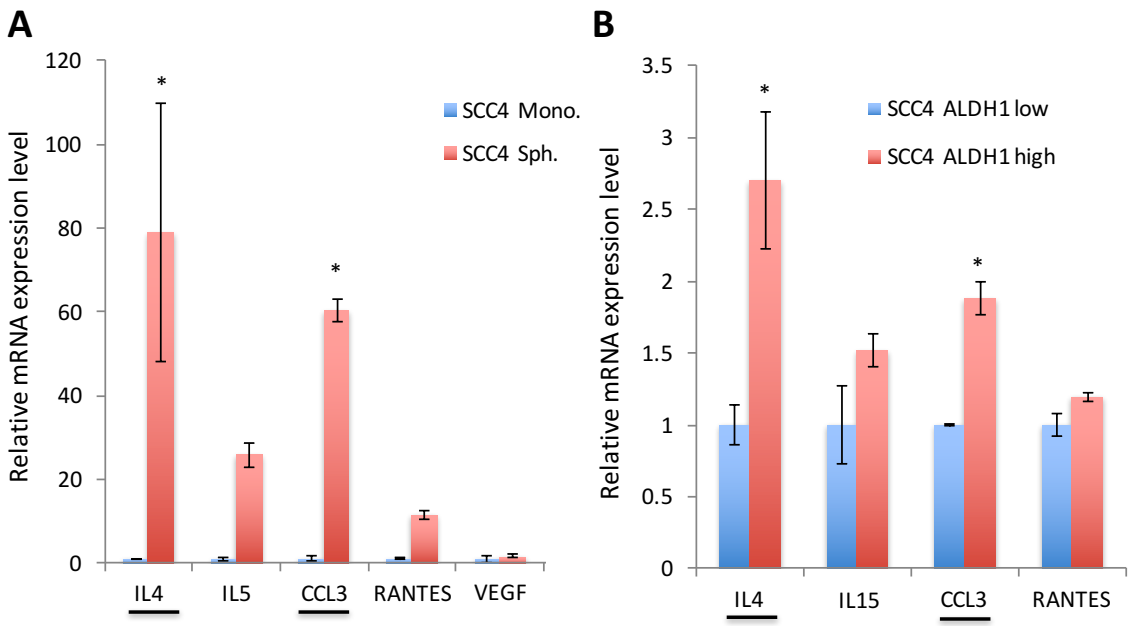
A
Relative mRNA expression level
120
100
80
60
40
20
0
SCC4 Mono.
SCC4 Sph.
*
*
IL4
IL5
CCL3
RANTES
VEGF
B
Relative mRNA expression level
3.5
3
2.5
2
1.5
1
0.5
0
SCC4 ALDH1 low
SCC4 ALDH1 high
*
*
IL4
IL15
CCL3
RANTES

Figure 17. Orai1-NFATc3 cytokines are upregulated in CSC population.

(A) Expression level of cytokines was compared between SCC4 monolayer and spheres. Spheres were prepared by performing sphere assay using $1x10^4$ SCC4 cells. Sphere cells were collected at day 7 with the monolayers and cytokine genes expression change was determined by qPCR. Ct values of each gene was normalized against GAPDH. Cytokines upregulated in HOK-16B/Orai1 cells are underlined. *$P < 0.025$ by two-tailed Student's *t* test. (B) Expression level of cytokines was compared between $ALDH1^{high}$ and $ALDH1^{low}$ population. $ALDH1^{high}$ and $ALDH1^{low}$ cells are prepared by using Aldehyde Dehydrogenase-Based Cell Detction Kit (STEMCELL). Total 3 x 10^7 cells were used for fluorescent data acquisition and sorting by using a BD FACScan flow cytometer (BD Biosciences). * $P < 0.05$ by two-tailed Student's *t* test.

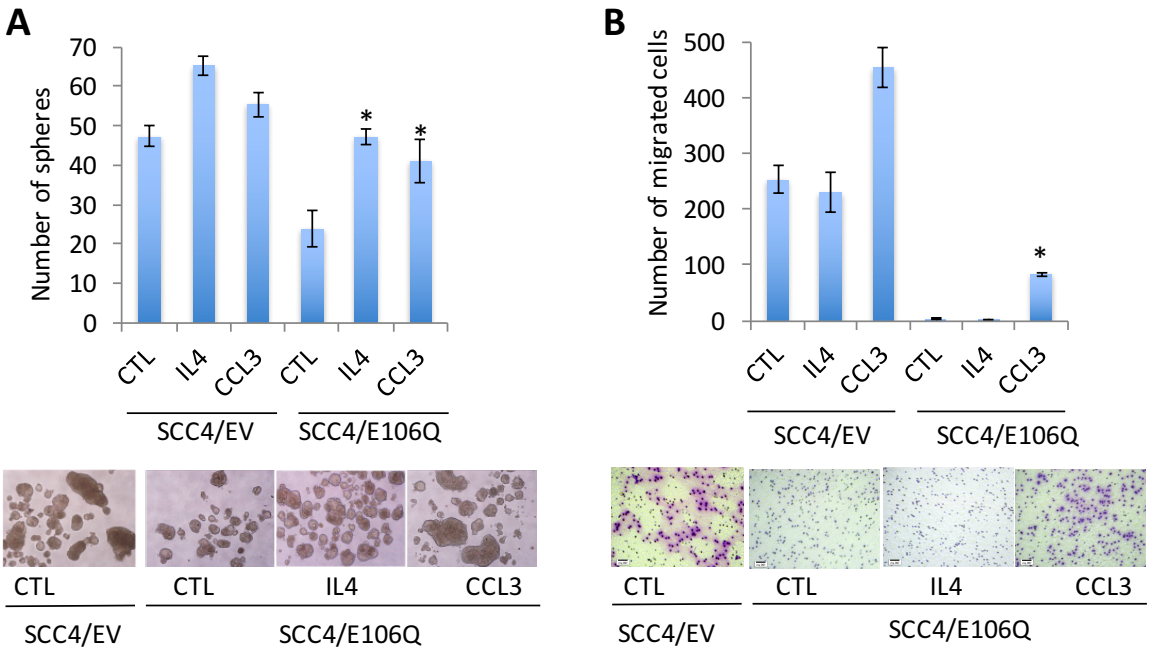
A
Number of spheres
70
60
50
40
30
20
10
0
CTL
IL4
CCL3
CTL
IL4
CCL3
*
*
SCC4/EV
SCC4/E106Q
CTL
CTL
IL4
CCL3
SCC4/EV
SCC4/E106Q
B
Number of migrated cells
500
400
300
200
100
0
CTL
IL4
CCL3
CTL
IL4
CCL3
*
SCC4/EV
SCC4/E106Q
CTL
CTL
IL4
CCL3
SCC4/EV
SCC4/E106Q

Figure 18. IL4 and CCL3 rescued CSC phenotypes in Orai1-inhibited OSCC.

(A) Effect of IL4 and CCL3 treatment on self-renewal capacity in SCC4/E106Q was determined by performing sphere formation assay. **P* < 0.05 by two-tailed Student's *t* test. Representative image is shown below the graph. (B) Effect of IL4 and CCL3 on cell migration was determined by performing transwell migration assay. Representative image is shown below the graph. Migration ability was described as number of migrated cells per field with data as mean ± SD for *3 randomly selected fields*. **P* < 0.05 by two-tailed Student's *t* test.

A

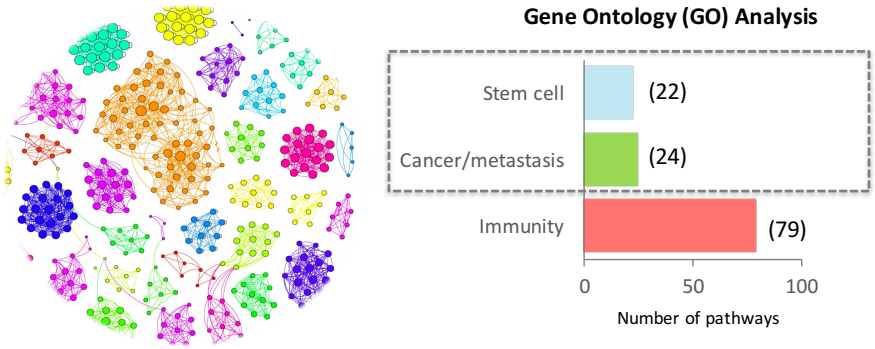

- Genes upregulated 2-folds or higher were used for the gene ontology (GO) analysis.
- Orai1 upregulated 275 pathways

B

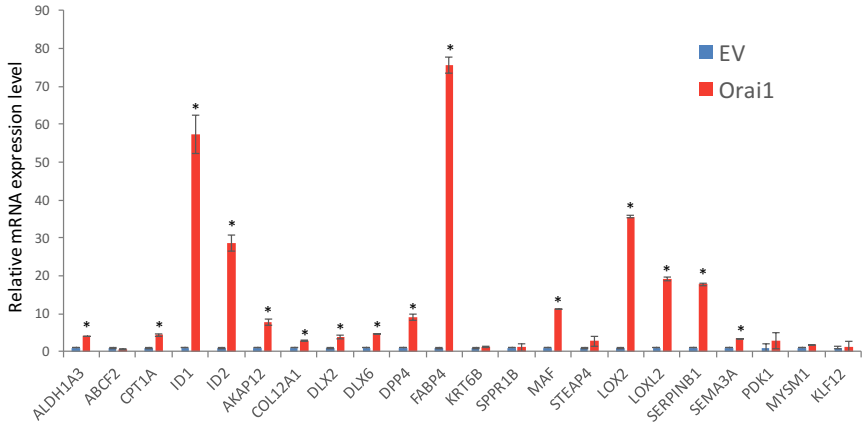

C

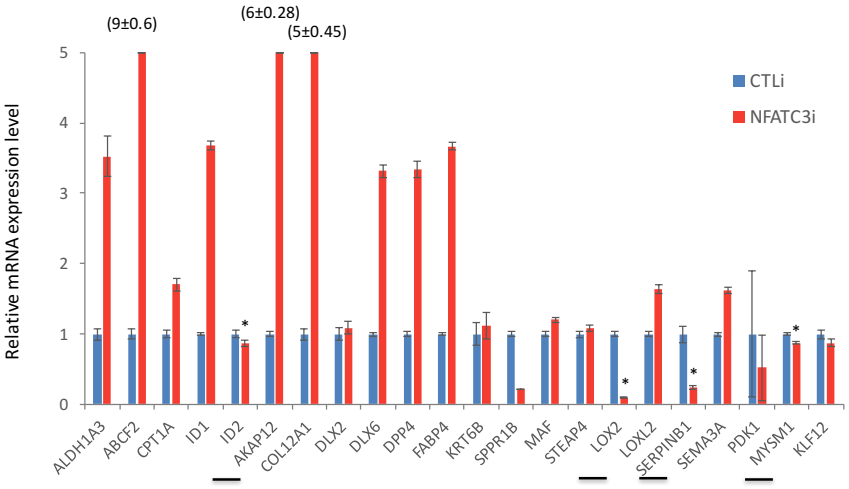

Figure 19. Orai1-induced stem cell and cancer/metastasis-related genes are regulated by NFATc3.

(A) Gene ontology analysis of genes upregulated 2 folds or higher revealed upregulation of 22 stem cell and 24 cancer/metastasis-related pathways out of 275 pathways upregulated by Orai1 in HOK-16B. (B) Validation of upregulated Orai1-induced genes in the HOK-16B by qRT-PCR revealed 15 genes upregulated by Orai1. Ct values of each gene was normalized against GAPDH. *$P < 0.01$ by two-tailed Student's *t* test. (C) 4 out of 15 Orai1-induced genes were regulated by NFATc3 and was determined by performing qRT-PCR using HOK-16B/Orai1/EV and HOK-16B/Orai1/NFATc3i cells. *$P < 0.01$ by two-tailed Student's *t* test.

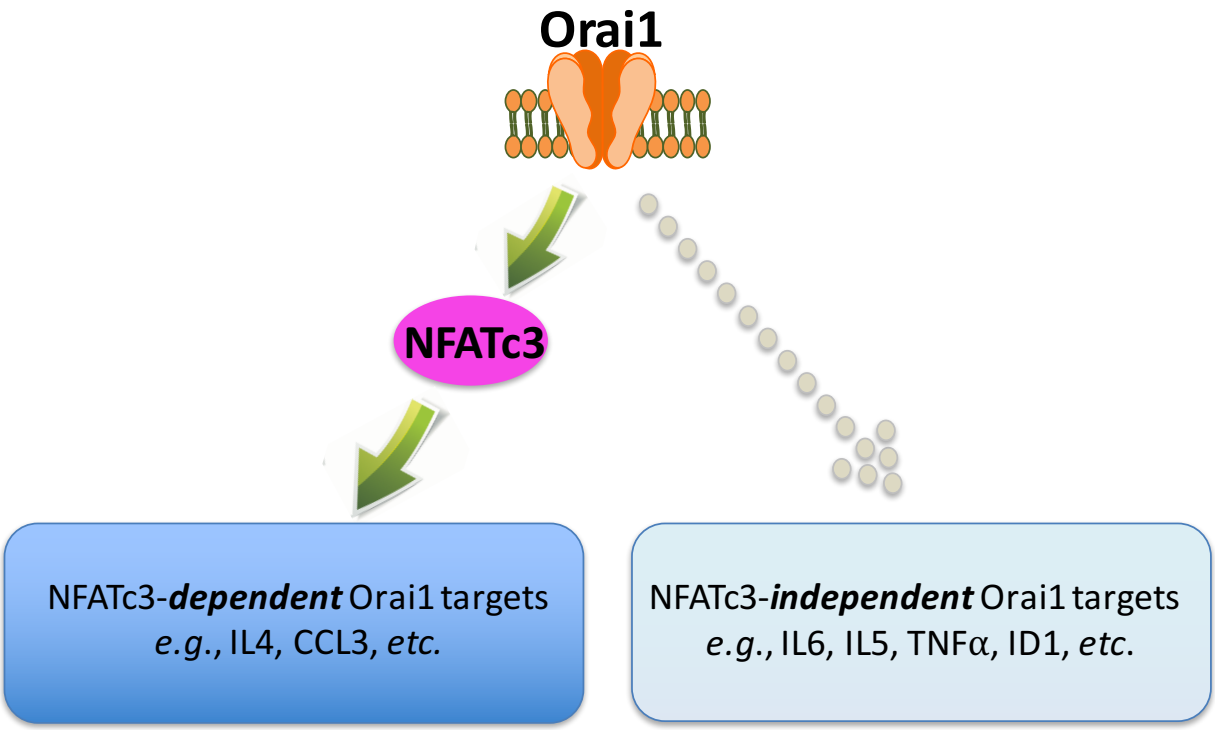
Orai1
NFATc3
NFATc3-*dependent* Orai1 targets
e.g., IL4, CCL3, *etc.*
NFATc3-*independent* Orai1 targets
e.g., IL6, IL5, TNFα, ID1, *etc.*

Figure 20. Orai1-induced genes are regulated in NFAT-dependent and NFAT-independent manner.

Figure demonstrating that Orai1 regulate CSC phenotypes via inducing upregulation of genes, *i.e*., *IL4* and *CCL3* regulated in NFATc3-dependent manner. Orai1-NFATc3 target cytokines have shown its rescue effect on CSC phenotypes in Orai1-inhibited OSCC, SCC4/E106Q. Also, further validation of Orai1-induced genes revealed group of genes, *i.e*., *IL6, IL5, TNFα, ID*1, *etc*., regulated by NFATc3-independent pathways.

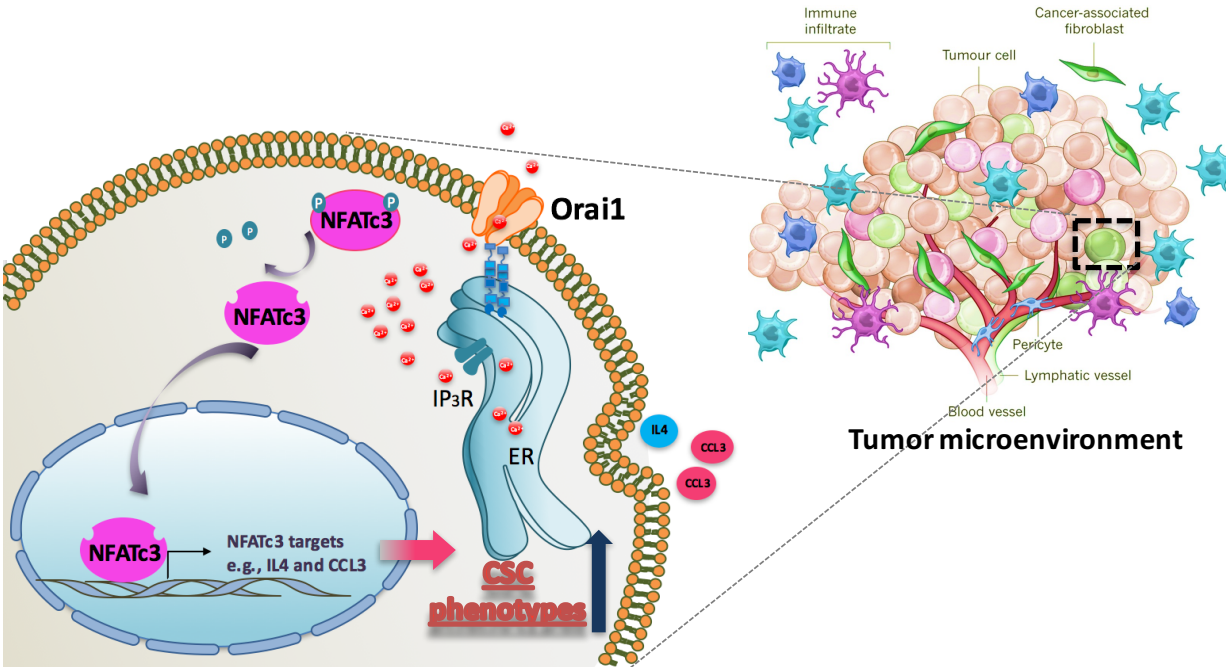
Immune infiltrate
Cancer-associated fibroblast
Tumour cell
Pericyte
Lymphatic vessel
Blood vessel
Tumor microenvironment
Orai1
NFATc3
NFATc3
IP3R
ER
IL4
CCL3
CCL3
NFATc3
NFATc3 targets
e.g., IL4 and CCL3
CSC
phenotypes

Figure 21. Proposed model: Orai1-NFATc3-Cytokine signaling governs cancer stemness in tumor microenvironment.

Schematic figure demonstrating the mechanism by which Orai1 promotes oral cancer progressing. This study reports noble CSCs regulation pathway, Orai1- NFATc3-Cytokine signaling pathway. This figure propose that Orai1-NFATc3-Cytokine axis may work in autocrine fashion to regulate CSC phenotypes and may also signals cells in the tumor microenvironment by paracrine fashion to drive more favorable tumor microenvironment for oral cancer growth, progression and metastasis.

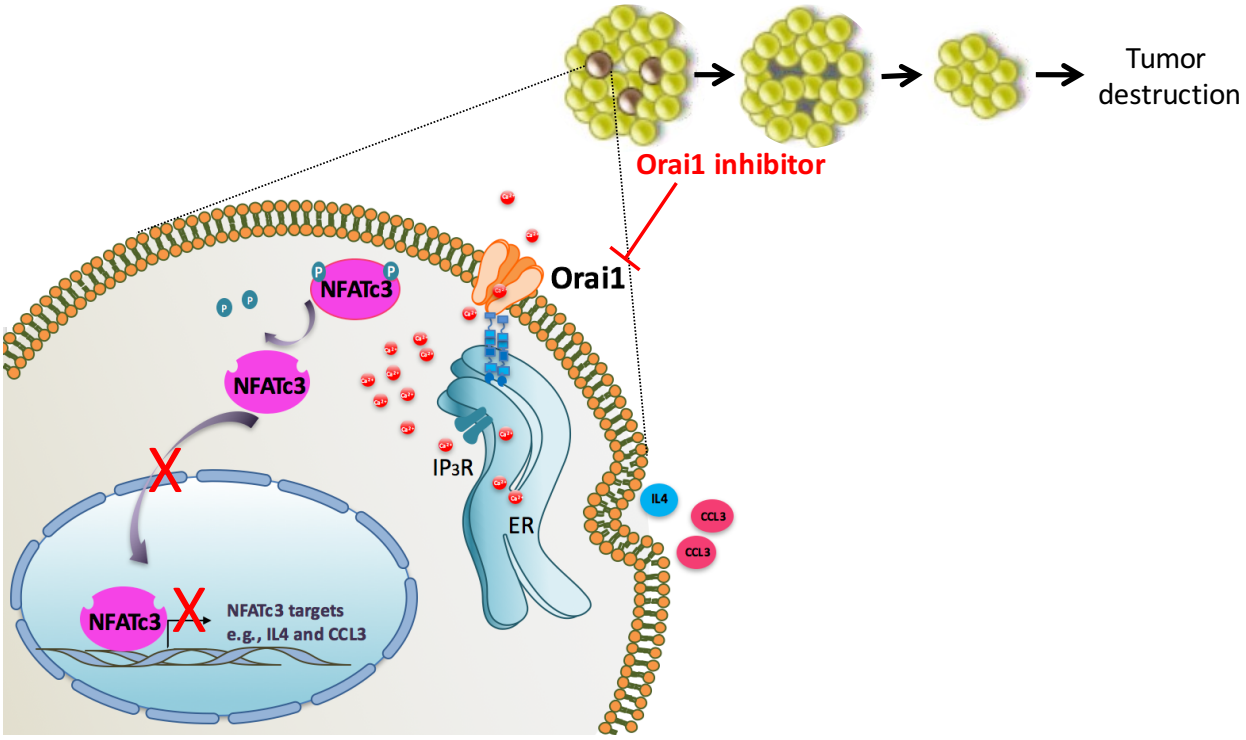
Tumor
destruction
Orai1 inhibitor
Orai1
NFATc3
NFATc3
IP3R
ER
IL4
CCL3
CCL3
NFATc3
NFATc3 targets
e.g., IL4 and CCL3

Figure 22. Orai1-mediated signaling may be a novel therapeutic target for oral cancer treatment.

This figure demonstrates the presence of oral CSCs regulated by Orai1-NFATc3-Cytokine axis within a tumor. As demonstrated in this study, Orai1is the key regulator of tumor formation as well as CSC phenotypes. Recently, potent Orai1 chemical blocker 5D has been identified to suppress Orai1 function (Kim *et al*., 2014). Therefore, our study proposes for the first time that targeting CSCs regulator, Orai1, by using Orai1 chemical inhibitor 5D may halt CSC growth and may offer a therapeutic modality against oral cancer.

Table 1. Human genes primer sequences used for real time qPCR

Gene	Forward (5'-3')	REVERSE
ABCF2	GAAGATCATTGGGCGATACG	CGTCTGACAAGTTCCGGATT
ALDH1	TTTGGTGGATTCAAGATGTCT	CACTGTGACTGTTTTGACCTC
ALDH1A3	TGGTGGCTTTAAAATGTCAGG	TATTCGGCCAAAGCGTATTC
AKAP12	AACGGTCAAGGAGCCCTAAA	TTCAGAGTCTCTCTGTCCAACCT
BMI1	CTGGTTGCCCATTGACAGC	CAGAAAATGAATGCGAGCCA
BMP2	CAGACCACCGGTTGGAGA	CCACTCGRRRCTGGTAGTTCTTC
BMP4	AGCCCTAAGACATCACTCACAG	TGAAGTCCACATAGAGCGAGTG
CMYC	CCACAAGGCCCTCAGTACC	CCTCTTCATCATCTTCATCATC
CCND1	CCATCCAGTGGAGGTTTGTC	GTGGGACAGGTGGCCTTT
COL12A1	CCCTGCTCCTGTCTTCCAT	TCCACCAGCAACACAATGTC
CPT1A	CCTCCAGTTGGCTTATCGTG	TTCTTCGTCTGGCTGGACAT
DLX2	AGCAGCTATGACCTGGGCTA	AATTTCAGGCTCAAGGTCCTC
DLX6	CCTCGGACCATTTATTCCAG	TTGTTCTGAAACCATATCTTCACC
DPP4	GCACGGCAACACATTGAA	TGAGGTTCTGAAGGCCTAAATC
GAPDH	AGCCACATCGCTCAGACAC	GCCCAATACGACCAAATCC
EZH2	ATGGCACCTGCAGAAGGA	TTGGGAAGCCGTCCTCTT
FABP4	CCACCATAAAGAGAAAACGAGAG	GTGGAAGTGACGCCTTTCAT
FGF4	TACTGCAACGTGGGCATC	GTGCACTCATCGGTGAAGAA
GLI1	AGGAATTTGACTCCCAAGAGC	GGCTTTGAAGGGCCTCAG
HES1	GTGAAGCACCTCCGGAAC	GTCACCTCGTTCATGCACTC
ID2	TGTCAAATGACAGCAAAGCAC	GTTGTTGTTGTGCAAAGAATAAAAG
ID1	CCAGAACCGCAAGGTGAG	GGTCCCTGATGTAGTCGATGA
KLF4	CTCCATTACCAAGAGCTCATG	GAACTCTTTGTGTAGGTTTTG
KLF12	GGGACTCTGTGTGAGGGAAA	TGTTCTTAGAGTCACATTGATCCTG
KRT6B	TGAGGAGATTGCTCAGAGGAG	GATCTGCAGCTCCTCGTACTTT
LIN28A	AAAAGGTACCGTGACTCAATT	AAAACTCGAGCCCGAGCTCGA
LOX	CTTTGCAAACGTGCCAGAA	GGGCAGTGTCTGGAGTGAAG
LOXL2	GGAGAGGACATACAATACCAAAGTG	CCATGGAGAATGGCCAGTAG
MAF	AGCGGCTTCCGAGAAAAC	GCGAGTGGGCTCAGTTATG
MYSM1	CAGGTGAAAGTGGCTTCAGA	GAGTATCTTCCTCCTAACAGACCAA
NANOG	AGATGCCTCACACGGAGACT	TCTCTGCAGAAGTGGGTTGTT
NFATc3	CAGTTTCTTTCAGTTCCTTCAC	TGCGAAATATAGGGGTGTGG
OCT4	GAAACCCACACTGCAGATCA	CGGTTACAGAACCACACTCG
ORAI1	CAGCAGCCAACGTCAGCACCA	CAGCTGGTCCTGTAAGCGGGCA
PDK1	GCTTCATCCAGGAACATTGG	CCGAGTCCCGCTAGAGAA
SEMA3A	TGAAATTGGACATCATCCTGAG	GGCCGTTTTCAAAATGTGAG
SERPINB1	TCAGCTTGCCCAGGTTCAAACTG	GGATGCTACCTGAGGAATTATGC
SOX2	TCTCATGATGTTCAACCATTCAC	CACATTTACATTCAAAGCACCAG

Table 1. ***Continued***

Gene	Forward (5'-3')	REVERSE
SPRR1B	CAGAGTATTCCTCTCTTCACACCA	CAAGGCTGTTTCACCTGCT
STEAP4	ACACAGAACACACGCTCCTT	TGACGGACTATGAGCCAGGA
STIM1	AGTGAGAAGGCGACAGGAAC	CTTGTCAATTCGGCAAAACTC
ZEB1	GGGAGGAGCAGTGAAAGAGA	TTTCTTGCCCTTCCTTTCTG
ZEB2	AAGCCAGGGACAGATCAG	CCACACTCTGTGCATTTGAAC

Table 2. Human cytokine gene primer sequences used for real time qPCR

Genes	Forward (5'-3')	Reverse (3'-5')
BRAK	AAGCTGAAATGAAGCCAAA	TGACCTCGGTACCTGGACAC
CCL3	GGCTCTCTGCAACCAGTTCT	AATCTGCCGGGAGGTGTAG
FGF2	TTCTTCCTGCGCATCCAC	CCTCTCTCTTCTGCTTGAAGTTG
IFNα	CTCGCCCTTTGCTTTACTGAT	CTCCTGTTATCCAGGCTGTGG
IFNβ	ATGACCAACAAGTGTCTCCTC	TGCCACAGGAGCTTCTGACAC
IFNγ	ACAAGTTATATCTTGGCTTTTC	TCCGCTACATCTGAATGACCT
IL1α	ATGGCCAAAGTTCCAGACATG	TGGAGTGGGCCATAGCTTACA
IL1β	TACCTGTCCTGCGTGTTGAA	TCTTTGGTAATTTTTGGGATC
IL2	AAGTTTTACATGCCCAAGAAGG	AAGTGAAAGTTTTTGCTTTGAGC
IL4	AACTGCTTCCCCCTCTGTTCT	TCTTCTGCTCTGTGAGGGTGT
IL5	ATCCTTTAAACAAGTGGATTAGGC	GCTCTTTGGGAAGGCAAACT
IL6	AAATTCGGTACATCCTCGAC	CAGGAACTGGATCAGGACTT
IL7	TGGCAATATAGAAACACGAACTTT	TTCCACTCTGAAAAACTGCATAAG
IL8	TGCGCCAACACAGAATTAT	ATGAATCCATCCCCCTGTT
IL18	CATGTACAAAGACAGTGAAGT	TTTCAGGTGGATCCATTTCC
IL15	ATTTTGGGCTGTTTCAGTGC	TTACTTTGCAACTGGGGTGA
IL36RN	GGATTCAGCCTTGAAGGTACT	GGGACAACACTGATCTCCTCA
IL13	CTCCTCAATCCTCTCCTGTT	GTTGAACCGTCCCTCGCGAAA
MMP 3	GGTGAGGACACCAGCATGA	ATCCCTGGAAAGTCTTCAGC
RANTES	CCTCGCTGTCATCCTCATTGC	GGAGCACTTGCCACTGGTGTA
SDF1	CCAAACTGTGCCCTTCAGAT	CTTTAGCTTCGGGTCAATGC
TGFβ	TGGCGTTACCTTGGTAACC	GGTGTTGAGCCCTTTCCAG
TNFα	GGTGCTTGTTCCTCAGCCTCT	GAGAGAGGTCCCTGGGGAACT
VEGF	TCCAGGAGTACCCTGATGAGA	ATCTGCATGGTGATGTTGGAC

6. BIBLIOGRAPHY

Abdullah, L. N., and Chow, E. K. (2013). Mechanisms of chemoresistance in cancer stem cells. Clin Transl Med *2*, 3.

`Akiri, G., Sabo, E., Dafni, H., Vadasz, Z., Kartvelishvily, Y., Gan, N., Kessler, O., Cohen, T., Resnick, M., Neeman, M., and Neufeld, G. (2003). Lysyl oxidase-related protein-1 promotes tumor fibrosis and tumor progression in vivo. Cancer Res *63*, 1657-1666.

Al-Swiahb, J. N., Chen, C. H., Chuang, H. C., Fang, F. M., Tasi, H. T., and Chien, C. Y. (2010). Clinical, pathological and molecular determinants in squamous cell carcinoma of the oral cavity. Future Oncol *6*, 837-850.

Arabzadeh, A., Chan, C., Nouvion, A. L., Breton, V., Benlolo, S., DeMarte, L., Turbide, C., Brodt, P., Ferri, L., and Beauchemin, N. (2013). Host-related carcinoembryonic antigen cell adhesion molecule 1 promotes metastasis of colorectal cancer. Oncogene *32*, 849-860.

Asiedu, M. K., Ingle, J. N., Behrens, M. D., Radisky, D. C., and Knutson, K. L. (2011). TGFbeta/TNF(alpha)-mediated epithelial-mesenchymal transition generates breast cancer stem cells with a claudin-low phenotype. Cancer Res *71*, 4707-4719.

Baba, T., Naka, K., Morishita, S., Komatsu, N., Hirao, A., and Mukaida, N. (2013). MIP-1alpha/CCL3-mediated maintenance of leukemia-initiating cells in the initiation process of chronic myeloid leukemia. J Exp Med *210*, 2661-2673.

Balkwill, F., and Coussens, L. M. (2004). Cancer - An inflammatory link. Nature *431*, 405-406.

Balkwill, F., and Mantovani, A. (2001). Inflammation and cancer: back to Virchow? The Lancet *357*, 539-545.

Bani-Yaghoub, M., Tremblay, R. G., Lei, J. X., Zhang, D., Zurakowski, B., Sandhu, J. K., Smith, B., Ribecco-Lutkiewicz, M., Kennedy, J., Walker, P. R., and Sikorska, M. (2006). Role of Sox2 in the development of the mouse neocortex. Dev Biol *295*, 52-66.

Beck, B., and Blanpain, C. (2013). Unravelling cancer stem cell potential. Nat Rev Cancer *13*, 727-738.

Benzaquen, L. R., Brugnara, C., Byers, H. R., Gattionicelli, S., and Halperin, J. (1995). Clotrimazole Inhibits Cell-Proliferation in-Vitro and in-Vivo (Vol 1, Pg 534, 1995). Nat Med *1*, 717-717.

Berridge, M. J., Lipp, P., and Bootman, M. D. (2000). The versatility and universality of calcium signalling. Nat Rev Mol Cell Biol *1*, 11-21.

Bhat-Nakshatri, P., Appaiah, H., Ballas, C., Pick-Franke, P., Goulet, R., Badve, S., Srour, E. F., and Nakshatri, H. (2010). SLUG/SNAI2 and Tumor Necrosis Factor Generate Breast Cells With CD44+/CD24-Phenotype. Bmc Cancer *10*.

Biteau, B., Hochmuth, C. E., and Jasper, H. (2008). JNK activity in somatic stem cells causes loss of tissue homeostasis in the aging Drosophila gut. Cell Stem Cell *3*, 442-455.
Blair, G. E., and Cook, G. P. (2008). Cancer and the immune system: an overview. Oncogene *27*, 5868.

Brundage, R. A., Fogarty, K. E., Tuft, R. A., and Fay, F. S. (1991). Calcium gradients underlying polarization and chemotaxis of eosinophils. Science *254*, 703-706.

Buchholz, M., Schatz, A., Wagner, M., Michl, P., Linhart, T., Adler, G., Gress, T. M., and Ellenrieder, V. (2006a). Overexpression of c-myc in pancreatic cancer caused by ectopic activation of NFATc1 and the Ca2+/calcineurin signaling pathway. EMBO J *25*, 3714-3724.

Buchholz, M., Schatz, A., Wagner, M., Michl, P., Linhart, T., Adler, G., Gress, T. M., and Ellenrieder, V. (2006b). Overexpression of c-myc in pancreatic cancer caused by ectopic activation of NFATc1 and the Ca2+/calcineurin signaling pathway. Embo J *25*, 3714-3724.

Cancela, J. M., Van Coppenolle, F., Galione, A., Tepikin, A. V., and Petersen, O. H. (2002). Transformation of local Ca2+ spikes to global Ca2+ transients: the combinatorial roles of multiple Ca2+ releasing messengers. Embo J *21*, 909-919.

Cao, Y., and Giovannucci, E. L. (2016). Alcohol as a Risk Factor for Cancer. Semin Oncol Nurs *32*, 325-331.

Carafoli, E. (1987). Intracellular calcium homeostasis. Annu Rev Biochem *56*, 395-433.

Castilho, R. M., Squarize, C. H., Leelahavanichkul, K., Zheng, Y., Bugge, T., and Gutkind, J. S. (2010). Rac1 is required for epithelial stem cell function during dermal and oral mucosal wound healing but not for tissue homeostasis in mice. PLoS One *5*, e10503.

Chambers, I., Colby, D., Robertson, M., Nichols, J., Lee, S., Tweedie, S., and Smith, A. (2003). Functional expression cloning of Nanog, a pluripotency sustaining factor in embryonic stem cells. Cell *113*, 643-655.

Chen, L., Glover, J. N., Hogan, P. G., Rao, A., and Harrison, S. C. (1998). Structure of the DNA-binding domains from NFAT, Fos and Jun bound specifically to DNA. Nature *392*, 42-48.

Chen, W., Yi, J. K., Shimane, T., Mehrazarin, S., Lin, Y. L., Shin, K. H., Kim, R. H., Park, N. H., and Kang, M. K. (2016). Grainyhead-like 2 regulates epithelial plasticity and stemness in oral cancer cells. Carcinogenesis *37*, 500-510.

Chen, Z. L., Zhao, S. H., Wang, Z., Qiu, B., Li, B. Z., Zhou, F., Tan, X. G., and He, J. (2011). Expression and unique functions of four nuclear factor of activated T cells isoforms in non-small cell lung cancer. Chin J Cancer *30*, 62-68.

Chiou, S. H., Yu, C. C., Huang, C. Y., Lin, S. C., Liu, C. J., Tsai, T. H., Chou, S. H., Chien, C. S., Ku, H. H., and Lo, J. F. (2008). Positive correlations of Oct-4 and Nanog in oral cancer stem-like cells and high-grade oral squamous cell carcinoma. Clin Cancer Res *14*, 4085-4095.

Chu, P. Y., Hu, F. W., Yu, C. C., Tsai, L. L., Yu, C. H., Wu, B. C., Chen, Y. W., Huang, P. I., and Lo, W. L. (2013). Epithelial-mesenchymal transition transcription factor ZEB1/ZEB2 co-expression predicts poor prognosis and maintains tumor-initiating properties in head and neck cancer. Oral Oncol *49*, 34-41.

Clay, M. R., Tabor, M., Owen, J. H., Carey, T. E., Bradford, C. R., Wolf, G. T., Wicha, M. S., and Prince, M. E. (2010). Single-Marker Identification of Head and Neck Squamous Cell Carcinoma Cancer Stem Cells with Aldehyde Dehydrogenase. Head Neck-J Sci Spec *32*, 1195-1201.

Clevers, H. (2011). The cancer stem cell: premises, promises and challenges. Nat Med *17*, 313-319.

Conticello, C., Pedini, F., Zeuner, A., Patti, M., Zerilli, M., Stassi, G., Messina, A., Peschle, C., and De Maria, R. (2004). IL-4 protects tumor cells from anti-CD95 and chemotherapeutic agents via up-regulation of antiapoptotic proteins. J Immunol *172*, 5467-5477.

Daniel, C., Gerlach, K., Väth, M., Neurath, M. F., and Weigmann, B. (2014). Nuclear factor of activated T cells—A transcription factor family as critical regulator in lung and colon cancer. International Journal of Cancer *134*, 1767-1775.

Davis, F. M., Peters, A. A., Grice, D. M., Cabot, P. J., Parat, M. O., Roberts-Thomson, S. J., and Monteith, G. R. (2012). Non-stimulated, agonist-stimulated and store-operated Ca2+ influx in MDA-MB-468 breast cancer cells and the effect of EGF-induced EMT on calcium entry. PLoS One *7*, e36923.

den Dekker, E., Molin, D. G., Breikers, G., van Oerle, R., Akkerman, J. W., van Eys, G. J., and Heemskerk, J. W. (2001). Expression of transient receptor potential mRNA isoforms and Ca(2+) influx in differentiating human stem cells and platelets. Biochimica et biophysica acta *1539*, 243-255.

Denissenko, M. F., Pao, A., Tang, M., and Pfeifer, G. P. (1996). Preferential formation of benzo[a]pyrene adducts at lung cancer mutational hotspots in P53. Science *274*, 430-432.

Di Stefano, A. B., Iovino, F., Lombardo, Y., Eterno, V., Hoger, T., Dieli, F., Stassi, G., and Todaro, M. (2010). Survivin Is Regulated by Interleukin-4 in Colon Cancer Stem Cells. J Cell Physiol *225*, 555-561.

Dickson, M. A., Hahn, W. C., Ino, Y., Ronfard, V., Wu, J. Y., Weinberg, R. A., Louis, D. N., Li, F. P., and Rheinwald, J. G. (2000). Human keratinocytes that express hTERT and also bypass a p16(INK4a)-enforced mechanism that limits life span become immortal yet retain normal growth and differentiation characteristics. Molecular and Cellular Biology *20*, 1436-1447.

Du, Q. S., Ren, X. R., Xie, Y., Wang, Q., Mei, L., and Xiong, W. C. (2001). Inhibition of PYK2-induced actin cytoskeleton reorganization, PYK2 autophosphorylation and focal adhesion targeting by FAK. J Cell Sci *114*, 2977-2987.

Du, X., Squier, C. A., Kremer, M. J., and Wertz, P. W. (2000). Penetration of N-nitrosonornicotine (NNN) across oral mucosa in the presence of ethanol and nicotine. J Oral Pathol Med *29*, 80-85.

Endo, Y., Uzawa, K., Mochida, Y., Shiiba, M., Bukawa, H., Yokoe, H., and Tanzawa, H. (2004). Sarcoendoplasmic reticulum Ca(2+) ATPase type 2 downregulated in human oral squamous cell carcinoma. Int J Cancer *110*, 225-231.

Erler, J. T., Bennewith, K. L., Nicolau, M., Dornhofer, N., Kong, C., Le, Q. T., Chi, J. T., Jeffrey, S. S., and Giaccia, A. J. (2006). Lysyl oxidase is essential for hypoxia-induced metastasis. Nature *440*, 1222-1226.

Ezeh, U. I., Turek, P. J., Reijo, R. A., and Clark, A. T. (2005). Human embryonic stem cell genes OCT4, NANOG, STELLAR, and GDF3 are expressed in both seminoma and breast carcinoma. Cancer-Am Cancer Soc *104*, 2255-2265.

Feghali, C. A., and Wright, T. M. (1997). Cytokines in acute and chronic inflammation. Front Biosci *2*, d12-26.

Flourakis, M., Lehen'kyi, V., Beck, B., Raphael, M., Vandenberghe, M., Abeele, F. V., Roudbaraki, M., Lepage, G., Mauroy, B., Romanin, C.*, et al.* (2010). Orai1 contributes to the establishment of an apoptosis-resistant phenotype in prostate cancer cells. Cell death & disease *1*, e75.

Fong, S. F., Dietzsch, E., Fong, K. S., Hollosi, P., Asuncion, L., He, Q., Parker, M. I., and Csiszar, K. (2007). Lysyl oxidase-like 2 expression is increased in colon and esophageal tumors and associated with less differentiated colon tumors. Genes Chromosomes Cancer *46*, 644-655.

Francipane, M. G., Alea, M. P., Lombardo, Y., Todaro, M., Medema, J. P., and Stassi, G. (2008). Crucial role of interleukin-4 in the survival of colon cancer stem cells. Cancer Res *68*, 4022-4025.

Gales, D., Clark, C., Manne, U., and Samuel, T. (2013). The Chemokine CXCL8 in Carcinogenesis and Drug Response. ISRN Oncol *2013*, 859154.

Giles, R. H., van Es, J. H., and Clevers, H. (2003). Caught up in a Wnt storm: Wnt signaling in cancer. Bba-Rev Cancer *1653*, 1-24.

Ginestier, C., Hur, M. H., Charafe-Jauffret, E., Monville, F., Dutcher, J., Brown, M., Jacquemier, J., Viens, P., Kleer, C. G., Liu, S. L.*, et al.* (2007). ALDH1 is a marker of normal and malignant human mammary stem cells and a predictor of poor clinical outcome. Cell Stem Cell *1*, 555-567.

Grimm, M., Krimmel, M., Polligkeit, J., Alexander, D., Munz, A., Kluba, S., Keutel, C., Hoffmann, J., Reinert, S., and Hoefert, S. (2012). ABCB5 expression and cancer stem cell hypothesis in oral squamous cell carcinoma. Eur J Cancer *48*, 3186-3197.

Grivennikov, S. I., Greten, F. R., and Karin, M. (2010). Immunity, inflammation, and cancer. Cell *140*, 883-899.

Gwack, Y., Srikanth, S., Feske, S., Cruz-Guilloty, F., Oh-hora, M., Neems, D. S., Hogan, P. G., and Rao, A. (2007). Biochemical and functional characterization of Orai proteins. J Biol Chem *282*, 16232-16243.

Hansson, B. G., Rosenquist, K., Antonsson, A., Wennerberg, J., Schildt, E. B., Bladstrom, A., and Andersson, G. (2005). Strong association between infection with human papillomavirus and oral and oropharyngeal squamous cell carcinoma: A population-based case-control study in southern Sweden. Acta Oto-Laryngol *125*, 1337-1344.

Hazelton, B., Mitchell, B., and Tupper, J. (1979). Calcium, magnesium, and growth control in the WI-38 human fibroblast cell. J Cell Biol *83*, 487-498.

Hecht, S. S. (2003). Tobacco carcinogens, their biomarkers and tobacco-induced cancer. Nat Rev Cancer *3*, 733-744.

Hermann, P. C., Huber, S. L., Herrler, T., Aicher, A., Ellwart, J. W., Guba, M., Bruns, C. J., and Heeschen, C. (2007). Distinct populations of cancer stem cells determine tumor growth and metastatic activity in human pancreatic cancer. Cell Stem Cell *1*, 313-323.

Hickie, R. A., Wei, J. W., Blyth, L. M., Wong, D. Y., and Klaassen, D. J. (1983). Cations and calmodulin in normal and neoplastic cell growth regulation. Can J Biochem Cell Biol *61*, 934-941.

Horsley, V., Aliprantis, A. O., Polak, L., Glimcher, L. H., and Fuchs, E. (2008). NFATc1 balances quiescence and proliferation of skin stem cells. Cell *132*, 299-310.

Hsu, C. J., Wu, M. H., Chen, C. Y., Tsai, C. H., Hsu, H. C., and Tang, C. H. (2013). AMP-activated protein kinase activation mediates CCL3-induced cell migration and matrix metalloproteinase-2 expression in human chondrosarcoma. Cell Commun Signal *11*, 68.

Jordan, N. V., Johnson, G. L., and Abell, A. N. (2011). Tracking the intermediate stages of epithelial-mesenchymal transition in epithelial stem cells and cancer. Cell Cycle *10*, 2865-2873.

Kahl, C. R., and Means, A. R. (2003). Regulation of cell cycle progression by calcium/calmodulin-dependent pathways. Endocr Rev *24*, 719-736.

Kellokoski, J. K., Syrjanen, S. M., Chang, F., Yliskoski, M., and Syrjanen, K. J. (1992). Southern Blot Hybridization and Pcr in Detection of Oral Human Papillomavirus (Hpv) Infections in Women with Genital Hpv Infections. J Oral Pathol Med *21*, 459-464.

Kim, J. H., Lkhagvadorj, S., Lee, M. R., Hwang, K. H., Chung, H. C., Jung, J. H., Cha, S. K., and Eom, M. (2014a). Orai1 and STIM1 are critical for cell migration and proliferation of clear cell renal cell carcinoma. Biochem Biophys Res Commun *448*, 76-82.

Kim, K. D., Srikanth, S., Tan, Y. V., Yee, M. K., Jew, M., Damoiseaux, R., Jung, M. E., Shimizu, S., An, D. S., Ribalet, B.*, et al.* (2014b). Calcium signaling via Orai1 is essential for induction of the nuclear orphan receptor pathway to drive Th17 differentiation. J Immunol *192*, 110-122.

Kim, K. D., Srikanth, S., Yee, M. K., Mock, D. C., Lawson, G. W., and Gwack, Y. (2011). ORAI1 deficiency impairs activated T cell death and enhances T cell survival. Journal of immunology *187*, 3620-3630.

Kim, R. H., Lieberman, M. B., Lee, R., Shin, K. H., Mehrazarin, S., Oh, J. E., Park, N. H., and Kang, M. K. (2010). Bmi-1 extends the life span of normal human oral keratinocytes by inhibiting the TGF-beta signaling. Experimental cell research *316*, 2600-2608.

Kligerman, J., Lima, R. A., Soares, J. R., Prado, L., Dias, F. L., Freitas, E. Q., and Olivatto, L. O. (1994). Supraomohyoid neck dissection in the treatment of T1/T2 squamous cell carcinoma of oral cavity. Am J Surg *168*, 391-394.

Lang, S. H., Frame, F. M., and Collins, A. T. (2009). Prostate cancer stem cells. J Pathol *217*, 299-306.

Lasorella, A., Rothschild, G., Yokota, Y., Russell, R. G., and Iavarone, A. (2005). Id2 mediates tumor initiation, proliferation, and angiogenesis in Rb mutant mice. Mol Cell Biol *25*, 3563-3574.

Lee, C. H., Lee, J. M., Wu, D. C., Hsu, H. K., Kao, E. L., Huang, H. L., Wang, T. N., Huang, M. C., and Wu, M. T. (2005a). Independent and combined effects of alcohol intake, tobacco smoking and betel quid chewing on the risk of esophageal cancer in Taiwan. Int J Cancer *113*, 475-482.

Lee, E. J., Kim, J., Lee, S. A., Kim, E. J., Chun, Y. C., Ryu, M. H., and Yook, J. I. (2005b). Characterization of newly established oral cancer cell lines derived from six squamous cell carcinoma and two mucoepidermoid carcinoma cells. Exp Mol Med *37*, 379-390.

Lee, H. J., Zhuang, G., Cao, Y., Du, P., Kim, H. J., and Settleman, J. (2014). Drug resistance via feedback activation of Stat3 in oncogene-addicted cancer cells. Cancer Cell *26*, 207-221.

Lee, J., Kim, H. K., Rho, J. Y., Han, Y. M., and Kim, J. (2006). The human OCT-4 isoforms differ in their ability to confer self-renewal. J Biol Chem *281*, 33554-33565.

Lee, S. H., Hong, H. S., Liu, Z. X., Kim, R. H., Kang, M. K., Park, N. H., and Shin, K. H. (2012a). TNFalpha enhances cancer stem cell-like phenotype via Notch-Hes1 activation in oral squamous cell carcinoma cells. Biochem Biophys Res Commun *424*, 58-64.

Lee, S. H., Lee, C. R., Rigas, N. K., Kim, R. H., Kang, M. K., Park, N. H., and Shin, K. H. (2015). Human papillomavirus 16 (HPV16) enhances tumor growth and cancer stemness of HPV-negative oral/oropharyngeal squamous cell carcinoma cells via miR-181 regulation. Papillomavirus Res *1*, 116-125.

Lee, W. J., Roberts-Thomson, S. J., Holman, N. A., May, F. J., Lehrbach, G. M., and Monteith, G. R. (2002). Expression of plasma membrane calcium pump isoform mRNAs in breast cancer cell lines. Cell Signal *14*, 1015-1022.

Lee, Y. F., Miller, L. D., Chan, X. B., Black, M. A., Pang, B., Ong, C. W., Salto-Tellez, M., Liu, E. T., and Desai, K. V. (2012b). JMJD6 is a driver of cellular proliferation and motility and a marker of poor prognosis in breast cancer. Breast Cancer Res *14*.

Lehen'kyi, V., Flourakis, M., Skryma, R., and Prevarskaya, N. (2007). TRPV6 channel controls prostate cancer cell proliferation via Ca(2+)/NFAT-dependent pathways. Oncogene *26*, 7380-7385.

Li, B. H., Yang, M. Z., Li, P. D., Yuan, Q., Liu, X. H., Yuan, J., and Zhang, W. H. (2008). IL-4/Stat6 activities correlate with apoptosis and metastasis in colon cancer cells. Biochem Bioph Res Co *369*, 554-560.

Lin, C. J., Grandis, J. R., Carey, T. E., Gollin, S. M., Whiteside, T. L., Koch, W. M., Ferris, R. L., and Lai, S. Y. (2007). Head and neck squamous cell carcinoma cell lines: Established models and rationale for selection. Head Neck-J Sci Spec *29*, 163-188.

Lin, W. W., and Karin, M. (2007). A cytokine-mediated link between innate immunity, inflammation, and cancer. J Clin Invest *117*, 1175-1183.

Liu, H., Hughes, J. D., Rollins, S., Chen, B., and Perkins, E. (2011). Calcium entry via ORAI1 regulates glioblastoma cell proliferation and apoptosis. Exp Mol Pathol *91*, 753-760.

Liu, J. F., Zhao, S. H., and Wu, S. S. (2013). Depleting NFAT1 expression inhibits the ability of invasion and migration of human lung cancer cells. Cancer Cell Int *13*, 41.

Liu, S. L., Dontu, G., Mantle, I. D., Patel, S., Ahn, N. S., Jackson, K. W., Suri, P., and Wicha, M. S. (2006). Hedgehog signaling and Bmi-1 regulate self-renewal of normal and malignant human mammary stem cells. Cancer Res *66*, 6063-6071.

Liu, Z. H., Dai, X. M., and Du, B. (2015). Hes1: a key role in stemness, metastasis and multidrug resistance. Cancer Biol Ther *16*, 353-359.

Lukyanenko, V., Gyorke, I., Wiesner, T. F., and Gyorke, S. (2001). Potentiation of Ca(2+) release by cADP-ribose in the heart is mediated by enhanced SR Ca(2+) uptake into the sarcoplasmic reticulum. Circ Res *89*, 614-622.

Mancini, M., and Toker, A. (2009). NFAT proteins: emerging roles in cancer progression. Nat Rev Cancer *9*, 810-820.

Mani, S. A., Guo, W., Liao, M. J., Eaton, E. N., Ayyanan, A., Zhou, A. Y., Brooks, M., Reinhard, F., Zhang, C. C., Shipitsin, M.*, et al.* (2008). The epithelial-mesenchymal transition generates cells with properties of stem cells. Cell *133*, 704-715.

Marcial, V. A., Pajak, T. F., Mohiuddin, M., Cooper, J. S., al Sarraf, M., Mowry, P. A., Curran, W., Crissman, J., Rodriguez, M., and Velez-Garcia, E. (1990). Concomitant cisplatin chemotherapy and radiotherapy in advanced mucosal squamous cell carcinoma of the head and neck. Long-term results of the Radiation Therapy Oncology Group study 81-17. Cancer-Am Cancer Soc *66*, 1861-1868.

Martinez-Martinez, S., and Redondo, J. M. (2004). Inhibitors of the calcineurin/NFAT pathway. Curr Med Chem *11*, 997-1007.

Mignen, O., and Shuttleworth, T. J. (2000). I(ARC), a novel arachidonate-regulated, noncapacitative Ca(2+) entry channel. J Biol Chem *275*, 9114-9119.

Min, B. M., Baek, J. H., Shin, K. H., Gujuluva, C. N., Cherrick, H. M., and Park, N. H. (1994). Inactivation of the P53 Gene by Either Mutation or Hpv Infection Is Extremely Frequent in Human Oral Squamous-Cell Carcinoma Cell-Lines. Oral Oncology-European Journal of Cancer Part B *30B*, 338-345.

Monet, M., Lehen'kyi, V., Gackiere, F., Firlej, V., Vandenberghe, M., Roudbaraki, M., Gkika, D., Pourtier, A., Bidaux, G., Slomianny, C.*, et al.* (2010). Role of cationic channel TRPV2 in promoting prostate cancer migration and progression to androgen resistance. Cancer Res *70*, 1225-1235.

Monroe, M. M., Anderson, E. C., Clayburgh, D. R., and Wong, M. H. (2011). Cancer stem cells in head and neck squamous cell carcinoma. Journal of oncology *2011*, 762780.

Monteith, G. R., McAndrew, D., Faddy, H. M., and Roberts-Thomson, S. J. (2007). Calcium and cancer: targeting Ca2+ transport. Nat Rev Cancer *7*, 519-530.

Morel, A. P., Lievre, M., Thomas, C., Hinkal, G., Ansieau, S., and Puisieux, A. (2008). Generation of breast cancer stem cells through epithelial-mesenchymal transition. PloS one *3*, e2888.

Mueller, S. N., Hosiawa-Meagher, K. A., Konieczny, B. T., Sullivan, B. M., Bachmann, M. F., Locksley, R. M., Ahmed, R., and Matloubian, M. (2007). Regulation of homeostatic chemokine expression and cell trafficking during immune responses. Science *317*, 670-674.

Neal, J. W., and Clipstone, N. A. (2003). A constitutively active NFATc1 mutant induces a transformed phenotype in 3T3-L1 fibroblasts. J Biol Chem *278*, 17246-17254.

O'Hayre, M., Salanga, C. L., Handel, T. M., and Allen, S. J. (2008). Chemokines and cancer: migration, intracellular signalling and intercellular communication in the microenvironment. The Biochemical journal *409*, 635-649.

Oguma, K., Oshima, H., Aoki, M., Uchio, R., Naka, K., Nakamura, S., Hirao, A., Saya, H., Taketo, M. M., and Oshima, M. (2008). Activated macrophages promote Wnt signalling through tumour necrosis factor-alpha in gastric tumour cells. Embo J *27*, 1671-1681.

Ota, N., Ohno, J., Seno, K., Taniguchi, K., and Ozeki, S. (2014). In vitro and in vivo expression of aldehyde dehydrogenase 1 in oral squamous cell carcinoma. Int J Oncol *44*, 435-442.

Padar, S., van Breemen, C., Thomas, D. W., Uchizono, J. A., Livesey, J. C., and Rahimian, R. (2004). Differential regulation of calcium homeostasis in adenocarcinoma cell line A549 and its Taxol-resistant subclone. Br J Pharmacol *142*, 305-316.

Pan, G., and Thomson, J. A. (2007). Nanog and transcriptional networks in embryonic stem cell pluripotency. Cell Res *17*, 42-49.

Pande, G., Kumar, N. A., and Manogaran, P. S. (1996). Flow cytometric study of changes in the intracellular free calcium during the cell cycle. Cytometry *24*, 55-63.

Panner, A., and Wurster, R. D. (2006). T-type calcium channels and tumor proliferation. Cell Calcium *40*, 253-259.

Parekh, A. B. (2007). Functional consequences of activating store-operated CRAC channels. Cell calcium *42*, 111-121.

Parekh, A. B., and Putney, J. W., Jr. (2005). Store-operated calcium channels. Physiological reviews *85*, 757-810.

Park, N. H., Gujuluva, C. N., Baek, J. H., Cherrick, H. M., Shin, K. H., and Min, B. M. (1995). Combined Oral Carcinogenicity of Hpv-16 and Benzo(a)Pyrene - an in-Vitro Multistep Carcinogenesis Model. Oncogene *10*, 2145-2153.

Park, N. H., Min, B. M., Li, S. L., Huang, M. Z., Cherick, H. M., and Doniger, J. (1991). Immortalization of Normal Human Oral Keratinocytes with Type 16 Human Papillomavirus. Carcinogenesis *12*, 1627-1631.

Peng, L., Ran, Y. L., Hu, H., Yu, L., Liu, Q., Zhou, Z., Sun, Y. M., Sun, L. C., Pan, J., Sun, L. X., *et al.* (2009). Secreted LOXL2 is a novel therapeutic target that promotes gastric cancer metastasis via the Src/FAK pathway. Carcinogenesis *30*, 1660-1669.

Perez-Sayans, M., Somoza-Martin, J. M., Barros-Angueira, F., Reboiras-Lopez, M. D., Gandara Rey, J. M., and Garcia-Garcia, A. (2009). Genetic and molecular alterations associated with oral squamous cell cancer (Review). Oncology reports *22*, 1277-1282.

Pfeifer, G. P., Denissenko, M. F., Olivier, M., Tretyakova, N., Hecht, S. S., and Hainaut, P. (2002). Tobacco smoke carcinogens, DNA damage and p53 mutations in smoking-associated cancers. Oncogene *21*, 7435-7451.

Pinton, P., Ferrari, D., Magalhaes, P., Schulze-Osthoff, K., Di Virgilio, F., Pozzan, T., and Rizzuto, R. (2000). Reduced loading of intracellular Ca(2+) stores and downregulation of capacitative Ca(2+) influx in Bcl-2-overexpressing cells. J Cell Biol *148*, 857-862.

Prevarskaya, N., Skryma, R., and Shuba, Y. (2011). Calcium in tumour metastasis: new roles for known actors. Nat Rev Cancer *11*, 609-618.

Prokopchuk, O., Liu, Y., Henne-Bruns, D., and Kornmann, M. (2005). Interleukin-4 enhances proliferation of human pancreatic cancer cells: evidence for autocrine and paracrine actions. Br J Cancer *92*, 921-928.

Ribatti, D. (2012). Cancer stem cells and tumor angiogenesis. Cancer Letters *321*, 13-17.
Richard, V., Sebastian, P., Nair, M. G., Nair, S. N., Malieckal, T. T., Kumar, T. R. S., and Pillai, M. R. (2013). Multiple drug resistant, tumorigenic stem-like cells in oral cancer. Cancer Lett *338*, 300-316.

Rivera, C., and Venegas, B. (2014). Histological and molecular aspects of oral squamous cell carcinoma (Review). Oncol Lett *8*, 7-11.

Rizzuto, R., Pinton, P., Ferrari, D., Chami, M., Szabadkai, G., Magalhaes, P. J., Di Virgilio, F., and Pozzan, T. (2003). Calcium and apoptosis: facts and hypotheses. Oncogene *22*, 8619-8627.
Roderick, H. L., and Cook, S. J. (2008). Ca2+ signalling checkpoints in cancer: remodelling Ca2+ for cancer cell proliferation and survival. Nat Rev Cancer *8*, 361-375.

Rooney, M., Kish, J., Jacobs, J., Kinzie, J., Weaver, A., Crissman, J., and Al-Sarraf, M. (1985). Improved complete response rate and survival in advanced head and neck cancer after three-course induction therapy with 120-hour 5-FU infusion and cisplatin. Cancer-Am Cancer Soc *55*, 1123-1128.

Saito, K., Uzawa, K., Endo, Y., Kato, Y., Nakashima, D., Ogawara, K., Shiba, M., Bukawa, H., Yokoe, H., and Tanzawa, H. (2006). Plasma membrane Ca2+ ATPase isoform 1 down-regulated in human oral cancer. Oncology reports *15*, 49-55.
Sansone, P., Storci, G., Tavolari, S., Guarnieri, T., Giovannini, C., Taffurelli, M., Ceccarelli, C.,

Santini, D., Paterini, P., Marcu, K. B.*, et al.* (2007). IL-6 triggers malignant features in mammospheres from human ductal breast carcinoma and normal mammary gland. J Clin Invest *117*, 3988-4002.

Schall, T. J., Bacon, K., Camp, R. D., Kaspari, J. W., and Goeddel, D. V. (1993). Human macrophage inflammatory protein alpha (MIP-1 alpha) and MIP-1 beta chemokines attract distinct populations of lymphocytes. J Exp Med *177*, 1821-1826.

Schmidt, S., Liu, G., Liu, G., Yang, W., Honisch, S., Pantelakos, S., Stournaras, C., Hönig, A., and Lang, F. (2014). Enhanced Orai1 and STIM1 expression as well as store operated Ca 2+ entry in therapy resistant ovary carcinoma cells).

Schoenhals, M., Kassambara, A., De Vos, J., Hose, D., Moreaux, J., and Klein, B. (2009). Embryonic stem cell markers expression in cancers. Biochem Biophys Res Commun *383*, 157-162.

Schrodl, K., Oelmez, H., Edelmann, M., Huber, R. M., and Bergner, A. (2009). Altered Ca2+-homeostasis of cisplatin-treated and low level resistant non-small-cell and small-cell lung cancer cells. Cell Oncol *31*, 301-315.

Seitz, H. K., and Becker, P. (2007). Alcohol metabolism and cancer risk. Alcohol Res Health *30*, 38-41, 44-37.

Shiboski, C. H., Schmidt, B. L., and Jordan, R. C. K. (2005). Tongue and tonsil carcinoma - Increasing trends in the US population ages 20-44 years. Cancer-Am Cancer Soc *103*, 1843-1849.

Shin, K. H., Kim, R. H., Yu, B., Kang, M. K., Elashoff, D., Christensen, R., Pucar, A., and Park, N. H. (2011). Expression and mutation analysis of heterogeneous nuclear ribonucleoprotein G in human oral cancer. Oral Oncol *47*, 1011-1016.

Sinevici, N., and O'Sullivan, J. (2016). Oral cancer: Deregulated molecular events and their use as biomarkers. Oral Oncol *61*, 12-18.

Singh, S., and Chellappan, S. (2014). Lung cancer stem cells: Molecular features and therapeutic targets. Mol Aspects Med *39*, 50-60.

Smith, E. M., Ritchie, J. M., Summersgill, K. F., Hoffman, H. T., Wang, D. H., Haugen, T. H., and Turek, L. P. (2004). Human papillomavirus in oral exfoliated cells and risk of head and neck cancer. Journal of the National Cancer Institute *96*, 449-455.

Sriuranpong, V., Park, J. I., Amornphimoltham, P., Patel, V., Nelkin, B. D., and Gutkind, J. S. (2003). Epidermal growth factor receptor-independent constitutive activation of STAT3 in head and neck squamous cell carcinoma is mediated by the autocrine/paracrine stimulation of the interleukin 6/gp130 cytokine system. Cancer Res *63*, 2948-2956.

Storci, G., Sansone, P., Mari, S., D'Uva, G., Tavolari, S., Guarnieri, T., Taffurelli, M., Ceccarelli, C., Santini, D., Chieco, P.*, et al.* (2010). TNFalpha up-regulates SLUG via the NF-kappaB/HIF1alpha axis, which imparts breast cancer cells with a stem cell-like phenotype. J Cell Physiol *225*, 682-691.

Sumida, T., Ishikawa, A., Nakano, H., Yamada, T., Mori, Y., and Desprez, P. Y. (2016). Targeting ID2 expression triggers a more differentiated phenotype and reduces aggressiveness in human salivary gland cancer cells. Genes Cells *21*, 915-920.

Sun, S., Liu, Y., Lipsky, S., and Cho, M. (2007). Physical manipulation of calcium oscillations facilitates osteodifferentiation of human mesenchymal stem cells. FASEB J *21*, 1472-1480.
Syrjanen, S. (1992). Viral-Infections in Oral-Mucosa. Scand J Dent Res *100*, 17-31.

Tai, M. H., Chang, C. C., Kiupel, M., Webster, J. D., Olson, L. K., and Trosko, J. E. (2005). Oct4 expression in adult human stem cells: evidence in support of the stem cell theory of carcinogenesis. Carcinogenesis *26*, 495-502.

Tanabe, Y., Sasaki, S., Mukaida, N., and Baba, T. (2016). Blockade of the chemokine receptor, CCR5, reduces the growth of orthotopically injected colon cancer cells via limiting cancerassociated fibroblast accumulation. Oncotarget.

Todaro, M., Alea, M. P., Di Stefano, A. B., Cammareri, P., Vermeulen, L., Iovino, F., Tripodo, C., Russo, A., Gulotta, G., Medema, J. P., and Stassi, G. (2007). Colon cancer stem cells dictate tumor growth and resist cell death by production of interleukin-4. Cell Stem Cell *1*, 389-402.

Todorova, M. G., Fuentes, E., Soria, B., Nadal, A., and Quesada, I. (2009). Lysophosphatidic acid induces Ca2+ mobilization and c-Myc expression in mouse embryonic stem cells via the phospholipase C pathway. Cell Signal *21*, 523-528.

Tsavaler, L., Shapero, M. H., Morkowski, S., and Laus, R. (2001). Trp-p8, a novel prostate-specific gene, is up-regulated in prostate cancer and other malignancies and shares high homology with transient receptor potential calcium channel proteins. Cancer Res *61*, 3760-3769.

Umar, S., Sarkar, S., Wang, Y., and Singh, P. (2009). Functional cross-talk between beta-catenin and NFkappaB signaling pathways in colonic crypts of mice in response to progastrin. J Biol Chem *284*, 22274-22284.

Vanden Abeele, F., Skryma, R., Shuba, Y., Van Coppenolle, F., Slomianny, C., Roudbaraki, M., Mauroy, B., Wuytack, F., and Prevarskaya, N. (2002). Bcl-2-dependent modulation of Ca(2+) homeostasis and store-operated channels in prostate cancer cells. Cancer Cell *1*, 169-179.

Velupillai, P., Sung, C. K., Tian, Y., Dahl, J., Carroll, J., Bronson, R., and Benjamin, T. (2010). Polyoma virus-induced osteosarcomas in inbred strains of mice: host determinants of metastasis. PLoS Pathog *6*, e1000733.

Voronov, E., Shouval, D. S., Krelin, Y., Cagnano, E., Benharroch, D., Iwakura, Y., Dinarello, C. A., and Apte, R. N. (2003). IL-1 is required for tumor invasiveness and angiogenesis. Proc Natl Acad Sci U S A *100*, 2645-2650.

Wang, B., Zhang, S., Yue, K., and Wang, X. D. (2013). The recurrence and survival of oral squamous cell carcinoma: a report of 275 cases. Chin J Cancer *32*, 614-618.

Wang, Y., Yu, Y., Tsuyada, A., Ren, X., Wu, X., Stubblefield, K., Rankin-Gee, E. K., and Wang, S. E. (2011). Transforming growth factor-beta regulates the sphere-initiating stem cell-like feature in breast cancer through miRNA-181 and ATM. Oncogene *30*, 1470-1480.

Warnakulasuriya, S. (2009). Global epidemiology of oral and oropharyngeal cancer. Oral Oncol *45*, 309-316.

Wen, L., Liang, C., Chen, E., Chen, W., Liang, F., Zhi, X., Wei, T., Xue, F., Li, G., Yang, Q.*, et al.* (2016). Regulation of Multi-drug Resistance in hepatocellular carcinoma cells is TRPC6/Calcium Dependent. Sci Rep *6*, 23269.

West, K. A., Castillo, S. S., and Dennis, P. A. (2002). Activation of the PI3K/Akt pathway and chemotherapeutic resistance. Drug Resist Updat *5*, 234-248.

Whitfield, J. F., Boynton, A. L., MacManus, J. P., Sikorska, M., and Tsang, B. K. (1979). The regulation of cell proliferation by calcium and cyclic AMP. Mol Cell Biochem *27*, 155-179.

Wu, Y., Li, Y. Y., Matsushima, K., Baba, T., and Mukaida, N. (2008). CCL3-CCR5 axis regulates intratumoral accumulation of leukocytes and fibroblasts and promotes angiogenesis in murine lung metastasis process. J Immunol *181*, 6384-6393.

Yang, N., Tang, Y., Wang, F., Zhang, H., Xu, D., Shen, Y., Sun, S., and Yang, G. (2013). Blockade of store-operated Ca(2+) entry inhibits hepatocarcinoma cell migration and invasion by regulating focal adhesion turnover. Cancer Lett *330*, 163-169.

Yang, S., Zhang, J. J., and Huang, X. Y. (2009a). Orai1 and STIM1 are critical for breast tumor cell migration and metastasis. Cancer Cell *15*, 124-134.

Yang, Z. H., Wang, X. H., Wang, H. P., and Hu, L. Q. (2009b). Effects of TRPM8 on the proliferation and motility of prostate cancer PC-3 cells. Asian J Androl *11*, 157-165.

Yasuda, K., Torigoe, T., Mariya, T., Asano, T., Kuroda, T., Matsuzaki, J., Ikeda, K., Yamauchi, M., Emori, M., Asanuma, H.*, et al.* (2014). Fibroblasts induce expression of FGF4 in ovarian cancer stem-like cells/cancer-initiating cells and upregulate their tumor initiation capacity. Lab Invest *94*, 1355-1369.

Yu, H., Kortylewski, M., and Pardoll, D. (2007). Crosstalk between cancer and immune cells: role of STAT3 in the tumour microenvironment. Nat Rev Immunol *7*, 41-51.

Yu, H., Pardoll, D., and Jove, R. (2009). STATs in cancer inflammation and immunity: a leading role for STAT3. Nat Rev Cancer *9*, 798-809.

Zhang, J., Chang, L., Jin, H., Xia, Y., Wang, L., He, W., Li, W., and Chen, H. (2016). Benzopyrene promotes lung cancer A549 cell migration and invasion through up-regulating cytokine IL8 and chemokines CCL2 and CCL3 expression. Exp Biol Med (Maywood) *241*, 1516-1523.

Zhang, J., Ni, S. S., Zhao, W. L., Dong, X. C., and Wang, J. L. (2013). High expression of JMJD6 predicts unfavorable survival in lung adenocarcinoma. Tumour biology : the journal of the International Society for Oncodevelopmental Biology and Medicine *34*, 2397-2401.

Zhong, F., Davis, M. C., McColl, K. S., and Distelhorst, C. W. (2006). Bcl-2 differentially regulates Ca2+ signals according to the strength of T cell receptor activation. J Cell Biol *172*, 127-137.

Zhu, H., Zhang, H., Jin, F., Fang, M., Huang, M., Yang, C. S., Chen, T., Fu, L., and Pan, Z. (2014). Elevated Orai1 expression mediates tumor-promoting intracellular Ca2+ oscillations in human esophageal squamous cell carcinoma. Oncotarget *5*, 3455-3471.